Universidad de Concepción

Facultad de Ingeniería

Doctorado en Energías

Assessment of the Impact of Wind–Solar Temporal Energy Complementarity on the Design of Stand-Alone Hybrid Renewable Energy Systems with Storage Using Artificial Intelligence

(Evaluación del Impacto de la Complementariedad Temporal Energética Eólico-Solar en el Diseño de Sistemas Híbridos de Energía Renovable Autónomos con Almacenamiento Utilizando Inteligencia Artificial)

Tesis presentada a la Facultad de Ingeniería de la Universidad de Concepción para optar al grado académico de Doctor en Energías.

Por: JOSÉ LUIS ALFREDO MUÑOZ PINCHEIRA

Profesor Guía: Dr. Felipe Sanhueza Gómez

Profesor Co-Guía: Dr. Lautaro Salazar Silva

Concepción, Chile, junio del 2025.

DEDICATORIA

Querida hija: que cada instante en que no estuve presente sea, al menos, semilla de un futuro más justo, donde otros también puedan encender sus sueños con la misma energía que ilumina el nuestro.

AGRADECIMIENTOS

A mi hija y esposa.

A mis padres.

A mis profesores guías y dirección del programa.

A mis compañeros de doctorado.

A mis colegas.

A la Dirección de Postgrado de la Universidad de Concepción por becarme durante mis estudios.

TABLE OF CONTENTS

LIST OF TABLES

LIST OF FIGURES

NOMENCLATURE

Symbol	Meaning	Units
HRES	Hybrid Renewable Energy System	
IPCC	Intergovernmental Panel on Climate Change	
GHG	Greenhouse gas	
IEA	International Energy Agency	
GIS	Geographic information system	
VRE	Variable Renewable Energy	
BESS	Battery Energy Storage System	
SEN	National Electric System	
MERRA-2	Modern-Era Retrospective analysis for Research and Applications, Version 2	
NPC	Net Present Cost	$
LCOE	Levelized Cost of Energy	$/kWh
LPSP	Loss of Power Supply Probability	%
D	Dumped Energy or curtailment	kWh
GA	Genetic algorithms	
ρ	Spearman's Correlation Coefficient	-
V	Wind Speed	m/s
GHI	Global Horizontal Irradiance	kWh/m²
PV	Photovoltaic Panel	-
WT	Wind Turbine	-
BS	Battery Storage Capacity	kWh
$P_{\mathrm{WT},t}^{single}$	Power generated by one wind turbine	kW
v	Hourly wind speed	m/s
$v_{\text{cut-in}}$	Minimum wind speed to start generating energy	m/s
v_{rated}	Nominal wind speed	m/s
$v_{\text{cut-out}}$	Maximum wind speed for safe operation	m/s
K_{WT}	wind turbine nominal capacity	kW
η_{WT}	Wind turbine efficiency	%
ϕ_{WT}	Wind turbine availability factor	-
P_{PV}	power generated by a photovoltaic panel	kW
K_{PV}	photovoltaic panel nominal capacity	kW
η_{PV}	Photovoltaic panel efficiency	%
ϕ_{PV}	Photovoltaic panel availability factor	-
x_1	total capacity of photovoltaic (PV) solar panels	kW
x_2	total wind turbine (WT) capacity	kW
x_3	total battery storage capacity	kW
C_{PV}	cost per kW of photovoltaic (PV) panels	$/kWp
C_{WT}	cost per kW of wind turbines	$/kW
C_{BS}	cost per kWh of batteries	$/kWh

OM_{PV}	annual operation and maintenance cost of PV (initial cost fraction)	% annual
OM_{WT}	annual operation and maintenance cost of WT (initial cost fraction)	% annual
K_{BS}	battery nominal capacity per unit	kW
r	discount rate	%
L	project life (years)	years
$C_{\mathrm{load},t}$	energy demand per hour	
I_t	solar irradiation	kWh/m^2 hour
v_t	wind speed	m^2/s
$E_{\mathrm{PV},t}$	total solar energy generated at hour t.	kWh
N_{PV}	number of photovoltaic panels	-
$E_{\mathrm{WT},t}$	total wind energy generated by wind turbines at hour t	kWh
$E_{\mathrm{WT},t}^{\mathrm{single}}$	energy generated by a single wind turbine at hour t.	kWh
N_{WT}	number of wind turbines.	-
$E_{\mathrm{bat},t}$	Energy stored in the batteries at the end of hour t	kWh
$E_{\mathrm{bat,\ pre},t}$	Battery energy before adjustment at time t	kWh
$E_{\mathrm{total},t}$	Energy generated by the system (solar + wind) at hour t.	kWh
$C_{load,t}$	Load or demand for energy at hour t.	kWh
N_{BT}	number of batteries.	-

ABSTRACT

The transition towards a 100% renewable energy matrix faces significant technical challenges, primarily due to the variability of solar and wind resources and their high geographic concentration. These characteristics have led to problems in centralized power systems, such as transmission network congestion and forced energy curtailment, which undermine the efficiency and economic viability of renewable projects. This thesis addresses this issue through two complementary studies.

The first study analyzes the temporal complementarity between solar and wind energy in Chile, using hourly data from 2004 to 2016 across 176 locations. Using Spearman's rank correlation coefficient, four zones with different levels of energy synergy were identified: positive (A1), negative (A2 and B), and neutral (C). This classification enabled the construction of a strategic map to locate more efficient hybrid systems with lower storage requirements.

The second study incorporates these findings into an optimization model for the design of stand-alone Hybrid Renewable Energy Systems (HRES), consisting of solar panels, wind turbines, and batteries. The model, implemented in GNU Octave, uses genetic algorithms to simulate optimal configurations under different levels of complementarity and demand profiles (constant and variable). Key performance metrics are evaluated, including Net Present Cost (NPC), Levelized Cost of Energy (LCOE), and Loss of Power Supply Probability (LPSP).

The results show that higher complementarity reduces costs, storage size, and simplifies system design, particularly under high continuity requirements (low LPSP). It is concluded that explicitly considering temporal complementarity improves the technical and economic performance of off-grid HRES and strengthens local energy resilience. Furthermore, promoting distributed generation in areas with high solar-wind complementarity supports energy system decentralization, reducing pressure on transmission networks and mitigating renewable energy curtailment. The thesis therefore proposes incorporating this metric as a key criterion in territorial energy planning to guide investments towards more sustainable, resilient, and cost-effective configurations.

RESUMEN

La transición hacia una matriz energética 100% renovable enfrenta importantes desafíos técnicos, principalmente debido a la variabilidad de los recursos solar y eólico, así como a su alta concentración geográfica. Estas características han generado problemas en los sistemas eléctricos centralizados, como la congestión de las redes de transmisión y la generación forzada de vertimientos energéticos, lo que afecta la eficiencia y viabilidad económica de los proyectos renovables. Esta tesis aborda dicha problemática mediante dos estudios complementarios.

El primer estudio analiza la complementariedad temporal entre la energía solar y eólica en Chile, utilizando datos horarios desde 2004 hasta 2016 en 176 localidades. A través del coeficiente de correlación por rangos de Spearman, se identificaron cuatro zonas con distintos niveles de sinergia energética: positiva (A1), negativa (A2 y B) y neutra (C). Esta clasificación permitió construir un mapa estratégico para ubicar sistemas híbridos más eficientes y con menores requerimientos de almacenamiento.

El segundo estudio incorpora estos hallazgos en un modelo de optimización para el diseño de Sistemas Híbridos de Energía Renovable autónomos (HRES, por sus siglas en inglés), compuestos por paneles solares, aerogeneradores y baterías. El modelo, implementado en GNU Octave, utiliza algoritmos genéticos para simular configuraciones óptimas bajo distintos niveles de complementariedad y perfiles de demanda (constante y variable). Se evalúan métricas clave de desempeño, como el Costo Neto Actualizado (NPC), el Costo Nivelado de la Energía (LCOE) y la Probabilidad de Pérdida de Suministro de Energía (LPSP).

Los resultados muestran que una mayor complementariedad reduce los costos, el tamaño del almacenamiento y simplifica el diseño del sistema, especialmente bajo altos requerimientos de continuidad (bajo LPSP). Se concluye que considerar explícitamente la complementariedad temporal mejora el desempeño técnico y económico de los HRES autónomos y fortalece la resiliencia energética local. Además, fomentar la generación distribuida en zonas con alta complementariedad solar-eólica apoya la descentralización del sistema energético, reduciendo la presión sobre las redes de transmisión y mitigando los vertimientos renovables. Por lo tanto, la tesis propone incorporar esta métrica como un criterio clave en la planificación energética territorial para orientar las inversiones hacia configuraciones más sostenibles, resilientes y costo-efectivas.

INTRODUCTION

Global Context and Energy Challenge

The world is undergoing a profound transformation of its energy systems, driven by the urgent need to address climate change and reduce dependence on fossil fuels. Various international reports, such as those from the Intergovernmental Panel on Climate Change (IPCC, 2023), warn that limiting the global temperature increase to 1.5 °C requires a drastic reduction in greenhouse gas (GHG) emissions, with the energy sector being one of the main contributors (IEA, 2023).

In this context, the transition toward an energy matrix based on renewable sources, particularly photovoltaic solar and wind energy, has become a global strategic priority. These technologies have experienced rapid growth due to declining costs, supportive public policies, and the development of regulatory frameworks that promote their adoption (World Economic Forum, 2024). However, both sources share a characteristic that complicates their large-scale integration: their temporal variability and intermittency (Ringkjøb et al., 2020).

Solar and wind power generation depend on local and fluctuating weather conditions, complicating real-time management of the balance between generation and demand. This condition imposes significant technical and economic challenges, particularly in centralized power systems where large-scale energy storage is not economically feasible (Hossain Lipu et al., 2025). Without appropriate mechanisms to mitigate this variability, there is an increased risk of overinvestment in installed capacity, energy curtailment (Pérez Odeh & Watts, 2019), or the need for backup from fossil sources - undermining decarbonization goals (Ahmed Adam et al., 2024).

In response to this scenario, HRES, which combine multiple renewable sources with storage systems, have emerged as a technically viable solution. Their implementation reduces dependence on a single energy source, enhances supply stability, and facilitates the operation of isolated power systems or those with limited transmission infrastructure (León Gómez et al., 2023). However, the efficient design of these systems requires addressing complex challenges related to optimal sizing, energy management, demand-side management, and storage, all of which are critical to ensuring their technical and economic feasibility (Maghami & Mutambara, 2023).

Specific Problem

Despite the technological and regulatory advances that have supported the growth of renewable energy, the effective integration of these sources into centralized power systems continues to face significant challenges, particularly in countries with limited infrastructure or extensive transmission networks. One of the main issues is grid congestion (ZeroHedge, 2024), which occurs when transmission capacity is insufficient to transport the energy generated in high-production zones to consumption centers. This has led to forced renewable energy curtailment, reducing overall system efficiency and discouraging further investment in clean generation (Newbery, 2025).

Another major challenge is the geographic concentration of renewable resources, such as solar energy in northern Chile or wind power in the south. This dependency exposes the system to seasonal variability and extreme weather events (Pérez Odeh & Watts, 2019). In Chile, this spatial concentration, combined with a rapid increase in renewable generation in certain regions, has led to a sustained rise in curtailment, even after the commissioning of the Cardones–Polpaico transmission line in 2019. Although this infrastructure improved the integration of the national grid, evacuation capacity has once again been exceeded during peak production hours, resulting in near-zero marginal prices and record curtailment levels reaching 1,600 GWh in 2022 (Fraunhofer, 2022). This situation highlights the need for structural solutions that enable more flexible absorption of renewable generation, including continued grid reinforcement, large-scale energy storage deployment, and, most importantly, a decentralized energy planning approach that encourages the strategic siting of projects in areas with high complementarity and closer to demand centers.

In this context, HRES represent a viable solution, especially in remote or poorly connected regions. Integrating complementary technologies (solar, wind, and storage), enable decentralized local generation, reduce transmission losses, and enhance energy autonomy.

However, most current HRES design models do not explicitly incorporate the temporal complementarity between renewable sources. This represents a missed opportunity to improve the combined use of resources, reduce storage system size, and optimize the technical and economic performance of the proposed solutions (Jurasz et al., 2020). This limitation becomes particularly critical in contexts where continuous power supply is required, such as rural communities or industrial applications sensitive to interruptions.

Research Justification

The transition toward a sustainable energy matrix requires overcoming the challenges of intermittency and variability associated with solar and wind resources, especially in off-grid systems. In this context, HRES are a promising alternative, combining complementary resources and energy storage to ensure continuous supply.

However, in Chile, no systematic studies have been conducted to characterize the temporal complementarity between solar and wind resources at the national level. Internationally, the effect of renewable sources temporal complementarity on the techno-economic design of hybrid renewable systems with storage has not been adequately addressed in the scientific literature. This research gap is particularly relevant in the context of Chile's high renewable energy penetration and pronounced climatic variability.

Moreover, although there are metrics to assess temporal complementarity, their relationship with key parameters such as NPC, LCOE, LPSP, or the installed storage capacity in HRES has not yet been thoroughly explored. In addition, some of these metrics require refinement to better capture the relationship between complementarity, reliability, and cost, since greater complementarity does not always imply lower overall system costs (Jurasz et al., 2020).

This research is justified by both its methodological and practical contributions. First, it proposes a geospatial characterization of solar-wind temporal complementarity in Chile based on hourly data from 176 locations. Second, it develops an optimization model for the design of stand-alone HRES in GNU Octave using genetic algorithms. Third, it quantifies the impact of different levels of complementarity on key HRES performance indicators, providing evidence that can inform design decisions, territorial planning, and investment in distributed generation.

In this way, the study contributes to both scientific advancement in hybrid renewable systems and the development of practical criteria for designing decentralized, resilient, and cost-effective energy solutions, particularly relevant for isolated communities, industrial applications, and regions undergoing energy transition.

Hypothesis

An increase in the temporal complementarity between non-conventional renewable energy sources—wind and solar—leads to a reduction in both the NPC and the LPSP in the optimal design of an off-grid HRES.

Objectives

General Objective

To evaluate the influence of temporal complementarity between non-conventional renewable energy sources on the reduction of NPC and LPSP in the optimal design of an off-grid HRES that includes storage.

Specific Objectives

1. To design a methodology for evaluating temporal energy complementarity.
2. To develop the first temporal solar-wind energy complementarity map for Chile.
3. To program an artificial intelligence algorithm to find the optimal solution of a stand-alone HRES with storage.
4. To assess the impact of different levels of solar-wind temporal complementarity on the optimal design of an HRES for various load profiles, quantifying their influence on the solution.

Conceptual Framework of the Research

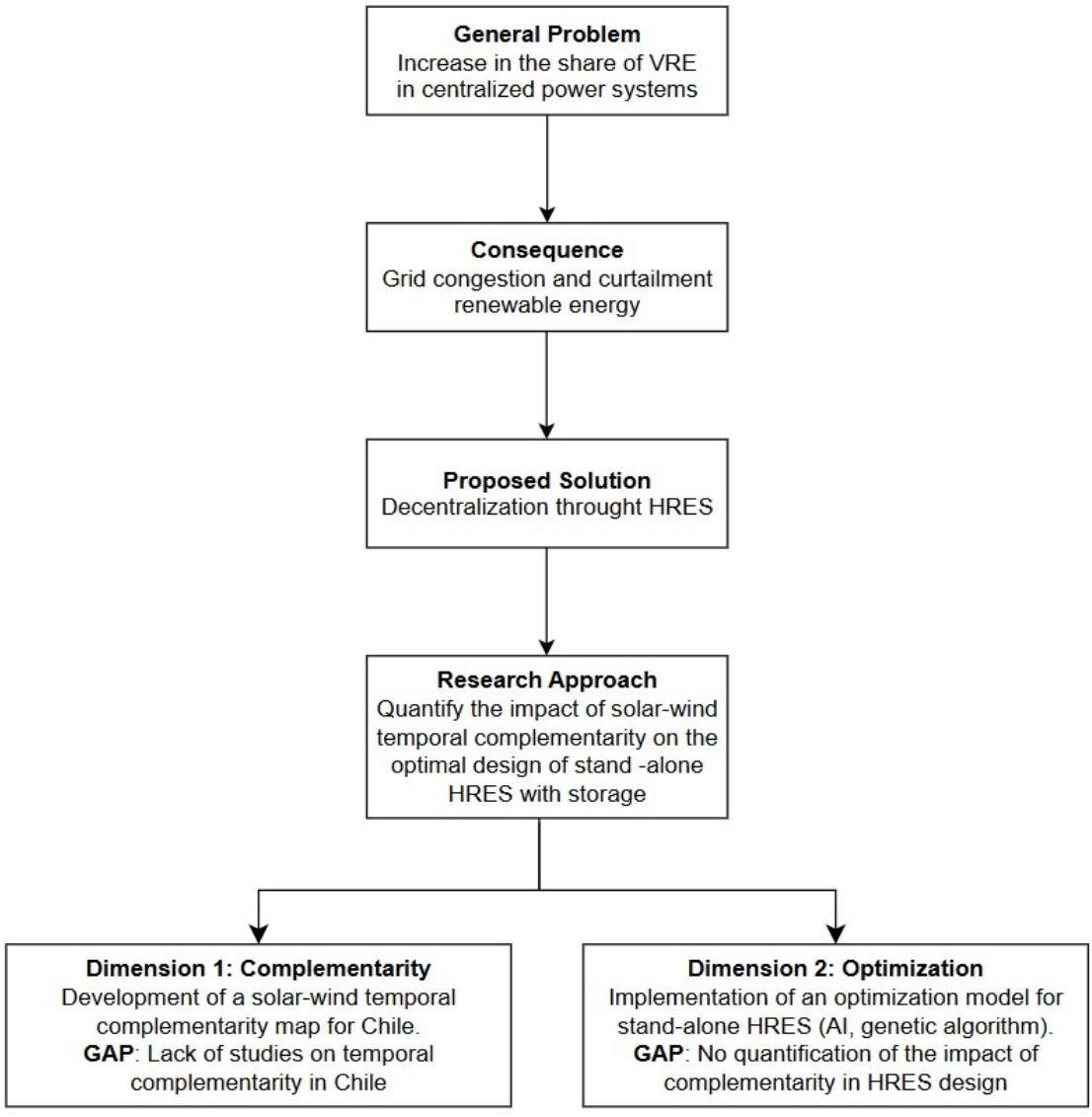

Diagram 1 Conceptual Framework of the Research
Source: Own elaboration

General Methodology

This research is structured in two complementary stages. It aims to characterize the temporal complementarity between solar and wind resources across Chile and evaluating its impact on the optimal design of stand-alone Hybrid Renewable Energy Systems, through the use of artificial intelligence techniques and statistical analysis.

Stage 1: Geospatial and statistical analysis of solar-wind complementarity: In the first stage, a quantitative characterization of the temporal complementarity between solar irradiation and wind speed is performed across 176 geographically distributed locations in Chile. Hourly data from 2004–2016, obtained from the Solar Explorer platform (Ministerio de Energía, n.d.) are used. Complementarity is measured using Spearman's rank correlation coefficient, which captures non-linear relationships between the two variables.

As a result, the locations are classified into four groups based on their level of complementarity: positive, negative, null, and moderate. This classification is represented geographically in a complementarity map, which serves as a key input for the subsequent HRES design analysis.

To validate the significance of the differences observed among zones, a statistical significance analysis is conducted through hypothesis testing and one-way ANOVA. This allows for the evaluation of whether the identified complementarity patterns are statistically distinct across regions.

Stage 2: Optimization of off-grid HRES design and statistical analysis: The second stage focuses on evaluating the impact of different levels of complementarity on the optimal design of a stand-alone HRES composed of solar panels, wind turbines, and a battery bank. The model is implemented in the GNU Octave environment and uses a genetic algorithm as a metaheuristic optimization technique. The objective is to minimize the NPC while satisfying a reliability constraint defined by the Loss of Power Supply Probability (LPSP).

Various scenarios are simulated by varying the complementarity coefficient ($\rho = -0.95$ to $\rho = 0.95$), considering two demand profiles: (1) a constant load typical of industrial processes, and (2) a variable load representative of residential communities.

The optimal number of panels, turbines, and batteries is determined for each configuration, along with key performance indicators: NPC, LCOE, LPSP, curtailed energy, and installed capacity.

This stage also includes a sensitivity analysis on three critical variables:

- Maximum allowable LPSP (%),
- Unit cost of batteries ($/kWh),
- Discount rate (%).

This enables an assessment of the system's robustness under varying technical and economic conditions.
Additionally, a second round of simulations is carried out using multiple random seeds to ensure the statistical validity of the genetic algorithm results. A one-way ANOVA is then applied to determine the significance of the differences in NPC observed under different levels of complementarity.

Expected Results and Contribution

This research is expected to provide robust quantitative evidence on the impact of temporal complementarity between solar and wind resources on the optimal design of off-grid HRES. In particular, it is anticipated that high levels of complementarity, negative correlations between solar and wind generation over time—will significantly reduce the NPC and the LCOE, by decreasing storage requirements and enhancing the joint utilization of both sources. Additionally, improvements in system reliability (lower LPSP) and reductions in curtailed energy are projected, especially in scenarios with constant demand or strict continuity-of-supply requirements.

From a methodological perspective, the thesis will contribute a reproducible energy optimization model that explicitly integrates complementarity as an input variable in HRES design. This approach will demonstrate that complementarity should not be regarded solely as a geophysical property, but as a strategic technical criterion for the efficient sizing of renewable systems in regions with variable generation profiles.

In practical terms, the results will:

- Identify areas within Chile with high solar-wind complementarity, supporting investment decisions in distributed generation.
- Provide a technical framework for territorial energy planning, particularly in remote regions or areas with low grid reliability.

- Support public policies that promote the development of decentralized, resilient, and cost-effective energy solutions.

Finally, from a scientific standpoint, this thesis aims to fill a gap in the literature regarding quantifying the effect of temporal complementarity on the techno-economic design of stand-alone hybrid systems, contributing an analytical foundation that can be replicated or extended in other geographical contexts with similar characteristics.

INTRODUCCIÓN

Contexto Global y Desafío Energético

El mundo está experimentando una profunda transformación de sus sistemas energéticos, impulsada por la urgente necesidad de abordar el cambio climático y reducir la dependencia de los combustibles fósiles. Diversos informes internacionales, como los del Panel Intergubernamental sobre Cambio Climático (IPCC, 2023), advierten que limitar el aumento de la temperatura global a 1,5 °C requiere una drástica reducción de las emisiones de gases de efecto invernadero (GEI), siendo el sector energético uno de los principales responsables (IEA, 2023).

En este contexto, la transición hacia una matriz energética basada en fuentes renovables, particularmente la energía solar fotovoltaica y eólica, se ha convertido en una prioridad estratégica global. Estas tecnologías han experimentado un rápido crecimiento debido a la disminución de sus costos, el respaldo de políticas públicas y el desarrollo de marcos regulatorios que promueven su adopción (World Economic Forum, 2024). Sin embargo, ambas fuentes comparten una característica que dificulta su integración a gran escala: su variabilidad e intermitencia temporal (Ringkjøb et al., 2020).

La generación de energía solar y eólica depende de condiciones meteorológicas locales y fluctuantes, lo que complica la gestión en tiempo real del equilibrio entre generación y demanda. Esta condición impone desafíos técnicos y económicos significativos, especialmente en sistemas eléctricos centralizados donde el almacenamiento de energía a gran escala no es económicamente viable (Hossain Lipu et al., 2025). Sin mecanismos adecuados para mitigar esta variabilidad, aumenta el riesgo de sobreinversión en capacidad instalada, vertimiento de energía (Pérez Odeh & Watts, 2019), o la necesidad de respaldo con fuentes fósiles, lo cual socava los objetivos de descarbonización (Ahmed Adam et al., 2024).

Ante este escenario, los Sistemas Híbridos de Energía Renovable (HRES, por sus siglas en inglés), que combinan múltiples fuentes renovables con sistemas de almacenamiento, han surgido como una solución técnicamente viable. Su implementación reduce la dependencia de una única fuente de energía, mejora la estabilidad del suministro y facilita la operación de sistemas eléctricos aislados o con infraestructura de transmisión limitada (León Gómez et al., 2023). Sin embargo, el diseño eficiente de estos sistemas requiere abordar desafíos complejos relacionados con el dimensionamiento óptimo, la gestión energética,

la gestión del lado de la demanda y el almacenamiento, todos ellos críticos para asegurar su viabilidad técnica y económica (Maghami & Mutambara, 2023).

Problema Específico

A pesar de los avances tecnológicos y regulatorios que han respaldado el crecimiento de las energías renovables, la integración efectiva de estas fuentes en sistemas eléctricos centralizados continúa enfrentando importantes desafíos, especialmente en países con infraestructura limitada o redes de transmisión extensas. Uno de los principales problemas es la congestión de la red (ZeroHedge, 2024), que ocurre cuando la capacidad de transmisión es insuficiente para transportar la energía generada en zonas de alta producción hacia los centros de consumo. Esto ha provocado vertimientos forzados de energía renovable, reduciendo la eficiencia general del sistema y desincentivando nuevas inversiones en generación limpia (Newbery, 2025).

Otro desafío importante es la concentración geográfica de los recursos renovables, como la energía solar en el norte de Chile o la energía eólica en el sur. Esta dependencia expone al sistema a la variabilidad estacional y a eventos meteorológicos extremos (Pérez Odeh & Watts, 2019). En Chile, esta concentración espacial, combinada con un rápido aumento de la generación renovable en ciertas regiones, ha generado un incremento sostenido en los vertimientos, incluso después de la puesta en marcha de la línea de transmisión Cardones–Polpaico en 2019. Aunque esta infraestructura mejoró la integración del sistema eléctrico nacional, la capacidad de evacuación volvió a ser superada durante las horas de máxima producción, lo que ha provocado precios marginales cercanos a cero y niveles récord de vertimiento que alcanzaron los 1.600 GWh en 2022 (Fraunhofer, 2022). Esta situación pone de manifiesto la urgencia de implementar soluciones estructurales que permitan una integración más flexible de la generación renovable, lo que implica no solo el fortalecimiento continuo de la infraestructura de transmisión y el desarrollo de sistemas de almacenamiento a gran escala, sino también — y de manera prioritaria — la adopción de un enfoque descentralizado de planificación energética que favorezca la localización estratégica de proyectos en zonas con alta complementariedad de recursos y cercanas a los centros de consumo.

En este contexto, los Sistemas Híbridos de Energía Renovable representan una solución viable, especialmente en regiones remotas o con baja conectividad. La integración de tecnologías complementarias (solar, eólica y almacenamiento)

permite una generación local descentralizada, reduce las pérdidas por transmisión y mejora la autonomía energética.

Sin embargo, la mayoría de los modelos actuales de diseño de HRES no incorporan explícitamente la complementariedad temporal entre las fuentes renovables. Esto representa una oportunidad desaprovechada para mejorar el uso combinado de los recursos, reducir el tamaño de los sistemas de almacenamiento y optimizar el desempeño técnico y económico de las soluciones propuestas (Jurasz et al., 2020). Esta limitación se vuelve especialmente crítica en contextos donde se requiere un suministro continuo de energía, como en comunidades rurales o aplicaciones industriales sensibles a interrupciones.

Justificación de la Investigación

La transición hacia una matriz energética sostenible requiere superar los desafíos de intermitencia y variabilidad asociados a los recursos solar y eólico, especialmente en sistemas fuera de red (off-grid). En este contexto, los HRES representan una alternativa prometedora al combinar fuentes complementarias con almacenamiento energético para garantizar un suministro continuo.

Sin embargo, en Chile no se han realizado estudios sistemáticos que caractericen la complementariedad temporal entre los recursos solar y eólico a nivel nacional. Por otro lado, a nivel internacional, el efecto de la complementariedad temporal de fuentes renovables sobre el diseño tecno-económico de sistemas híbridos con almacenamiento no ha sido abordado en profundidad en la literatura científica. Esta brecha de investigación resulta especialmente relevante considerando la alta penetración de energías renovables en Chile y su marcada variabilidad climática.

Además, aunque existen métricas para evaluar la complementariedad temporal, su relación con parámetros clave como el Costo Neto Actualizado (NPC), el Costo Nivelado de la Energía (LCOE), la Probabilidad de Pérdida de Suministro (LPSP) o la capacidad de almacenamiento instalada en los HRES no ha sido explorada en detalle. Asimismo, algunas de estas métricas requieren ser refinadas para captar mejor la relación entre complementariedad, confiabilidad y costo, ya que una mayor complementariedad no implica necesariamente menores costos totales del sistema (Jurasz et al., 2020).

Esta investigación se justifica tanto por sus aportes metodológicos como prácticos. En primer lugar, propone una caracterización geoespacial de la complementariedad temporal solar-eólica en Chile basada en datos horarios de

176 localidades. En segundo lugar, desarrolla un modelo de optimización para el diseño de HRES autónomos en GNU Octave utilizando algoritmos genéticos. En tercer lugar, cuantifica el impacto de distintos niveles de complementariedad sobre indicadores clave de desempeño de los HRES, entregando evidencia que puede orientar decisiones de diseño, planificación territorial e inversión en generación distribuida.

De este modo, el estudio contribuye tanto al avance científico en sistemas híbridos renovables como al desarrollo de criterios prácticos para diseñar soluciones energéticas descentralizadas, resilientes y costo-efectivas, particularmente relevantes para comunidades aisladas, aplicaciones industriales y regiones en transición energética.

Hipótesis

Un aumento en la complementariedad temporal entre fuentes de energía renovable no convencional — eólica y solar — conduce a una reducción tanto del Costo Neto Actualizado (NPC) como de la Probabilidad de Pérdida de Suministro (LPSP) en el diseño óptimo de un sistema híbrido de energía renovable autónomo (HRES) con almacenamiento.

Objetivos

Objetivo General

Evaluar la influencia de la complementariedad temporal entre fuentes de energía renovable no convencional en la reducción del NPC y del LPSP en el diseño óptimo de un HRES autónomo con almacenamiento.

Objetivos Específicos

1. Diseñar una metodología para evaluar la complementariedad energética temporal.
2. Desarrollar el primer mapa de complementariedad temporal solar-eólica para Chile.
3. Programar un algoritmo de inteligencia artificial para encontrar la solución óptima de un HRES autónomo con almacenamiento.

4. Evaluar el impacto de distintos niveles de complementariedad temporal solar-eólica en el diseño óptimo de un HRES para diversos perfiles de carga, cuantificando su influencia en la solución.

Marco Conceptual de la Investigación

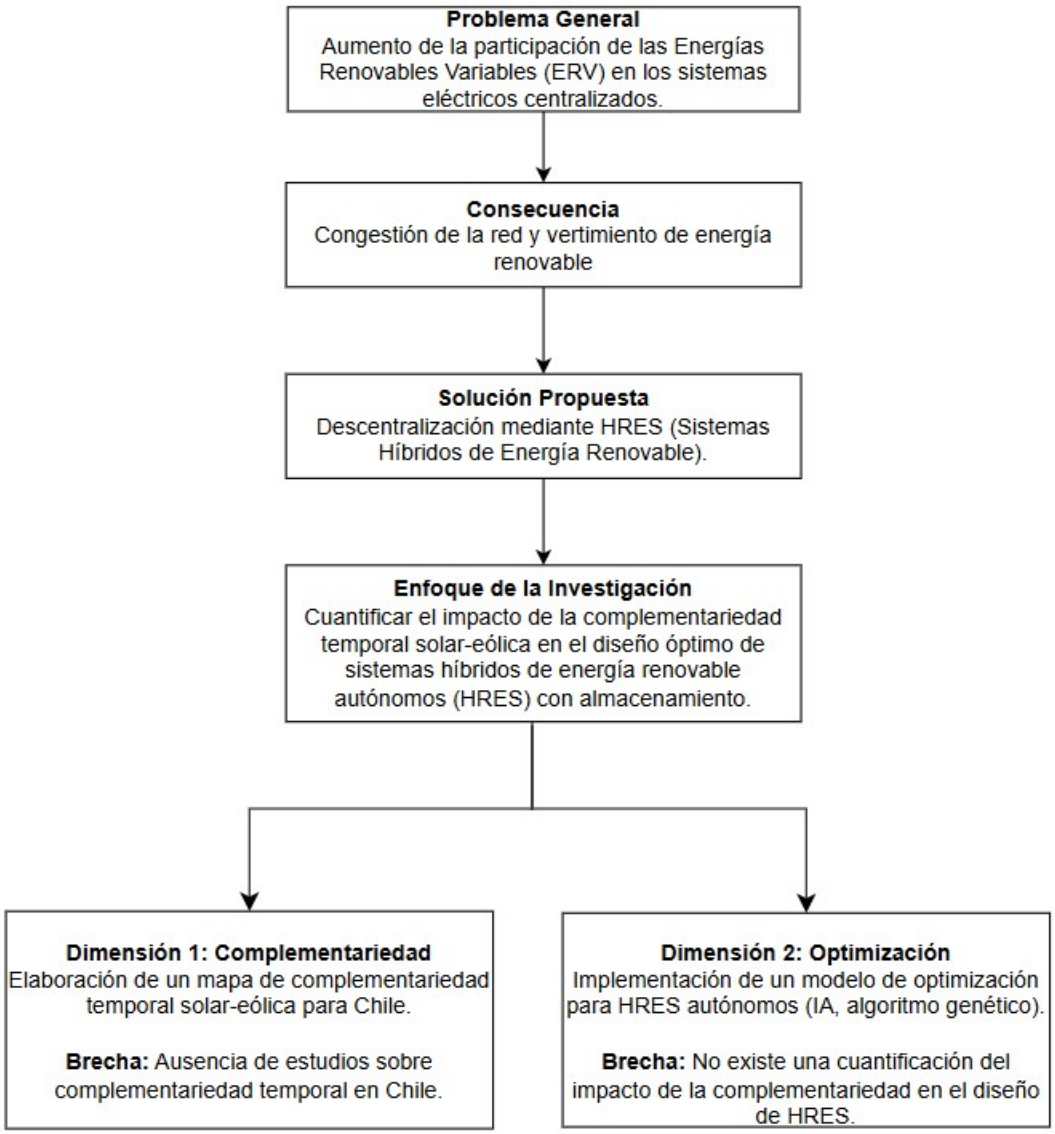

Diagrama 2: Marco Conceptual de la investigación
Fuente: Elaboración propia.

Metodología General

Esta investigación se estructura en dos etapas complementarias. Su objetivo es caracterizar la complementariedad temporal entre los recursos solar y eólico a lo largo del territorio chileno y evaluar su impacto en el diseño óptimo de Sistemas Híbridos de Energía Renovable autónomos (HRES), mediante el uso de técnicas de inteligencia artificial y análisis estadístico.

Etapa 1: Análisis geoespacial y estadístico de la complementariedad solar-eólica.

En la primera etapa se realiza una caracterización cuantitativa de la complementariedad temporal entre la irradiación solar y la velocidad del viento en 176 localidades distribuidas geográficamente en Chile. Se utilizan datos horarios del período 2004 – 2016, obtenidos desde la plataforma Solar Explorer (Ministerio de Energía, s.f.). La complementariedad se mide mediante el coeficiente de correlación por rangos de Spearman, que permite capturar relaciones no lineales entre ambas variables.

Como resultado, las localidades se clasifican en cuatro grupos según su nivel de complementariedad: positiva, negativa, nula y moderada. Esta clasificación se representa geográficamente en un mapa de complementariedad, que sirve como insumo clave para el análisis posterior de diseño de HRES.

Para validar la significancia de las diferencias observadas entre zonas, se realiza un análisis estadístico mediante pruebas de hipótesis y análisis de varianza unidireccional (ANOVA). Esto permite evaluar si los patrones de complementariedad identificados son estadísticamente distintos entre regiones.

Etapa 2: Optimización del diseño de HRES autónomos y análisis estadístico:

La segunda etapa se centra en evaluar el impacto de distintos niveles de complementariedad en el diseño óptimo de un HRES autónomo compuesto por paneles solares, aerogeneradores y un banco de baterías. El modelo se implementa en el entorno GNU Octave y utiliza un algoritmo genético como técnica de optimización metaheurística. El objetivo es minimizar el Costo Neto Actualizado (NPC), cumpliendo con una restricción de confiabilidad definida por la Probabilidad de Pérdida de Suministro (LPSP).

Se simulan diversos escenarios variando el coeficiente de complementariedad ($\rho=-0{,}95$ a $\rho=0{,}95$), considerando dos perfiles de demanda: (1) una carga

constante típica de un proceso industrial, y (2) una carga variable representativa de comunidades residenciales.

Para cada configuración se determina el número óptimo de paneles, turbinas y baterías, junto con los indicadores clave de desempeño: NPC, LCOE, LPSP, energía vertida y capacidad instalada.

Esta etapa también incluye un análisis de sensibilidad sobre tres variables críticas:

- Límite máximo permitido de LPSP (%),
- Costo unitario de las baterías (US$/kWh),
- Tasa de descuento (%).

Esto permite evaluar la robustez del sistema bajo condiciones técnicas y económicas variables.

Adicionalmente, se realiza una segunda ronda de simulaciones utilizando múltiples semillas aleatorias para asegurar la validez estadística de los resultados del algoritmo genético. Posteriormente, se aplica un análisis de varianza unidireccional (ANOVA) para determinar la significancia de las diferencias observadas en el NPC bajo distintos niveles de complementariedad.

Resultados Esperados y Contribución

Se espera que esta investigación entregue evidencia cuantitativa sólida sobre el impacto de la complementariedad temporal entre los recursos solar y eólico en el diseño óptimo de sistemas híbridos de energía renovable autónomos (HRES). En particular, se anticipa que altos niveles de complementariedad — es decir, correlaciones negativas entre la generación solar y eólica a lo largo del tiempo — reducirán significativamente tanto el Costo Neto Actualizado (NPC) como el Costo Nivelado de la Energía (LCOE), al disminuir los requerimientos de almacenamiento y mejorar la utilización conjunta de ambas fuentes. Asimismo, se proyectan mejoras en la confiabilidad del sistema (menores valores de LPSP) y reducciones en la energía vertida, especialmente en escenarios con demanda constante o exigencias estrictas de continuidad de suministro.

Desde una perspectiva metodológica, la tesis aportará un modelo de optimización energética reproducible que integra explícitamente la complementariedad como una variable de entrada en el diseño de HRES. Este enfoque permitirá demostrar

que la complementariedad no debe considerarse únicamente como una propiedad geofísica, sino también como un criterio técnico estratégico para el dimensionamiento eficiente de sistemas renovables en regiones con perfiles de generación variables.

En términos prácticos, los resultados permitirán:

- Identificar zonas dentro de Chile con alta complementariedad solar-eólica, apoyando decisiones de inversión en generación distribuida.
- Proporcionar un marco técnico para la planificación energética territorial, particularmente en regiones remotas o con baja confiabilidad de red.
- Respaldar políticas públicas que promuevan el desarrollo de soluciones energéticas descentralizadas, resilientes y costo-efectivas.

Finalmente, desde una perspectiva científica, esta tesis busca llenar una brecha en la literatura relacionada con la cuantificación del efecto de la complementariedad temporal en el diseño tecno-económico de sistemas híbridos autónomos, contribuyendo con una base analítica que pueda ser replicada o extendida en otros contextos geográficos con características similares.

CHAPTER 1

Chapter 1 addresses this thesis's first and second specific objectives by presenting a geographic characterization of the temporal energy complementarity between wind and solar sources across continental Chile. The content is organized in the format of a scientific article, including an introduction, literature review, methodology, results, statistical analysis, and conclusions.

This chapter addresses the three research questions:

i) What is the degree of temporal complementarity between solar and wind resources in the different regions of Chile?

ii) How does this complementarity vary over time?

iii) Which areas exhibit a synergistic behavior that allows for a more efficient integration of both resources?

A Python-based program processed more than 40 million hourly data points of solar irradiance and wind speed, corresponding to 176 locations throughout the country. Complementarity was measured using Spearman's rank correlation coefficient, and the results were graphically represented through maps generated with ArcGIS Pro software.

One of the maps also includes protected areas defined under Law No. 21,600, allowing the identification of regions with energy potential where projects could be developed in alignment with conservation criteria. The analysis covers the 2004 - 2016 period and captures possible interannual variations.

Four zones with different levels of complementarity were identified. To assess the consistency of the results, significance tests were applied to each point and mean tests by zone were conducted. Statistically significant correlations were found in 167 out of the 176 analyzed locations.

This chapter provides an analytical tool that serves as input for energy planning processes and the design of distributed HRES in Chile.

1 Temporal Complementarity Analysis of Wind and Solar Power Potential for Distributed Hybrid Electric Generation in Chile.

Article published in the journal Energies:

Muñoz-Pincheira JL, Salazar L, Sanhueza F, Lüer-Villagra A. Temporal Complementarity Analysis of Wind and Solar Power Potential for Distributed Hybrid Electric Generation in Chile. *Energies*. 2024; 17(8):1890. https://doi.org/10.3390/en17081890

Abstract

We evaluate the temporal complementarity in daily averages between wind and solar power potential in Chile using Spearman's correlation coefficient. We used hourly wind speed and solar radiation data for 176 geographic points from 2004 to 2016. The results allow us to identify four zones: Zone A1 in the coast and valleys in the north of Chile between latitudes 18°S and 36°S, with moderate positive correlation; Zone A2 in the north Andes between latitudes 25°S and 33°S, with weak negative correlation; Zone B in the center-south part of the country between latitudes 36°S and 51°S with moderate negative correlation; and Zone C in the south, between latitudes 51°S and 55°S with null or weak positive correlation. On the one hand, the interannual analysis shows that Zone A1 keeps uniform correlation values with negative asymmetry, i.e., higher correlation values. On the other hand, there is positive asymmetry in most the years in Zone A2, i.e., lower (or negative) correlation values. Zone B shows an interannual oscillation of the median correlation, while Zone C shows a larger dispersion in the interannual results. Significance analysis shows that 163 out of the 176 points are statistically significant, while Zones A1, A2, and B have significant correlations, with Zone C being marginally significant. The results obtained are relevant information for further studies on the location of hybrid generation facilities. We expect our methodology to be instrumental in Chile's energetic transition to a 100% renewable generation matrix.

Keywords: Energy complementarity; hybrid distributed generation; HRES; Spearman's correlation coefficient; wind power potential; solar power potential; Chilean energy transition

1.1 Introduction and literature review

There is abundant empirical evidence that shows the increase in mean global temperature on our planet is attributed mainly to the emission of greenhouse effect gases and is significantly caused by human activities, such as the combustion of fossil fuels (IPCC, 2023). Because of this, multiple countries have signed the Paris Agreement (ONU, 2015), committing to modify their electric energy generation matrices. This change aims to transition towards more sustainable and less pollutant energy sources to mitigate the impact of climate change, together with meeting the global emission reduction goals.

The current trend in energy transition is moving from fossil fuels to renewable energy sources, such as photovoltaic solar and wind. This trend has been pushed forward by the constant reduction in the costs of renewable technologies, the expansion of energy markets, and the development of public policies promoting the transformation in the energy generation sector. It has been estimated that following the global policies, a 7,5 Gigaton of equivalent CO_2 will be achieved by 2030, according to the latest update on the roadmap to achieve zero net emissions (IEA, 2023). The change towards solar and wind energy is expected to account for 5 Gt.

Chile, as a country, has the goal of having a completely renewable electric energy generation matrix by 2030. By this time, all the thermoelectric plants using coal are expected to have ceased operation. The country aims to duplicate the current variable renewable energy (VRE) generation capacity, such as photovoltaic solar and wind, from 12 Gigawatts (GW) to 24 GW by 2030, which is about 55% of the total projected installed capacity (Coordinador eléctrico nacional, 2022). Given the variable nature of solar and wind sources, a significant increase in the storage capacity is expected, reaching about 13.2 GW by 2026. This increase will focus on using battery-based energy storage (BESS) in northern Chile.

Table 1-1 shows the current electric energy installed generation capacity for the central electric system in Chile (SEN). Variable renewable energy sources (VRE), such as solar photovoltaic and wind, have about 25.2% and 13% shares, respectively (Generadoras de Chile, 2023). It is expected that VRE will increase its share up to 55% by 2030, and the total share of renewable energy sources will increase from 63.5% to 100% in the same period (Coordinador eléctrico nacional, 2022), as **Fig 1-1** shows.

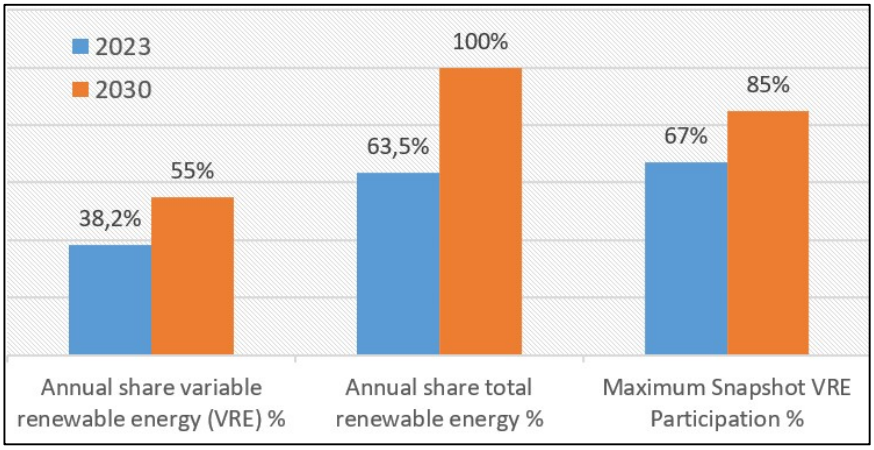

Fig 1-1 Renewable energy projection for Sistema Eléctrico Nacional (SEN), data from (Coordinador eléctrico nacional, 2022)

Most of the production in Chile is devoted to mining. Chile is the world's largest copper producer and the second largest for lithium. The transition to renewable energy sources would decrease the uncertainty in the supply by reducing the dependence on fossil energy sources, which Chile must import. Furthermore, from the environmental perspective, this energy transition will allow Chile to reduce its carbon footprint, contributing to reducing the emission of greenhouse effect gasses.

Table 1-1 *Installed electric energy generation capacity, (SEN, 2023).*

Technology	Power (MW)	% Total
Photovoltaic	8,292	25.2%
Wind	4,270	13%
Run-of-the-river hydroelectricity	4,002	12.2%
Dams	3,501	10.6%
Biofuel	597	1.8%
Solar thermal	114	0.3%
Geothermal	95	0.3%
Renewable	***20,871***	***63.5%***
Coal	4,595	14%
Natural gas	3,873	11.8%
Derived from oil	3,541	10.8%
Thermal	***12,009***	***36.5%***
Total	***32,880***	

Source: Report of Chilean generators, September 2023.

The transition towards a 100% renewable electric generation matrix with a high share of VRE implies excellent challenges that must be solved. In the energy section, generation must meet the demand at every moment, and energy cannot be stored on a large scale. Both photovoltaic and wind sources are by nature, variable and are known to have non-manageable generation. The geographical concentration of VRE plants to take advantage of solar and wind potentials generates congestion in the transmission systems. This congestion creates energy dumping and distortions in the price of energy, causing disinterest in new-generation investments (Pérez Odeh & Watts, 2019).

Multiple alternatives to mitigate the problems of using VRE in the generation matrix have been proposed, mainly oriented to the demand, i.e., changing the users' behavior, and the offer, i.e., generation.

1.1.1 Demand

Demand can be satisfied by augmenting energy efficiency to avoid expanding the generation capacity of the VREs. In 2021, the Chilean Energy Minister created a Law and National Plan for Energy Efficiency to reduce the energy intensity by 10% by 2030. The plan considers residential energy efficiency, labeling electric devices according to efficiency, and increasing efficiency in buildings, transport, and productive sectors (Ministerio de energía, Gobierno de Chile, 2022). Outside Chile, the report "The evolution of energy efficiency policy to support clean energy transitions" from (International Energy Agency, 2023) indicates that energy efficiency is the first step towards a renewable electric energy generation matrix that reduces the emission of greenhouse effect gasses, increases the energy security and decreases the energy consumption costs. Another way to influence the users is to adjust the generation demand curve (offer curve) through pricing. This strategy implies the implementation of a smart grid in the system and modifying the electric market. A relevant example of this is the model proposed by the Arabic government of using intelligent energy, (tele)communication, and intelligent information systems, considering projects oriented to innovation, the development of human resources, and industrial viability (Khan et al., 2023).

1.1.2 Offer

From the point of view of the offer, there is also a set of solutions to meet the demand, considering the generation variability of VRE. We highlight the following:

1.1.2.1 Increase in the VRE generation capacity

The generation variability can be decreased by increasing the photovoltaic and wind generation to cover the demand peaks, or storing the over-generation *for later use*. (Rey-Costa et al., 2023), for the Australian electric market, that the decrease in the costs of photovoltaic and wind electric generation technologies allows 100% renewable generation systems to be economically viable. To meet the demand, the installed capacity must be four times the demand if no energy storage is considered, reducing the current generation cost by 28% or if energy storage is considered, by 55%, compared with the current prices.

1.1.2.2 Increase in storage capacity

Adding storage using different technologies and autonomy scales implies increased investment costs. Still, it is a way to solve the VRE generation variability problem. An alternative solution is deploying energy storage systems shared by multiple renewable energy sources in different locations. (Song et al., 2023) argues that this strategy may reduce infrastructure costs while enabling a high penetration of renewable energy sources in the system. In (Auguadra et al., 2023), the authors conclude that energy storage is crucial for transforming the energy matrix toward renewable energy sources for the Spanish generation system. They suggest green hydrogen as a possible technology for energy storage towards a 100% renewable generation matrix.

1.1.2.3 Efficiency improvements in VRE generation

The increase in efficiency of photovoltaic panels and wind turbines implies a larger *electric energy generation* for the same installed capacity. The efficiency of a photovoltaic panel depends on parameters such as dust, reflection, inclination angle, orientation, shadows, radiation, and temperature. Such efficiency is around 6% and 20%. Recent studies point out that one of the parameters that affects the efficiency of photovoltaic panels the most is temperature, depending on the kind of cooling added to the panel (Akrouch et al., 2023).

1.1.2.4 Distributed hybrid generation

Its configuration uses two or more energy generation sources and one or more storage energy systems located in the same geographical location, which can generate and consume energy. **Fig 1-2** shows a distributed hybrid generation configuration with “s” storage systems, probably of different kinds, such as lead-acid, lithium, green hydrogen batteries, etc. The system receives energy from “m” resources, either solar, wind, hydro, etc. (Al Sumarmad et al., 2022). The systems

also receive energy from “n” diesel or other fuel generators. Finally, the energy supplied is used to serve the demand, where the excess energy is either stored or sent to a central system, which may also provide energy to this configuration.

When a hybrid generation system is not connected to a central system, it is denoted as an isolated hybrid generation system, requiring storage if the energy source is a VRE. Distributed generation has several advantages, compared with a centralized system, because generation may be closer to the consumption points, reducing the transmission losses, favoring the use of VRE, and thus reducing the emission of greenhouse effect gases. The resulting configuration is named a hybrid renewable energy system (HRES) if the sources are renewable. Distributed hybrid generation may improve the system's performance in meeting the demand compared to a centralized generation system when sources are VRE sources.

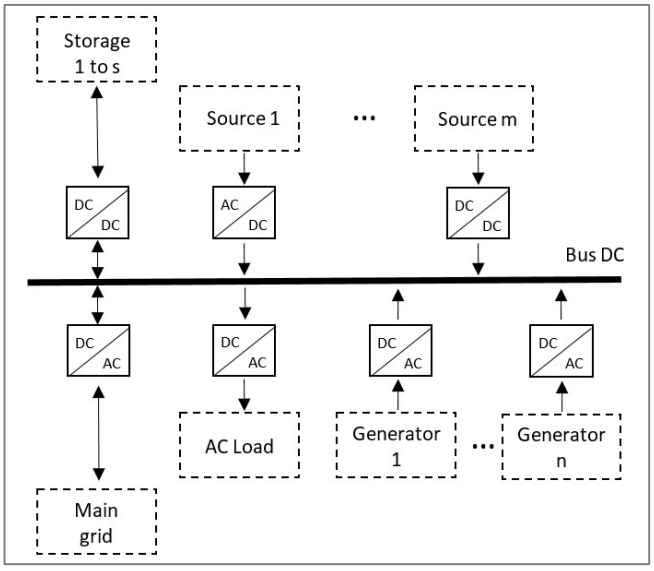

Fig 1-2 A distributed hybrid generation configuration.
Figure adapted from (Al Sumarmad et al., 2022).

Numerous studies have been conducted on optimizing HRES in terms of these systems' design, scheduling, and operation. For example, (Kharrich et al., 2023) present an algorithm to optimize the design of an HRES with photovoltaic panels, wind turbines, diesel generators and a battery energy storage system (BESS) to minimize the NPC. They consider the renewable fraction index, the probability of interruption of the energy supply and availability. The algorithm obtains a levelized

energy cost of 0.213 $/kWh, concluding on the role of storage as a management tool and the importance of the synergy between photovoltaic and wind systems. The authors (Naderipour et al., 2022) present a multicriteria model for a hybrid system with photovoltaic, wind, and batteries connected to the network, considering the components' costs, energy buying from the network, and CO_2 emissions. They consider a reliability constraint in terms of the probability of unsupplied energy. To solve the model, they use an artificial electric field algorithm that designs the components of the HRES. They compare two scenarios, connected and disconnected from the electric network, finding that the connected design achieves between 7% and 10% more reliability. The authors (Agajie et al., 2023) show a complete review of the state-of-the-art optimal sizing of HRES, considering the components, parameters, and methods used. They conclude that sizing HRES requires using multiple objectives, such as reliability, costs, and emissions. They also note that using metaheuristics is more efficient than other approaches.

1.1.2.5 Energy sources complementarity

The degree of association between two or more energy resources. Suppose the energy resource availability is variable in time, such as in wind and solar energy. In that case, it is essential to quantify this relationship to make proper decisions to meet the demand required by the system. In general terms, if the resources are in the same geographic region, it is denoted by temporal complementarity, and if not, it is spatial complementarity.

(Jurasz et al., 2020a) present different ways to quantify the complementarity through metrics (Pearson's correlation coefficient, Spearman's and Kendall's range correlation coefficients, autocorrelation, cross-correlation, etc.) and indices (of complementarity through wavelets, temporal complementarity index, etc.) Other authors (Pedruzzi et al., 2023) review different methodologies, techniques, and wind and solar datasets to evaluate complementarity. After they analyzed different metrics and indices, they concluded that there is neither a unique standard nor a common methodology for assessing energy complementarity.

Fig 1-3 explains the concept of correlation coefficients for two resources whose availability is variable in time in three different scenarios. In Scenario (a), both resources have unit correlation (CC=1), meaning that both resources increase and decrease simultaneously and have their extremes simultaneously. In this scenario, there will be periods with energy deficit and surplus. In scenario (b), both resources are not correlated (CC=0), where their extremes do not happen

simultaneously, implying different deficit and surplus periods. In scenario (c), there is a negative correlation, meaning that both resources are complementary, where the maximum of one coincides in time with the minimum of the other, making it possible to meet the demand without deficit or surplus.

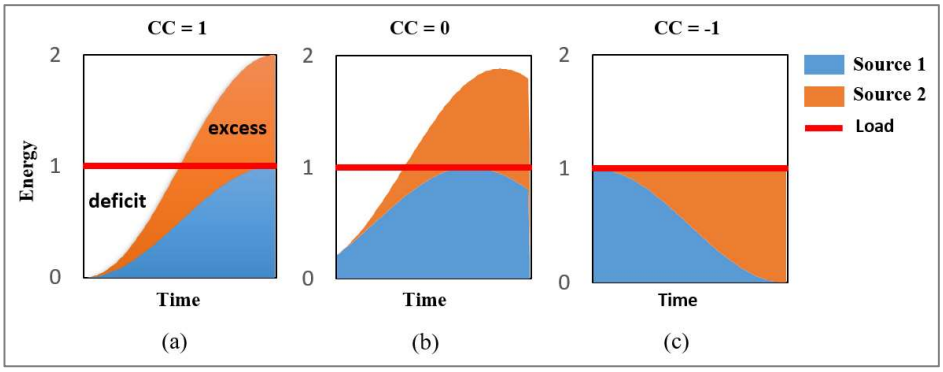

Fig 1-3 Conceptual explanation of correlation coefficient, adapted from (Jurasz et al., 2020a)

Given that energy complementarity is a relevant tool for defining, quantifying, and optimizing variable renewable resources for electric energy generation, multiple authors have studied complementarity in different regions and countries.

In Mexico, (Gallardo et al., 2020) performed a study on the wind-solar temporal complementarity using Pearson's correlation coefficient for all the Mexican territory using daily solar radiation and wind speed averages. They found that there are zones with good energy complementarity in the north-central zone of the country, together with specific zones in the southeast. (Magaña-González et al., 2023) find similar results using Spearman's coefficient to evaluate wind-solar complementarity, concluding that the north-central, northeast, and Baja California peninsula have good complementarity potential during summer. They also conclude that the Yucatán peninsula has significant energy complementarity during the year, making the location of wind parks in the sea beside photovoltaic energy on the coast. In North America, (Costoya et al., 2023) evaluate the wind-solar complementarity by evaluating different future climatic scenarios for the range between 2025 and 2054, including new indices to measure t complementarity. The results indicate that the greatest complementarity is in the coastline of Mexico's Gulf, some parts of the Caribbean Sea, and the oceanic region west of Mexico and the frontier between the United States of America and Canada.

For China, (Guo et al., 2023) evaluate wind-solar spatial complementary, proposing a new measurement model of complementarity. The results suggest that northern China has strong energy complementarity, increasing over time. Similarly, (Ren et al., 2019) studied the Chinese territory using Kendall's coefficient to evaluate both temporal and spatial complementarity of wind-solar resources. They use the hourly data of wind speed and solar radiation obtained from MERRA-2 (Gelaro et al., 2017) with 0.625° and 0.5° of longitude and latitude spatial resolution for five years, respectively. They conclude that wind energy is complementary with photovoltaic energy for every temporal scale in the maritime regions. Inside the country, the correlation varies from positive in the south to negative, i.e., complementarity, in the north. They suggest that wind parks must be scattered in future projects in regions with positive correlations. The authors finally note that each province in China owns independent wind-solar generation projects that should be optimized in a centralized way to assess energy complementarity.

In Portugal (Couto & Estanqueiro, 2021) evaluate the wind-solar complementarity to optimize energy generation by wind parks. They use information from 224 wind parks and, hourly wind speed, and solar radiation data from 2015 and 2016 for places near the parks. Their results indicate that wind and solar resources are complementary, and they propose to develop hybrid plants from the existing wind parks.

Different energy complementarity studies have been performed in Brazil. (Nogueira et al., 2023) evaluate the complementarity between the maritime wind resources and those that supply energy to the Brazilian electric system, such as photovoltaic, hydro, and thermal. Their analysis uses Pearson's coefficient with hourly data obtained from MERRA-2 and the national system operator. They conclude that, considering the increasing demand projection, adding maritime wind energy is an excellent complement to hydroelectric power. They also conjecture that it may help, in the long term, to reduce seasonal variability and possible impacts of droughts. (Fernandes et al., 2022) perform a temporal and spatial complementarity analysis for wind-solar resources on the northeast coast of Brazil, using a non-dimensional temporal complementarity index proposed by (Beluco et al., 2008). They used wind speed and solar radiation time series from 2004 to 2014. They obtain temporal and spatial complementary maps, identifying high-complementarity areas. They expect these maps to help plan future wind parks and photovoltaic plants. (Cantão et al., 2017) evaluate temporal and spatial complementarity between hydro and wind resources for Brazil, creating correlation maps based on Voronoi diagrams. The study shows that the wind

correlation has a sizeable temporal similarity for the whole Brazilian territory and that spatial complementarity is larger than temporal complementarity.

In Colombia, (Cantor et al., 2022) analyze the wind-hydro energy complementarity for the energy supplied to the Colombian electric market. The authors indicate that correlation coefficients are not the best way to evaluate complementarity. They propose three new metrics: total variation complementarity index, variance complementarity index, and standard deviation index. Because of Colombia's dependence on hydroelectric generation, the authors (Henao et al., 2020), performed a complementarity study between runoff, precipitation, solar radiation, and wind speed on an annual and interannual scale. Their results show that wind and solar resources complement the hydroelectric sector, being an excellent alternative to electricity generation for periods of drought.

Two works are particularly relevant for Latin America. (Gonzalez-Salazar & Poganietz, 2021) evaluate the wind-solar and hydroelectric complementarity to mitigate the impact of El Niño (ENSO), based on data from the twentieth century and the relationship with different ENSO phases. The study concludes that adding 136 GW of solar and wind energy in locations with high complementarity may compensate for the variations in hydroelectric energy production due to ENSO. (Viviescas et al., 2019) evaluate the wind-solar complementarity and the impact of climate change on these resources for Latin America. They conclude that Brazil may be relevant in integrating wind-solar resources due to its good spatial complementarity with other countries. They also concluded that climate change may significantly negatively affect energy complementarity towards the end of the present century.

To the best of our knowledge, Chile has no temporal complementarity studies of variable renewable sources. There is work on spatial complementarity, like (Pérez Odeh & Watts, 2019), that evaluates the wind-solar-hydro spatial complementarity, concluding that spatial diversification has a solid and positive impact on the renewable energy market. From a different perspective, (Garcia G. & Oliva H., 2023) evaluate technically, economically, and in terms of CO_2 emissions a hybrid wind-solar plant to generate green hydrogen. The study is performed in four places in Chile without considering the energy complement, but even in these cases; they obtain results of competitive hydrogen prices. (Camargo et al., 2019) developed a model to size hybrid wind-solar resources with storage of 1MWh on the Chilean continental territory. They show that the capacity required for the hybrid system to obtain constant generation rates is very high. (Vargas-Ferrer et al., 2022) present a methodological framework for the long-term planning of inserting non-conventional renewable sources with low carbon emissions into the Chilean energy matrix. Their results indicate that hybrid generation is required

to achieve 90% renewable electric generation by combining hydroelectricity and solar concentration plants with thermal and battery energy storage, pumping storage, and electric generators moved by natural gas.

According to the literature review, multiple studies have analyzed the temporal complementarity between solar and wind energy sources in various countries, such as the United States, Mexico, China, Brazil, and members of the European Union. However, no studies of this kind with national coverage have been identified for the case of Chile, despite its high potential in both resources and its goal of achieving a 100% renewable electricity matrix by 2030. In this context, relevant research questions remain unaddressed, such as: i) what is the degree of temporal complementarity between solar and wind resources in the different regions of Chile?, ii) how does this complementarity vary over time?, and iii) which areas exhibit a synergistic behavior that allows for a more efficient integration of both resources?.

In line with these questions, the main objective of this study was to evaluate the temporal complementarity between wind and solar potential in Chile, using Spearman's correlation coefficient applied to hourly irradiance and wind speed data from 2004 to 2016. Additionally, georeferenced complementarity maps were generated to spatially visualize the areas with different levels of complementarity between both sources, providing a concrete tool for the efficient design of hybrid systems and strategic decision-making in the Chilean energy sector.

1.2 Methodology

We developed a methodology to evaluate the wind-solar complementarity at a national scale. This is particularly relevant for the Chilean case because it has not been done before, and it is a vital tool to support the decision regarding the presence of renewable energy sources in the Chilean energy matrix.

Our case study considers the hourly data of wind speed and solar power potential from 2004 to 2016 obtained from the database "Explorador Solar" (Molina et al., 2017) for each of the 176 geographical points under study, corresponding to all available data. For each point, it creates a time series with 113,880 elements.

Then, we compute the daily average radiation, in W/m^2, and average wind speed at 100 m. Then, the average wind potential, in W/m^2, is computed. After that, temporal complementarity is calculated using Spearman's correlation coefficient, computed for the respective solar and wind power potential time series. We use Spearman's because it is a non-parametric estimator of the intensity of the

relationship, perhaps non-linear, of two variables (Santabárbara, 2019). Our methodology, also shown in **Fig 1-4**, is the following.

Step 1: Beginning with the geographic map provided by the Chilean Militar Geographic Institute (Instituto Geográfico Militar de Chile) (IGM, n.d.), which uses a 25 km x 25 km grid. The measurement point selection is like (Zhang et al., 2016), where wind speed measurement points are separated by 1/4 degrees of latitude and 1/3 degrees of longitude.

We select points 50 km away in longitude and 100 km in latitude, obtaining 176 points covering the whole continental Chile territory. Each point is composed of an ID and its longitude and latitude.

Step 2: For each point obtained, we extract from "Explorador Solar" the hourly time series for solar radiation and wind speed at 5.5 meters from 2004 to 2016. "Explorador Solar" is a public database of superficial solar irradiance for Chile based on data obtained from a radiative transference irradiance model for clear skies and an empiric model from geostationary satellites for cloudy days. The mean percentage error of the model in the hourly time series of global horizontal irradiance is 0.73% (Molina et al., 2017).

Step 3: We then pre-process the resulting around 40 million values. If a point lacks information, it is computed interpolating two neighboring points.

Step 4: A usable database of hourly solar radiation and wind speed at 5.5 m from 2004 to 2016 is obtained on 176 geographical points selected in Step 1.

Step 5: The daily averages of solar radiation and wind speed at 5.5 m are computed using the Python programming language,. The pseudocode of this step and the following is shown in Algorithm 1.

Step 6: We compute the daily wind speed average at 100m using Hellman's exponential law for each day considered.

$$V_h = V_i * \left(\frac{h}{i}\right)^{\propto} \tag{1.1}$$

Where:

i: 5.5 m

h: 100 mm

V_i: wind speed at 5.5 m

V_h: wind speed at 100 m

α : Hellman's exponent, depending on the terrain rugosity.

Table 1-2 shows the different values considered for each point in the case study.

Algorithm 1. *Pseudocode to compute the daily averages of solar radiation and wind power.*

```
Receives:
  Points (set of points to study)
  vel (hourly 5m wind speed time series)
  ghi (hourly solar power time series)
Days ← ObtainDaysFromTimeSeries(vel, ghi)
Years ← ObtainYearsFromDays(Days)
for day in Days:
  for point in Points:
    Pot100m_eol[day, point] ← EstimatewindPower(vel[day,cell])
    meanPot100m_eol[day, point] ← ComputeDailywindPower(Eol_100m, day, ce point ll)
    meanGhi[day, point] ← ComputeDailySolarPower(ghi, day, point)
for point in Points:
  for year in Years:
    windPowerTimeSeriesYear ← windPowerTimeSeriesOfYear(meanPot100m_eol, point, year)
    SolarPowerTimeSeriesYear ← ExtractSolarPowerTimeSeriesOfYear(meanGhi, point, year)
    Spearman[point, year] ← computeSpearman(windPowerTimeSeriesYear,
SolarPowerTimeSeriesYear)
Returns:
  Spearman (the Spearman's rank correlation coefficient for each point and year)
```

Table 1-2 *Values of Hellman's exponent for different points of the area of study, based on information provided in (Wiernga, 1993).*

Point	α value	Kind of terrain
1 - 37	0.005	A featureless land with negligible cover
38-63	0.03	Flat terrain with grass or shallow vegetation.
64-83	0.1	Cultivated area, low crops, occasional obstacles separated by more than 20 obstacle heights H.
84-176	0.5	Heavily used landscape with open spaces = 10H, bushes, low orchards, Young dense forest

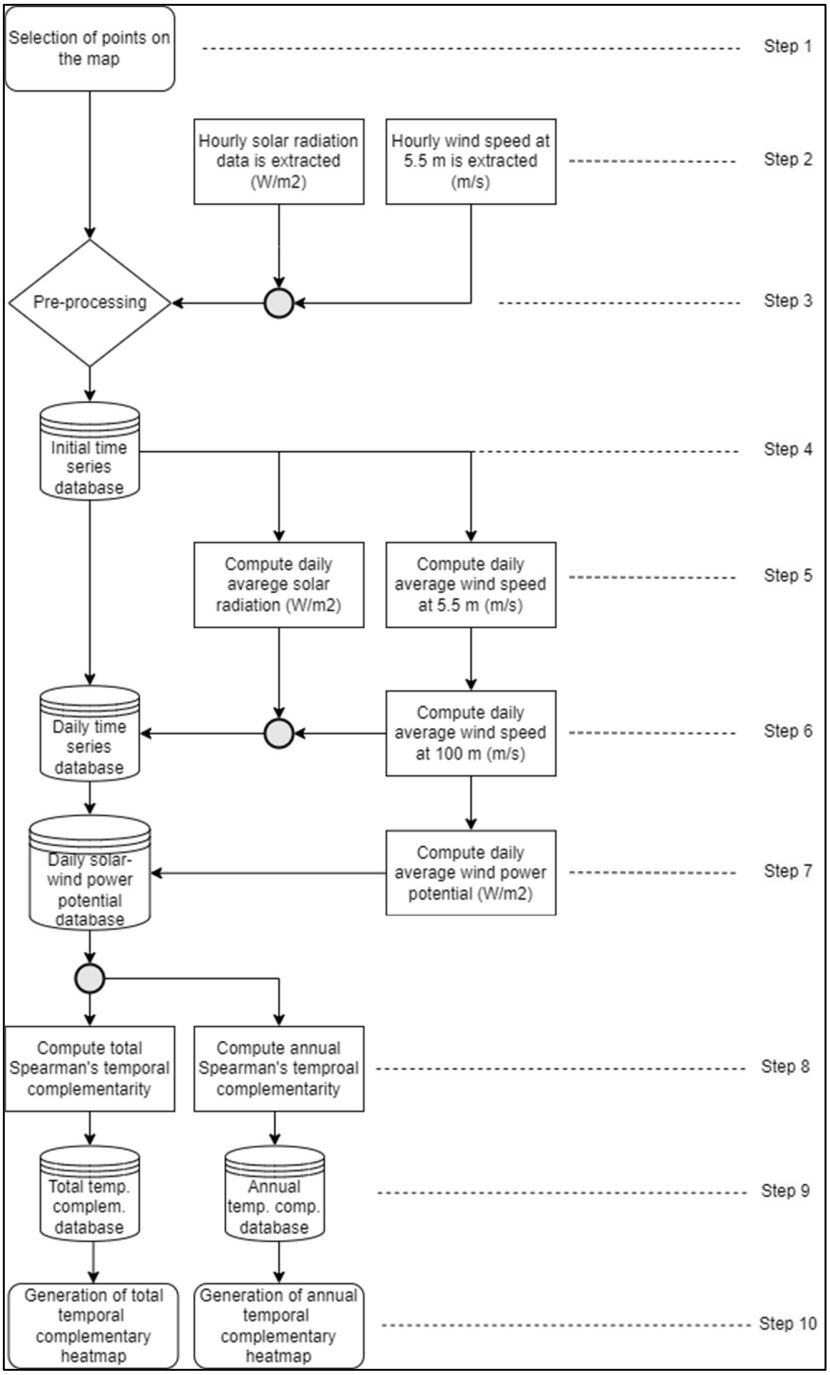

Fig 1-4 Flowchart of our methodology to evaluate temporal wind/solar complementarity Source: Own elaboration.

.

Step 7: Based on the daily average of wind speed at 100 m, we compute the daily average of wind potential in W/m^2, making comparable the wind and solar sources, based on the following expression,

$$\frac{P_e}{A} = \rho * V^3 \quad (1.2)$$

Where:

P_e/A: Daily average wind power potential (W/m^2)

ρ : air density (1,12 kg/m^2)

V: Daily average wind speed at 100 m (m/s)

Step 8: We use Spearman's correlation coefficient (Canales & Acuña, 2022) to calculate the temporal complementarity of each point's daily time series of wind and solar power potential from 2004 to 2016. To categorize correlation, we use the interpretation given in **Table 1-3**. We also compute this for the daily time series for each year. For further reference, equations 1.3 and 1.4 compute Spearman's coefficient.

$$\rho_s = 1 - \frac{6*S(d^2)}{T(T^2-1)} \quad (1.3)$$

$$S(d^2) = \sum_{t=1}^{T}\left[R\left(g_t^j\right) - R(g_t^k)\right]^2 \quad (1.4)$$

Where:

ρ_s: Spearman's correlation coefficient

$R\left(g_t^j\right)$: Range of resource *j* (average daily wind power) in day *t*

$R\left(g_t^k\right)$: Range of resource *k* (average daily solar power) in day *t*

T: Number of days considered in the analysis (4765 and 365 days, respectively)

S(d^2): Sum of range differences

Table 1-3 *Correlation coefficient interpretation. Adapted from (Santabárbara, 2019).*

Correlation	Interpretation	Kind of complementarity
-1 a -0.7	Strong negative	Strong complementarity
-0.7 a -0.3	Moderate negative	Moderate complementarity
-0.3 a 0	Weak negative	Weak complementarity
0	No relationship	No relationship
0 a 0.3	Weak positive	Weak correlation
0.3 a 0.7	Moderate positive	Moderate correlation
0.7 a 1	Strong positive	Strong correlation

Step 9: We obtain multiple databases: one for the average daily wind-solar temporal complementarity and one for each year from 2004 to 2016.

Step 10: The numerical results are then imported into ArcGIS Pro (ESRI Chile, 2024) to generate heat maps from the total and annual complementarity results.

Our methodology has some desirable properties, like the ease of obtaining new results if new or better information on wind speed or solar radiation is available and the possibility of providing graphical representations.

It also has some limitations and potential measurement errors. First, it aggregates information to points in the study area, adding potential errors to the model. Second, it is not dynamic, i.e., it does not prescribe or project its results to the future based on the present and past. Third, it is not guaranteed that different zones will be found each time our methodology is applied to a new dataset.

1.3 Results

1.3.1 Total daily average temporal complementarity

For each point selected, see **Fig 1-5**, we computed Spearman's correlation coefficient based on the daily average data of both wind power and solar radiation from 2004 to 2016. The results were entered into a geographical information system, creating a heat map. Red is assigned a correlation value of -1 (strong negative correlation), while blue is set to +1 (strong positive correlation). **Fig 1-6** shows the resulting map, where four zones can be identified.

A. Correlated zones: ranging from latitude 18°S to latitude 36°S, covering 72 points (Zone A). Given the different correlation values for the coast and valleys

compared to the mountains, we divided Zone A into two subzones: Zones A1 and A2.

A.1. Zone A1: At the coast and valleys, covering 45 points from latitude 18°S to latitude 36°S, there is a moderately positive correlated zone, with a median Spearman's correlation coefficient of +0.44 and an interquartile range of +0.23 to +0.6.

A.2. Zone A2: 27 analysis points were considered in the mountain area, from latitude 25°S to 33°S. There is weak negative complementarity, with a median of -0.18 and an interquartile range between -0.37 and -0.01.

B. Complementary zone: covering 77 points, from latitude 36°S to latitude 51°S, there is weak negative complementarity with a median of -0.18 and interquartile range from -0.33 to -0.07. (zone B).

C. Uncorrelated zone: covering 27 points, from latitude 51°S to latitude 55°S, there is weak positive to no correlation, with a median of +0.05 and an interquartile range from -0.04 to +0.12 (zone C).

Fig 1-7 briefly analyzes the resulting zones, showing the number of points and the range of values for Spearman's correlation coefficient. It shows that each zone has very different characteristics, see zones zones A1, B and C. And two zones are similar in dispersion, but they are geographical different, see zones A2 and B.

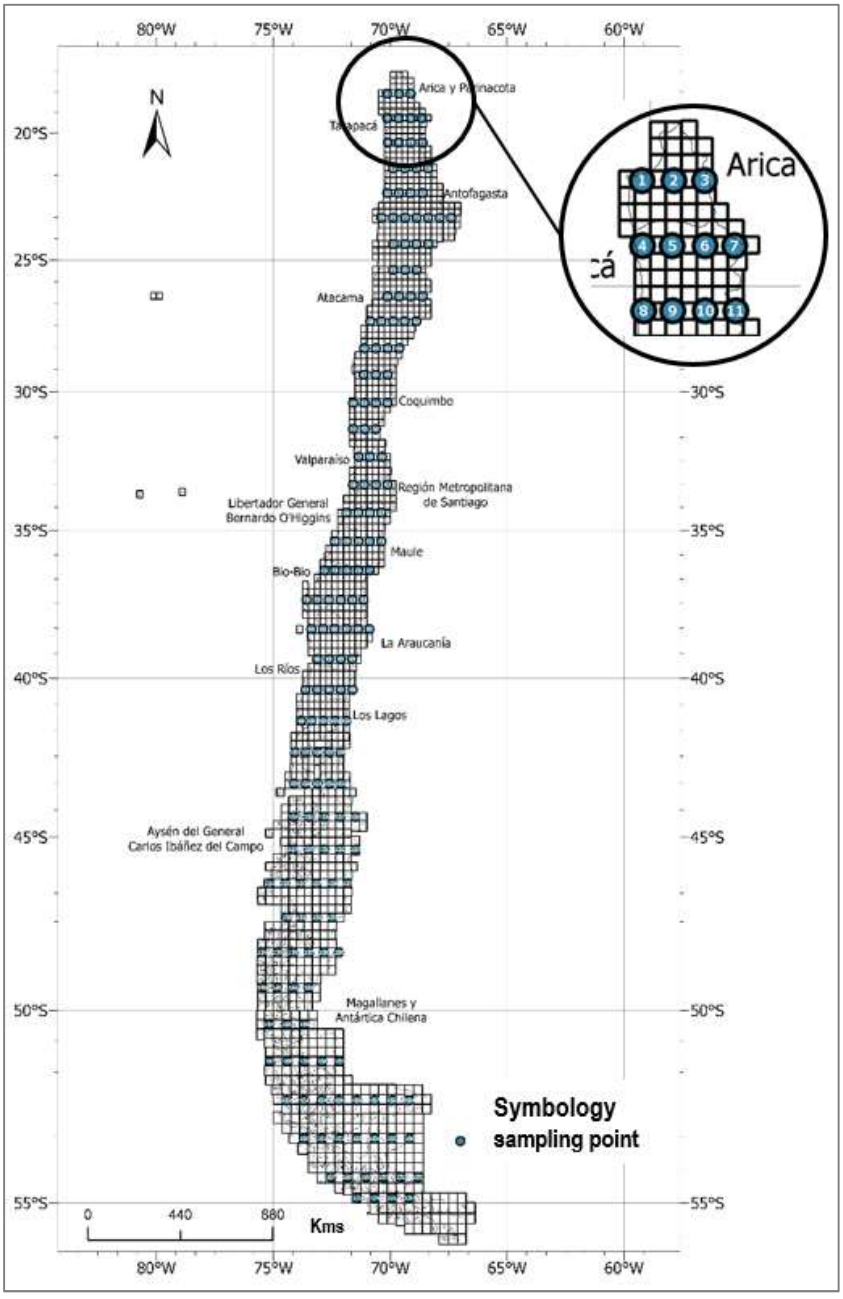

Fig 1-5 Points selected from the geographical map of continental Chile are presented as a 25km x 25km grid. Source: Own elaboration.

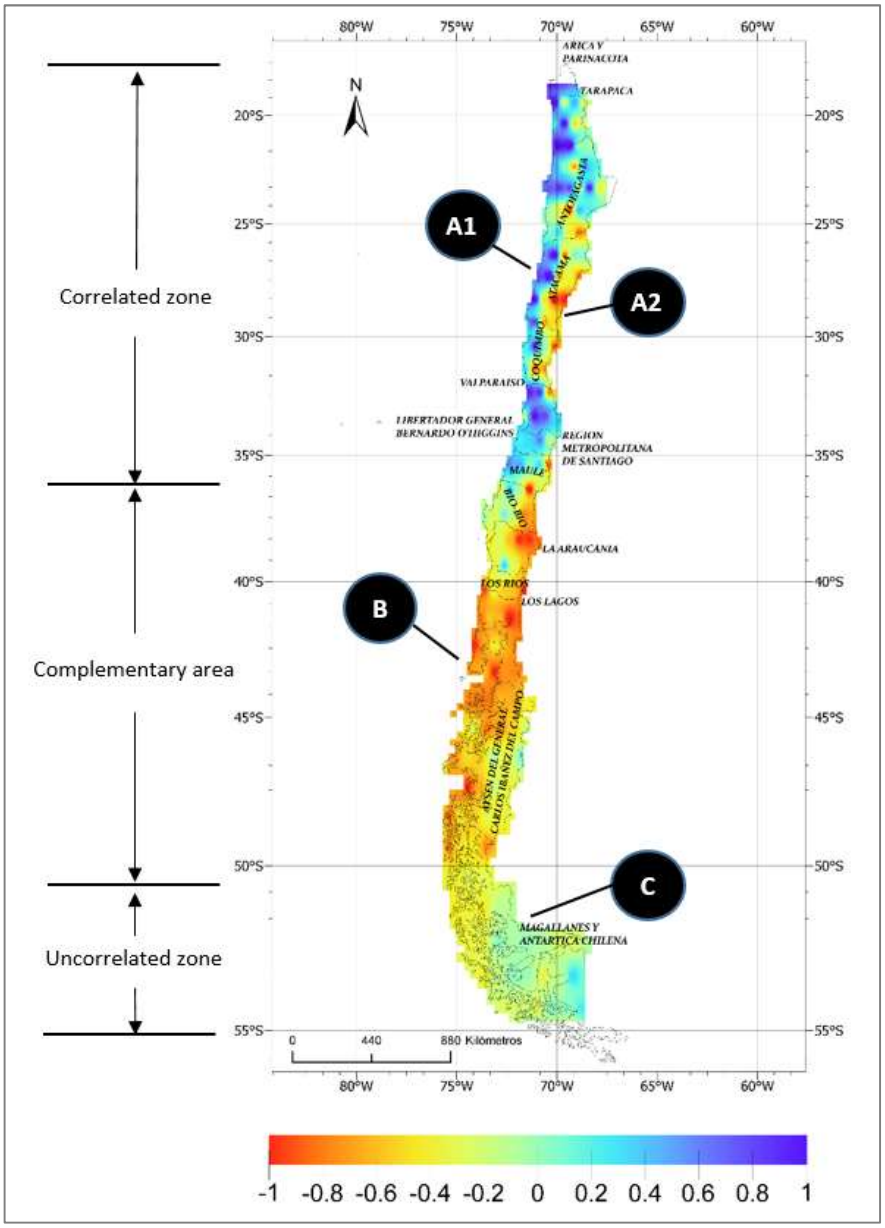

Fig 1-6 Total daily average temporal complementarity heat map created with ArcGIS Pro software for Spearman's correlation coefficient, ranging from -1 (red) to 1 (blue). Source: Own elaboration.

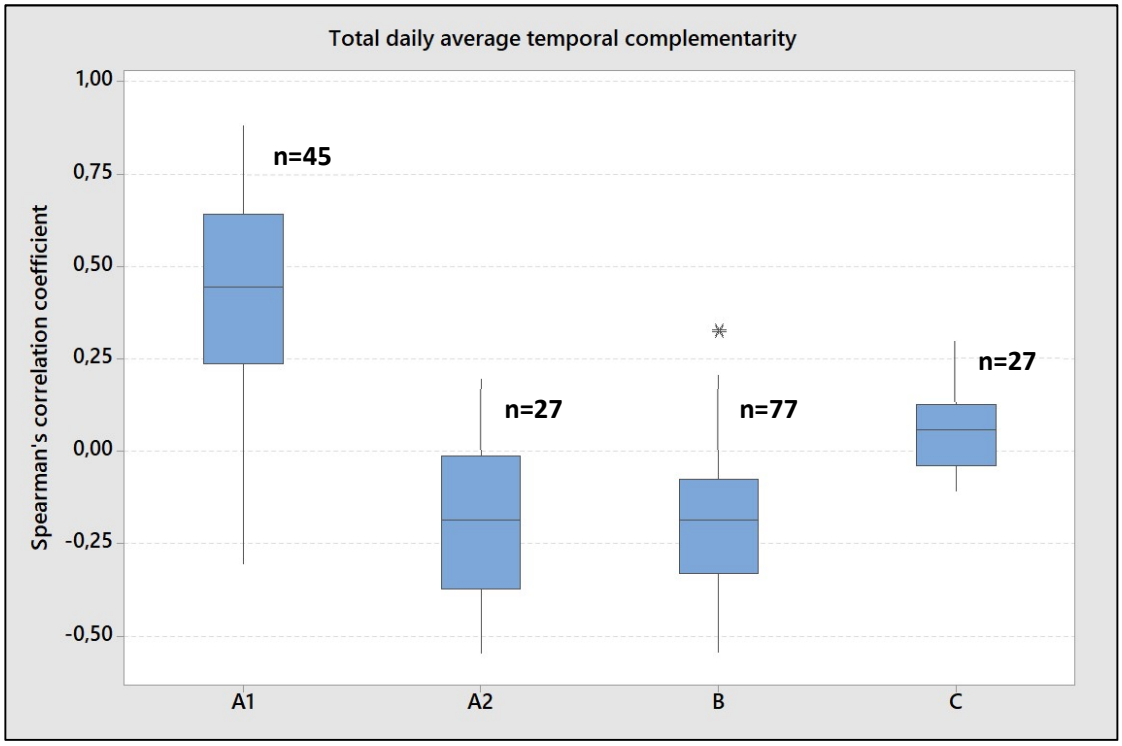

Fig 1-7 Dispersion diagram of Spearman's correlation coefficient for the point in the different zones found, created with Minitab software. Source: Own elaboration.

1.3.2 Daily average temporal complementarity per year

We now repeat the analysis for each year covered by the data. The results show that the zones identified before remain valid, with variations in the intensity of the complementarity, i.e., the level of correlation. **Fig 1-8** shows a comparison between the years 2004 and 2016.

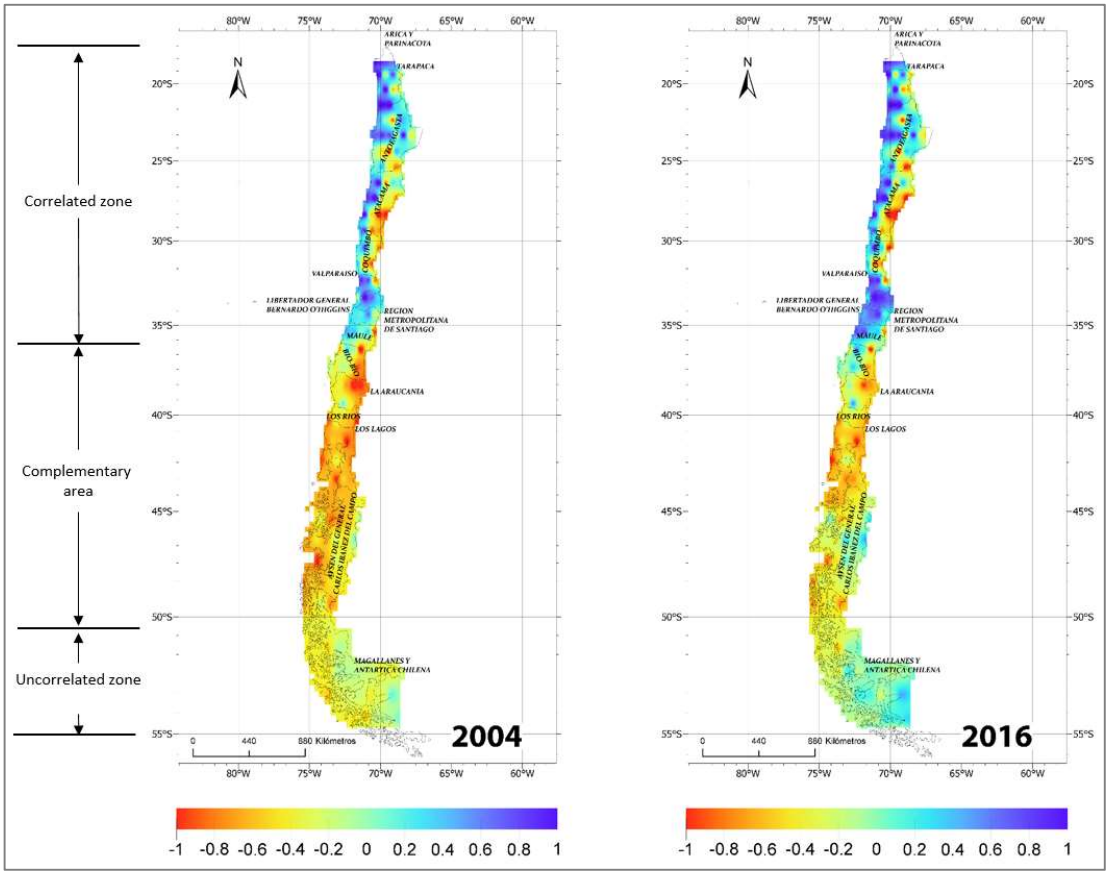

Fig 1-8 Daily average temporal complementarity per year. Comparison of 2004 versus 2016 for Spearman's correlation coefficient, ranging from -1 (red) to 1 (blue). Source: Own elaboration.

Fig 1-9a shows the daily average temporal complementarity values for zone A1 for each year considered. Note that the median is relatively stable, with the value of Spearman's coefficient around +0.5, i.e., moderate positive correlation, except for years 2010 and 2015, where it is reduced to around +0.25. There is also negative kurtosis, while interquartile ranges and extreme points remain uniform for the period studied.

Fig 1-9b is analogous to 9a, but this time for zone A2, where the median remains stable around -0.25, i.e., weak negative correlation, except for 2015, where it goes up to 0, i.e., no correlation. Positive kurtosis and stable extreme values, but dispersion in the interquartile ranges exist.

Fig 1-9c shows the results obtained for zone B, where the median varies in time without a clear tendency. Again, the extreme values remain uniform, with weak

dispersion of the interquartile ranges. Note also that there are more atypical data points than in the previous zones.

Fig 1-9d corresponds to zone C, where the median oscillates between -0.08 and +0.17, i.e., without correlation. There are also no clear tendencies in the interquartile ranges and extreme values.

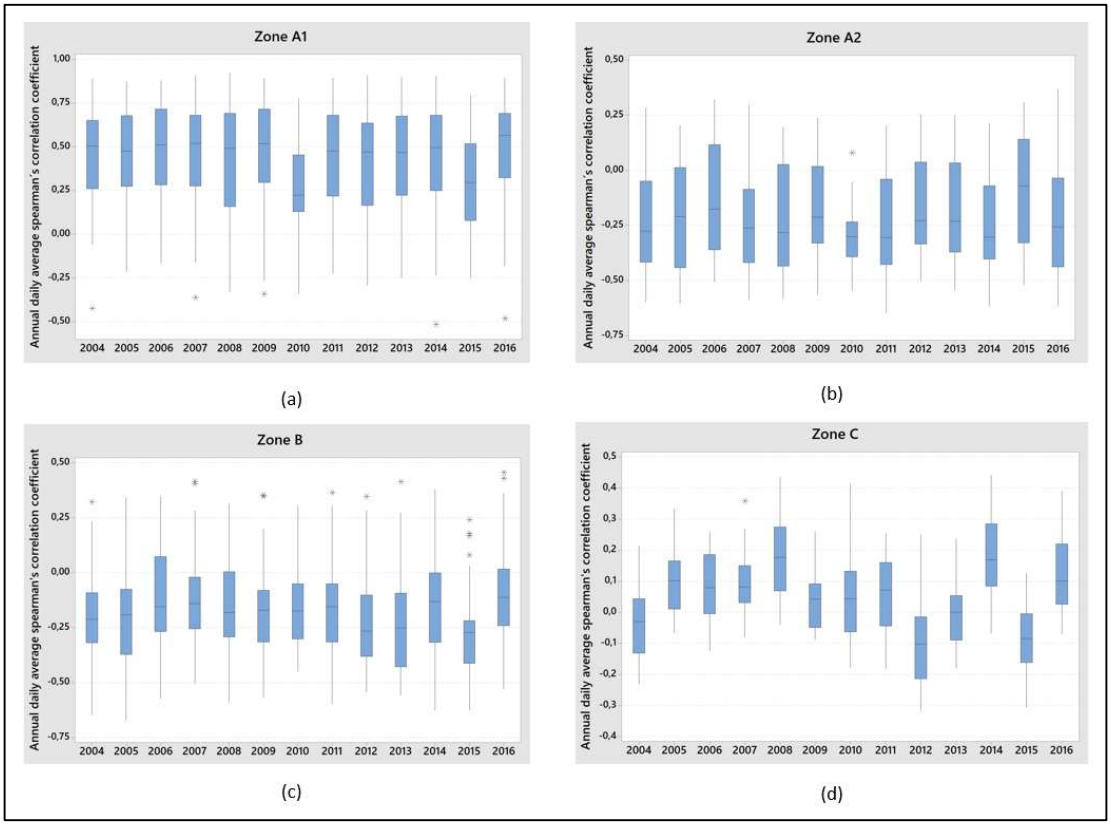

Fig 1-9 Evolution of daily average temporal complementarity from 2004 to 2016 for the previously identified zones (a) Zone A1; (b) Zone A2; (c) Zone B; (d) Zone C, and where * denotes outliers. Source: Own elaboration.

We now analyze the complementarity for points of interest graphically. We select a point inside each zone and then graph the daily averages for wind and solar power potential for 2014.

Fig 1-10 shows the results for Zone A1, where point 12 is selected. At this point, the value of Spearman's coefficient is +0.79, indicating a strong positive

correlation. In the figure, we plot a trend curve for both time series, which achieve their maximums in summer and minimums in winter, as expected.

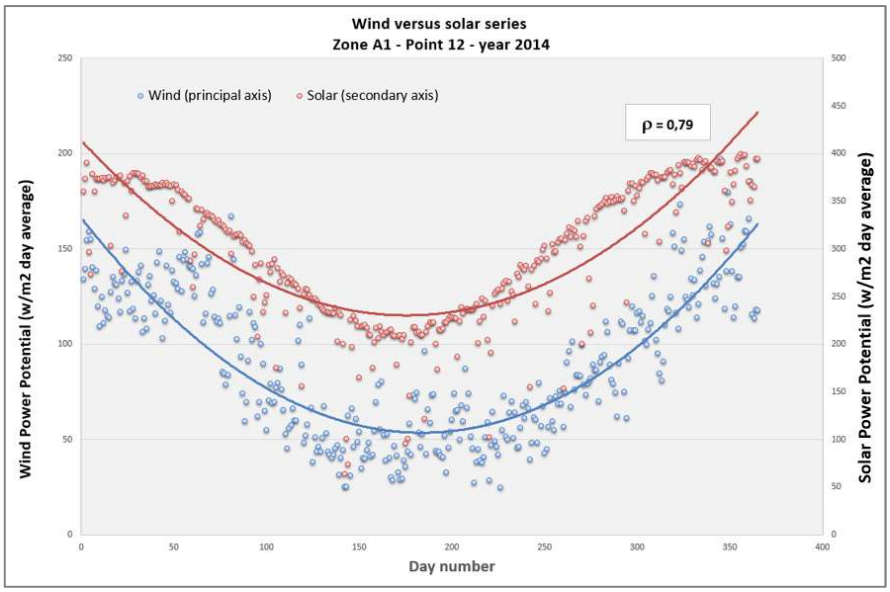

Fig 1-10 Wind and solar daily average power potential time series for Zone A1, point 12, year 2014. Source: Own elaboration.

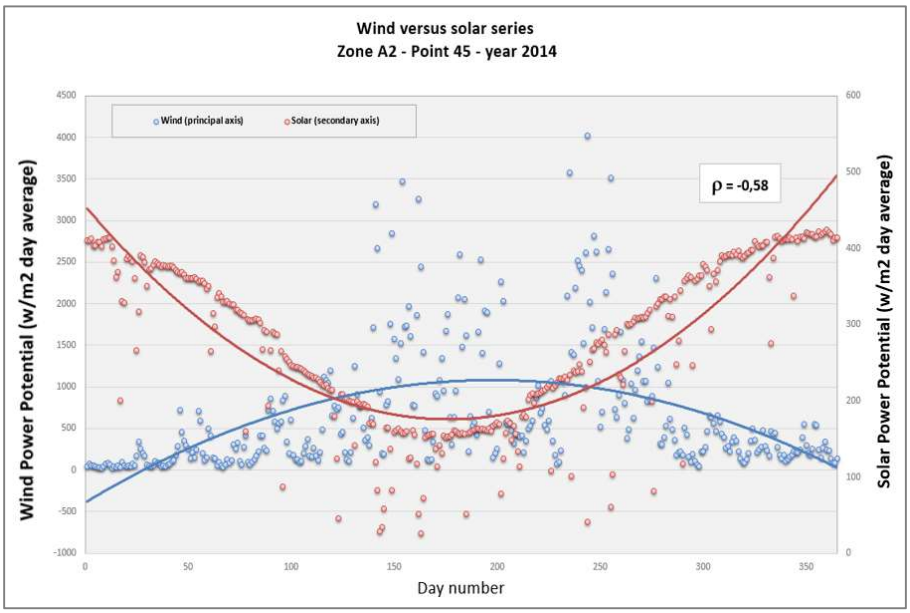

Fig 1-11 Wind and solar daily average power potential time series for Zone A2, point 45, year 2014. Source: Own elaboration.

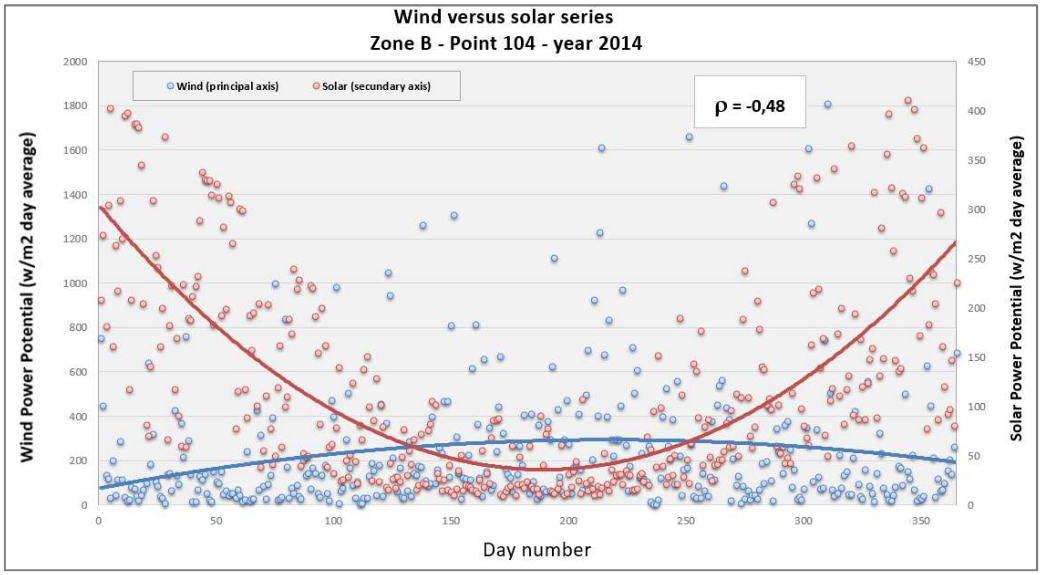

Fig 1-12 Wind and solar daily average power potential time series for Zone B, point 104, year 2014. Source: Own elaboration.

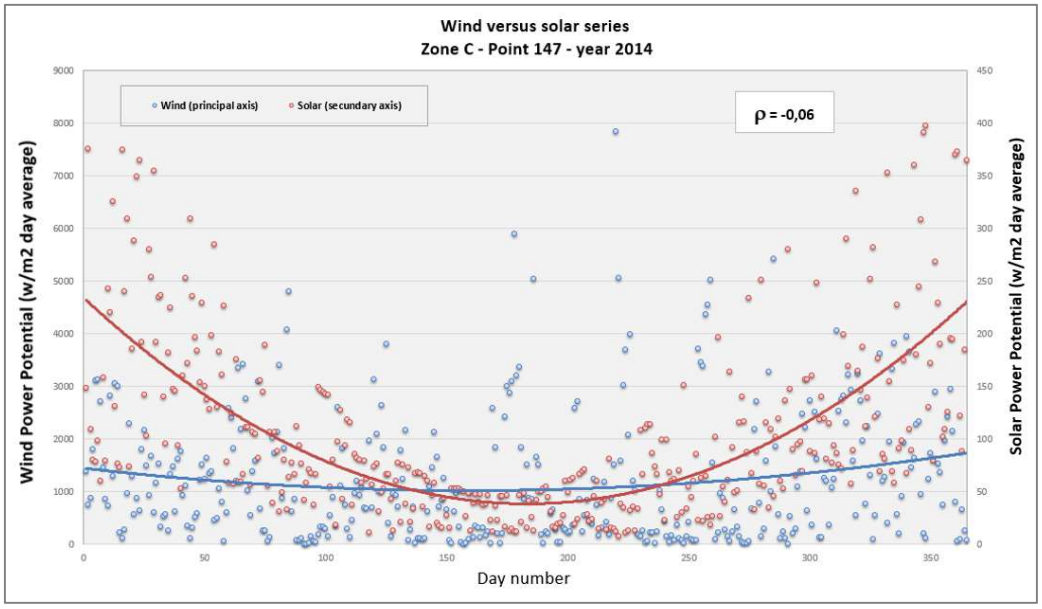

Fig 1-13 Wind and solar daily average power potential time series for Zone C, point 147, year 2014. Source: Own elaboration.

Fig 1-11 shows the results obtained for point 45 in zone A2, where Spearman's correlation coefficient value is -0.58, indicating a moderate negative correlation. The solar time series reaches its maximum in summer and minimum in winter, while the wind time series reaches its maximum in winter with a very high dispersion.

Fig 1-12 presents the results for point 104 in Zone B, where Spearman's correlation coefficient is -0.48, indicating a moderate negative correlation. We note that the solar radiation time series reaches its maximum in summer and minimum in winter, but the results have a significant dispersion. The wind time series reaches its maximum in winter, with a large dispersion in the values obtained.

Finally, **Fig 1-13** shows the results obtained for point 147 in zone B, where Spearman's correlation coefficient value is -0.06, indicating a weak to null negative correlation. The time series behavior is similar to the previous figure.

To provide a wind-solar temporal complementarity map as a tool for the formulation of public policies in the energy sector and to guide investment decisions in renewable energy generation, a map was developed that incorporates the protected areas defined by the Ministerio del Medio Ambiente, by Law No. 21,600 on the National System of Protected Areas (Sistema Nacional de Areas Protegidas, n.d.). These areas include natural monuments, national parks, national reserves, nature sanctuaries and conservation areas for indigenous peoples, among other protection categories.

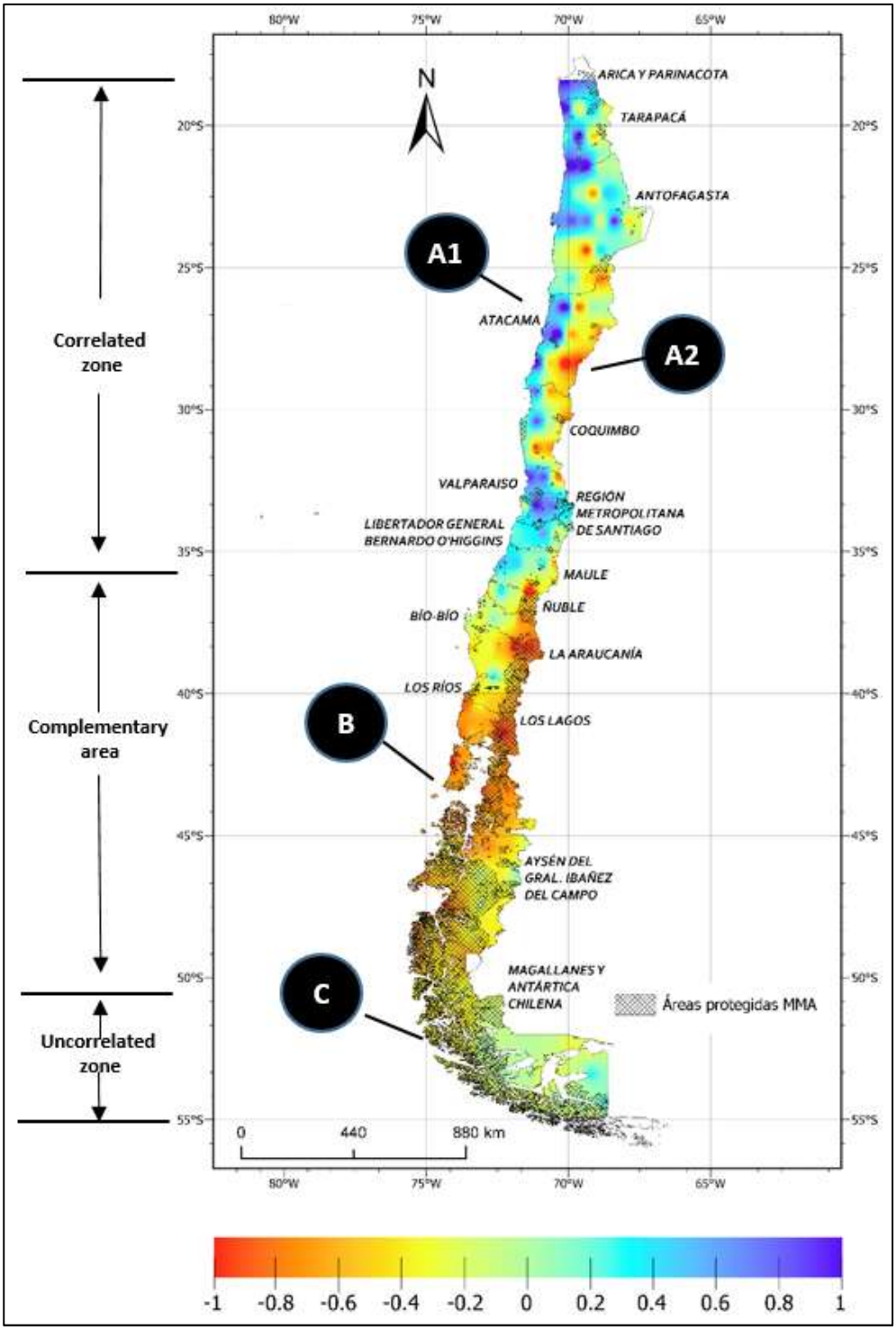

Fig 1-14 Wind–Solar Temporal Complementarity Map, Protected Areas in Chile.

1.3.3 Statistical analysis

In this section, we aim to check if the data used, and the zones obtained are valid statistically. We perform a significance test for each point, a statistical characterization and mean test for each zone and a statistical analysis of the annual evolution of the temporal complementarity for each zone.

1.3.3.1 Significance test for each point

We define as a sample the values of Spearman's coefficient obtained for each point in the timespan from 2004 to 2016 (Section 1.3.1) and the population accordingly.

Let,

-Null Hypothesis (H_0): There is no significant correlation between daily average solar radiation and daily average wind potential.

-Alternative Hypothesis (H_1): There is a significant correlation between daily average solar radiation and daily average wind potential.

We consider significance level α*=0.05* (5%) and number of data points *N=4745* for each geographical point, obtaining ρ_c = *+0.028* as the critical value of Spearman's coefficient. If $|\rho| > \rho_c$, we must reject H_0 and accept H_1, i.e., the correlation value is significant. If $|\rho| < \rho_c$, then we cannot reject H_0, i.e., the value of ρ is not statistically significant.

Fig 1-15 and ***Table 1-4*** show that the correlation coefficients are not statistically significant in 9 out of the 176 points. This means that if we select a year at random as a sample, in any of the 167 significant points, there is a probability of at least 95% that they may have a significant correlation. At the same time, it is impossible to make such a claim in the nine remaining. The nine non-significant points are shown in ***Table 1-4***.

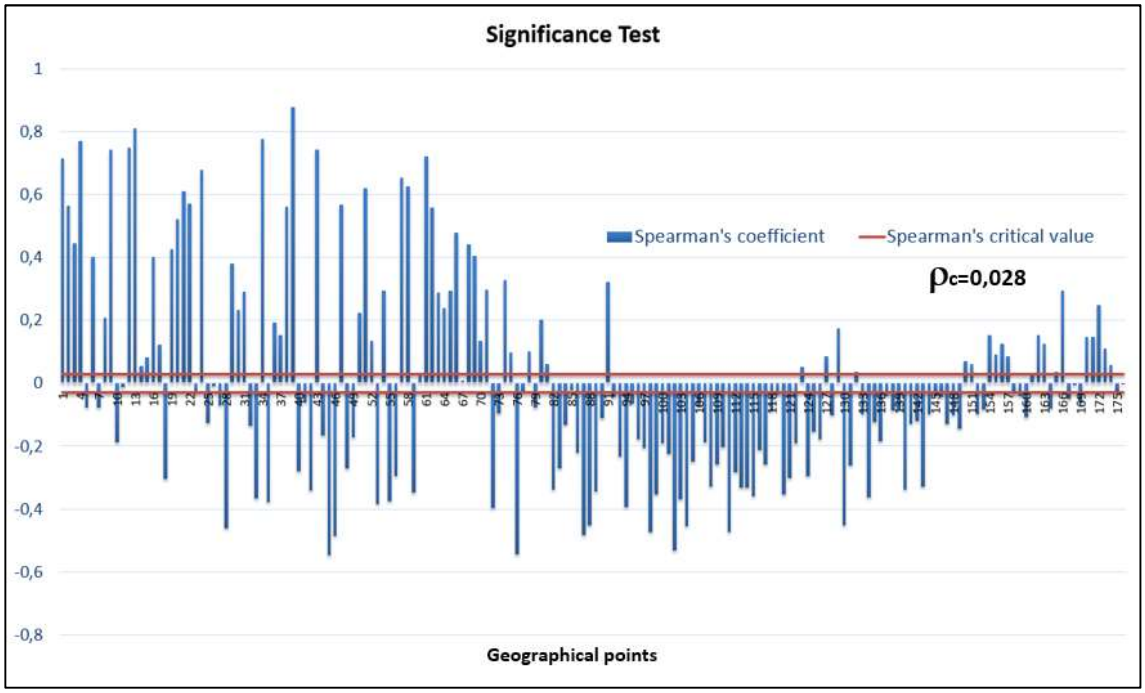

Fig 1-15 Spearman's coefficient significance level for each geographic point, corresponding to total daily average temporal complementarity. Source: Own elaboration.

Table 1-4 *List of statistically non-significative geographical points.*

Point	Zone	ρ_c	ρ
11	A1	0.028	0.014
26	A2	0.028	0.011
60	A1	0.028	0.028
67	A1	0.028	0.009
77	B	0.028	0.027
85	B	0.028	0.022
168	B	0.028	0.006
175	C	0.028	0.025
176	C	0.028	0.001

1.3.3.2 Significance test per zone

We want to know if each zone's correlation is statistically significant. We perform a mean test for each zone as follows. We define the mean of a zone as the average of the wind-solar complementarity computed using Spearman's correlation coefficient for all the points in the zone for the time considered. The

mean test and p-value are computed following (Delgado, 2007) and (Sleeper, 2011) .

Table 1-5 *Mean test for the correlations obtained in each zone.*

Sample (zone)	N	Mean	σ	Mean's standard error	95% CI for μ
A1	45	0.4227	0.2790	0.0416	(0.3389; 0.5066)
A2	27	-0.1948	0.2102	0.0404	(-0.2779; -0.1116)
B	77	-0.1793	0.1860	0.0212	(-0.2215; -0.1371)
C	27	0.0502	0.1057	0.0204	(0.0084; 0.0921)

In this case, we state,

-Null hypothesis $H_0: \mu = 0$

-Alternative hypothesis $H_1: \mu \neq 0$

Table 1-6 *Results of the mean test for each zone were obtained.*

Sample	T-value	p-value
A1	10.17	4.018E-13
A2	-4.82	5.469E-05
B	-8.46	1.466E-12
C	2.47	2.043E-02

The results show that, as $p < 0.05$ and the confidence intervals do not contain 0, we can reject the respective null hypotheses and accept the alternative hypotheses. Specifically, the correlation is significant in zones A1, A2, and B, while it is marginally significant in zone C.

1.4 Conclusions

This work studied the temporal complementarity between wind potential and solar radiation in the continental Chilean territory. We used Spearman's correlation coefficient to compute the complementarity, given that it is a non-parametric indicator that defines the strength and direction of the variable ranges. This coefficient can be used even if the relation is non-linear, the variables are non-normally distributed, and the variances are different.

For our analysis, we computed the daily average wind and solar power potential time series from 2004 to 2016 from hourly data from 176 geographical points extracted from a public database named "Explorador Solar" (Molina et al., 2017).

Our analysis showed four differentiated geographical zones in continental Chilean territory regarding complementarity.

Zone A1 corresponds to the coast and central valleys in the country's north, from latitude 18°S to latitude 36°S, It has a moderate positive correlation, a median of +0.44, and interquartile range of -0.3 to +0.87.

Zone A2 corresponds to the mountains in the country's north, ranging from 25°S to latitude 33°S, with weak negative complementarity, median -0.18, and interquartile range from -0.54 to +0.19.

Zone B, corresponding to the center and south part of the country, from latitude 36°S to latitude 51°S, has moderate negative complementarity, with a median of -0.18 and interquartile range from -0.54 to +0.32.

Finally, Zone C, located in the very south of the country, from latitude 51°S to latitude 55°S, has a weak positive to null correlation, a median of +0.05, and an interquartile range from -0.1 to +0.29.

After analyzing the complementarity in each year, we characterized each zone.

Zone A1 has a stable median, interquartile range, extreme values for the years considered, i.e., from 2004 to 2016, and negative kurtosis.

Zone A2 has uniform median and extreme values, but there is dispersion in the interquartile ranges. We also noted that shows positive kurtosis in most years.

Zone B has a non-uniform median, stable extreme values, and non-stable interquartile ranges.

Finally, Zone C has a non-uniform median, extreme values, and interquartile range.

We tested the statistical validity of our results through a significance test for Spearman's coefficient obtained in all the geographical points considered. The results obtained for 167 of the 176 are statistically significant. The significance test for each zone showed that zones A1, A2, and B have a statistically significant correlation, while zone C is marginally significant.

Unlike international studies conducted in countries such as China, Mexico, and Brazil, which have analyzed solar-wind complementarity at a regional level, generally using daily or monthly resolutions and partial territorial coverage—this work represents the first analysis with national coverage for Chile, based on hourly data and high spatial resolution. This approach enables a more accurate characterization that is highly useful for the design of hybrid systems. At the national level, although studies that have addressed the spatial complementarity between renewable sources or evaluated generation projects based on a single source (solar or wind), no prior research has systematically analyzed the temporal complementarity between both sources on a national scale. Therefore, this study fills an important gap in the literature and provides a concrete tool to support decentralized energy planning, the optimal design of hybrid systems, and informed decision-making in public policy and investment. Moreover, the results address the three research questions posed, by identifying the degree of temporal complementarity between resources, their variation over time, and the regions with the greatest solar-wind synergy across the Chilean territory.

Given that Chile aims to have a 100% renewable electric energy generation matrix by installing wind and photovoltaic generation and new storage systems, this work provides a way to this energy transition. We suggest incentivizing the development of distributed hybrid generation, taking advantage of the temporal complementarity stated in the zone identified in this work. We think that considering the complementarity heat maps we obtained is the first step in reducing energy generation and storage investment costs. A potential place for these incentives could be zone A2, where large mining companies are located, demanding massive amounts of electric energy. Implementing wind-solar hybrid generation systems could reduce the energy storage required to meet the demand, reducing investment and operation costs and reducing their carbon footprint.

As future research lines, we want to tackle:

a) Spatial complementarity, b) The sizing of distributed hybrid generation systems considering the existing complementarity levels. c) The effect of climate change on the wind-solar complementarity.

CHAPTER 2

Chapter 2 addresses the third and fourth specific objectives of this thesis. It presents a quantitative analysis of how the temporal complementarity between wind and solar resources influences the optimal design of off-grid HRES with storage. Based on the identified gap in the literature, the following research question is posed: How does the degree of temporal complementarity between solar and wind resources influence the NPC and the Loss of LPSP in the optimal design of such systems?.

To address this question, an optimization model is implemented in the OCTAVE environment using genetic algorithms to determine the most efficient configuration of solar panels, wind turbines, and batteries, minimizing NPC while meeting a reliability constraint defined by LPSP. Hourly wind speed and solar irradiance curves are generated with different levels of complementarity (ρ ranging from –0.95 to 0.95), while keeping the total daily energy potential constant. Two load profiles are considered: one constant (industrial) and one variable (residential).

The results establish a direct relationship between higher temporal complementarity and improved techno-economic performance, particularly in scenarios with strict reliability requirements. As LPSP decreases, complementarity becomes more important, enabling better use of renewable resources throughout the day and reducing the need for system oversizing.

A sensitivity analysis is also conducted on three key variables: maximum allowable LPSP, unit battery cost, and discount rate. In addition, a one-way ANOVA is performed to validate the statistical significance of the differences in NPC across complementarity scenarios. The chapter concludes with an environmental impact assessment and a case study on green hydrogen production, demonstrating the practical value of incorporating complementarity into energy system design.

2 Optimizing the design of stand-alone Hybrid Renewable Energy System with storage using genetic algorithms: Analysis of the impact of temporal complementarity of wind and solar sources

Article published in the journal Energy Conversion and Management.

Muñoz-Pincheira JL, Salazar L, Sanhueza F, Lüer-Villagra. "*Optimizing the design of stand-alone Hybrid Renewable Energy System with storage using genetic algorithms: Analysis of the impact of temporal complementarity of wind and solar sources"*. Energy Conversion and Management. Volume 341, 2025, 120016, ISSN 0196-8904, https://doi.org/10.1016/j.enconman.2025.120016

Abstract

This study analyzes the impact of temporal complementarity between wind and solar sources on the optimal design of stand-alone hybrid renewable energy systems with storage (HRES). A model was developed in GNU Octave that uses a fixed-seed genetic algorithm to ensure reproducibility and compare scenarios. The objective is to minimize the NPC while complying with a reliability constraint defined by the LPSP. Constant and variable load profiles are evaluated under different levels of complementarity, showing that their influence depends on the type of demand. Furthermore, a sensitivity analysis is performed on the LPSP, battery cost, and discount rate, demonstrating how these parameters affect the optimal configuration. The results indicate that high complementarity can significantly reduce the NPC, especially in contexts with strict reliability requirements. In environmental terms, an HRES supplying 1,470 kWh per day would avoid between 108 and 375 tons of CO_2 per year, compared to a fossil source. These findings are key to energy planning in countries moving toward decarbonization, supporting investment decisions in distributed generation and mitigating the effects of curtailment on centralized systems.

Keywords: Temporal Complementarity, HRES, Genetic Algorithms, Levelized Cost of Energy (LCOE), Distributed Generation.

2.1 Introduction and literature review

The world is facing a critical issue: climate change and the depletion of fossil fuel reserves. These challenges not only put the stability of ecosystems at risk but also threaten global energy security and the well-being of millions of people. As greenhouse gas emissions continue to rise and fossil fuel reserves decline, the need to find sustainable energy solutions becomes more urgent than ever. According to the latest Intergovernmental Panel on Climate Change (IPCC) report from 2023, it is imperative to drastically reduce carbon emissions to limit global warming to 1.5°C, underlining the urgency of adopting renewable energy sources soon. (IPCC, 2023)

One of the main challenges is meeting the growing energy demand. According to projections by the International Energy Agency, global electricity demand will increase by more than two-thirds by 2035. (International Energy Agency, 2020) This increase is driven by population growth and the expansion of industry, agriculture, and residential sectors, which require a constant and efficient energy supply. However, continuing to rely on fossil fuels exacerbates environmental problems and exposes economies to fluctuations in the prices and supply of these limited resources. Recent studies highlight that decarbonizing energy systems is key to meeting these challenges. (Sinha et al., 2024)

Faced with this scenario, the transition to renewable energy emerges as a viable and necessary solution. In recent years, many countries have begun to replace fossil fuels with renewable alternatives such as solar, wind, and biomass, among others. (REN21, 2023) These energy sources, in addition to being cleaner, have the potential to significantly reduce emissions of polluting gases and contribute to the stabilization of energy systems in the long term. The growing adoption of policies that encourage the use of renewable energy has been a key factor in this progress, with stricter regulatory frameworks and expanding national clean energy goals. (Daszkiewicz, 2020).

However, centralized power generation systems, still predominant in many countries and regions, have significant disadvantages regarding efficiency, costs, and the ability to meet increasingly volatile energy demands. These systems are often less efficient due to substantial losses during energy transmission and distribution, which can exceed 8% in some networks. (US EPA, 2015), (International Energy Agency, 2024). The high cost of maintaining and expanding infrastructure, such as long-distance transmission lines, also adds a considerable economic burden, especially in remote or low-population areas.

Congestion problems on power transmission networks have increased due to rising demand and a lack of transmission capacity, leading to bottlenecks that affect system stability and reliability. Congestion occurs when the capacity of transmission lines is insufficient to transport the electricity generated, forcing the use of more expensive and less efficient energy sources to meet demand. This has been a growing problem, especially in networks integrating renewable energy, such as areas with high wind penetration or photovoltaic farms.

For example, in the United States, costs related to power grid congestion reached $20.8 billion in 2022, a considerable increase compared to previous years. This cost increase is attributed to several factors, including a lack of investment in new transmission infrastructure, which limits the capacity to transport electricity from cheaper sources such as solar and wind to areas of higher demand. The construction of new high-capacity lines has decreased in recent years, exacerbating the congestion problem and affecting the system's efficiency. (Ross, 2023)

In addition, a lack of interregional capacity and increasing demand for electricity, driven by phenomena such as the rise in the use of electric vehicles, are creating bottlenecks in transmission networks. In some areas, this has forced using closer but more expensive generators to avoid overloading the network, reducing system efficiency and increases costs for consumers. (Rueger et al., 2023)

Renewable energy curtailment in Chile, particularly in the northern region, has posed a critical challenge due to excess solar generation in the face of limited demand and transmission capacity constraints. Between 2015 and 2017, marginal costs dropped to 0 USD/MWh numerous times, affecting the economic viability of several projects with Power Purchase Agreements (PPAs). Although the integration of the National Electric System (SEN) in 2018 and the commissioning of the Cardones-Polpaico transmission line in 2019 partially improved the situation, the issue persists. According to the Fraunhofer report (von Papp et al., 2022), renewable energy curtailment reached 1,600 GWh in one year, compared to 453 GWh recorded the previous year, with peaks observed in June and July 2023.

In contrast, HRES offer significant advantages over centralized systems. By combining multiple renewable energy sources, such as solar, wind, biomass, and others, with storage technologies, HRES enables more efficient, flexible, and reliable energy delivery. These systems do not rely on long transmission networks, reducing energy losses and avoiding congestion problems plaguing centralized systems. In addition, HRES can be deployed locally, which lowers operational and infrastructure costs while promoting decentralization and energy

resilience to natural disasters or grid failures. Thanks to their modularity and scalability, HRES can be tailored to the specific energy needs of communities and industrial sectors, providing customized and sustainable solutions. (Pérez Uc et al., 2024)

One of the most widely used stand-alone HRES architectures is the one in which several sources are coupled to a DC Bus, as shown in **Fig 2-1**. This is due to the ease of integration and the absence of power quality problems, such as harmonics and reactive power.

Fig 2-1 shows a schematic of a stand-alone HRES configuration coupled to a single DC bus line, composed of “s” storages systems of different types, such as lead acid batteries, lithium, green hydrogen, etc. The system is injected with energy from “m” resources, such as solar, wind, hydro, biomass, etc. The system is also fed by “n” generators, which can be diesel or another fuel type. Generating one or more fuel cells (FC) is also possible. Finally, the injected energy is used to feed the requested load, and the surplus can be sent to the storage system, which could also deliver it to the unit to meet the load.

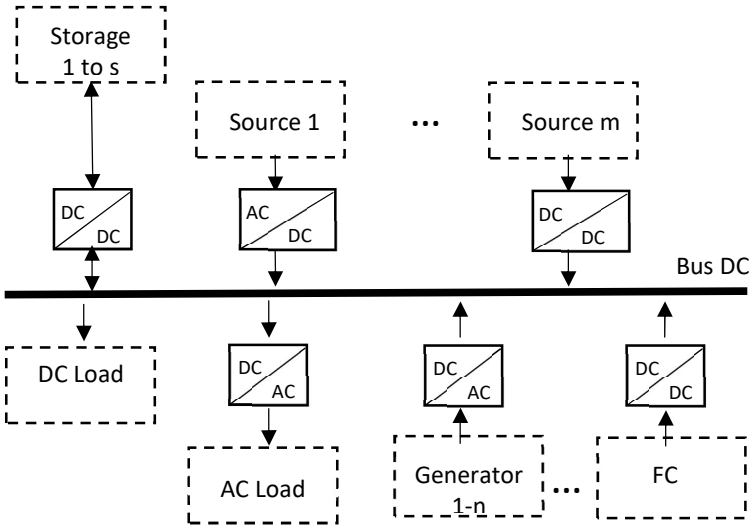

Fig 2-1 Autonomous HRES architecture. Scheme adapted from (Al Sumarmad et al., 2022).

One of the main challenges in HRES is finding an optimal combination of components due to the high initial costs, the increasing maintenance expenses, and the different depreciation rates that these systems present. These factors can complicate the economic viability of HRES, especially for projects with limited financial resources. The initial investment cost in infrastructure and technologies, such as solar panels, wind turbines, and energy storage systems, tends to be high and often deters investors, especially in rural or developing regions. (Kavadias & Triantafyllou, 2021).

Furthermore, the design of an HRES is influenced by several key factors, such as the availability of energy resources at the installation site, the system's technical specifications, environmental conditions, and social and technical constraints. For example, solar systems may be more efficient in areas with high solar radiation, but wind turbines may complement energy production in windy areas. This variability in energy resource conditions affects both the generation capacity and the cost of energy production. (Mishra et al., 2016)

In many cases, geographic location and social constraints, such as local community acceptance, affect the system's viability. These factors not only affect the design but also influence how much energy the system can produce and how it is distributed, which inevitably increases the overall cost of the system. (Cuesta et al., 2020)

To counter these challenges, a key strategy is to achieve an optimal configuration that maximizes system efficiency and reliability at the lowest possible cost. This requires careful design and balancing of the various available energy sources, technical capabilities, and regional energy demands. Optimizing system size and configuration is a complex process that involves a detailed understanding of local energy sources, climatic conditions, and technological specifications. In addition, economic factors such as long-term maintenance costs and component depreciation rates must be considered. (Al-falahi et al., 2017).

2.1.1 Optimization of HRES

Optimizing the design of an HRES requires knowing the load profile, the availability of energy sources, the evaluation parameters, the optimization technique, and the technical and economic data of the selected units to find a configuration that minimizes costs throughout the system's entire life stage while complying with the restrictions and the requested energy demand.

2.1.1.1 Evaluation Parameters

Various indicators have been used to evaluate HRES. The authors (Al-falahi et al., 2017) classified the indicators into four categories. The most important ones are shown in ***Table 2-1***.

Table 2-1 *HRES evaluation parameters*

Category	Indicator	Unit	Formula	Description
Economic	NPC (Net Present Cost)	$	$NPC = \sum_{t=1}^{T} \frac{C_t}{(1+r)^t}$	It represents the total present value of all future project costs (investment, operation, replacement costs, etc.), adjusted by the discount rate.
	COE (Cost of Energy)	$/kWh	$COE = \frac{C_{total}}{E_{total}}$	It reflects the average cost of producing a unit of energy.
	LCOE (Levelized Cost of Energy)	$/kWh	$LCOE = \frac{\sum_{t=1}^{T} \frac{C_t}{(1+r)^t}}{\sum_{t=1}^{T} \frac{E_t}{(1+r)^t}}$	The average cost of producing a unit of energy considering the discount rate or depreciation of costs over time.
Reliability	LPSP (Loss of Power Supply Probability)	%	$LPSP = \frac{\sum_{t=1}^{T} E_{\text{deficit},t}}{\sum_{t=1}^{T} E_{\text{demand},t}}$	It represents the probability that a system will not be able to satisfy the energy demand at a given time due to the lack of generated or stored energy availability.
	UL (Unmet Load)	kWh	$UL_t = E_{\text{demand},t} - E_{\text{supplied},t}$	Amount of energy or load demand that a power system cannot supply during a given period.
	D (dumped energy)	kWh	$D_t = E_{\text{generated},t} - E_{\text{demand},t} - E_{\text{stored},t}$	The amount of energy generated by a system that cannot be used or stored and is therefore discarded or "dumped"
Environmental	E (**Total CO_2 emissions**)	Ton CO_2	$E = \sum_{t=1}^{T} E_{\text{fuel},t} \cdot EF_{\text{fuel}}$	Amount of CO_2 emissions generated by the system
	LCA (Life Cycle Assessment)	Ton CO_2 equivalent		Methodology to evaluate the environmental impact of a product, process, or service throughout its entire life cycle.
Social	JC (Job Creation)	Total jobs	$JC = \text{Investment} \times \text{Employment ratio}$	Represents how many jobs are created per unit of investment or production in a specific industry or sector.

2.1.1.2 Size Optimization Techniques.

The authors of (Singh & Bansal, 2018) classified the optimization techniques for HRES configuration into three main categories: a) Artificial intelligence methods, b) Iterative methods, and c) Software tools for optimization. Some relevant works in each of these areas are reviewed below:

(a) Artificial intelligence methods

This approach includes the use of metaheuristics such as genetic algorithms (GA), tabu search (TS), simulated annealing (SA), and particle swarm optimization (PSO). These techniques effectively solve complex problems with multiple variables, such as optimizing the size and configuration of an HRES.

In (Vendoti et al., 2019), an optimization study is presented for an HRES using a Genetic Algorithm (GA) to provide an economical solution for rural electrification. They focus on a cluster of three villages in Kollegal block, Chamarajanagar district, Karnataka, India. The hybrid system includes solar photovoltaic (PV), wind, biomass, biogas, and fuel cells and aims to minimize the NPC and Cost of Energy (COE). Four models are evaluated, and the best combination (C1) includes solar PV, wind, biomass, biogas, fuel cells, and battery storage. The study concludes that combination C1 results in the lowest NPC of $856,013 with a COE of $0.163/kWh and suggests that this configuration meets the energy demands of the selected villages with no unmet loads.

In (Ogunjuyigbe et al., 2016) the optimal design of a hybrid renewable energy system to supply remote residential buildings using solar panels (PV), wind turbines, split diesel generators, and batteries is presented. It was carried out in an isolated residential environment and the objective was to minimize the life cycle cost (LCC), CO_2 emissions, and dump energy. For this, a genetic algorithm (GA) was used, which allowed them to optimize these three objectives simultaneously. The results show that the hybrid system combining PV, wind, split diesel generators and batteries is the most efficient option. This scenario reduce the LCC to $11,273, with a cost of energy (COE) of 0.13 $/kWh, wasted energy of 3 MWh and CO_2 emissions of 13,273 kg. The proposed system reduced costs by 46% and emissions by 82% compared to a diesel generator-only system.

The authors of (Merei et al., 2013) present the optimization of a hybrid off-grid power system combining solar (PV), wind, a diesel generator, and different battery technologies (lead-acid, lithium-ion, and redox flow). The study was conducted at

two locations with different climates: Aachen, Germany, and Quneitra, Syria. Component sizes and configurations were optimized using a genetic algorithm (GA) to minimize costs and emissions. The results show that the using redox flow batteries in combination with renewables is the most economical option, with an energy cost of 0.65 €/kWh in Aachen and 0.34 €/kWh in Quneitra. Furthermore, the hybrid system including solar panels, wind turbines, and redox flow batteries, is optimal in Germany, while in Syria, where diesel is cheaper and solar radiation is higher, a combination of solar panels and a diesel generator is preferred.

The article (Mahesh & Sandhu, 2020) proposes an optimization strategy for a grid-connected hybrid solar-wind-battery system, using a genetic algorithm (GA) an energy filter. The objective is to minimize the LCOE and reduce fluctuations in the energy injected into the grid. The technique was applied in a system combining solar panels, wind turbines and battery storage. The GA optimizes the size of the system components, considering constraints such as the loss of supply probability (LPSP) and power fluctuations. The results show that the proposed energy filter significantly improves the system stability by smoothing out power fluctuations. In the optimal configuration, an LCE of 0.4024 $/kWh is achieved, with reduced fluctuations in injected energy and an efficient use of solar and wind sources.

The authors in (Torres-Madroñero et al., 2020) present the optimal sizing of HRES for the Colombian context, specifically in Puerto Bolívar, La Guajira, a region with excellent solar and wind resources. They used two optimization methods, Genetic Algorithm (GA) and Particle Swarm Optimization (PSO), to minimize the LPSP and annual costs (TAC) or LCOE. The results show that PSO was more efficient than GA, achieving configurations that were better adjusted to energy demand, especially in non-interconnected areas. The optimal configuration included a combination of solar panels, wind turbines and batteries, reaching an LCOE of 0.16 USD/kWh. The study highlights the potential of HRES to improve energy coverage and reduce costs in remote areas of Colombia.

In (Marocco et al., 2022) the authors explore the optimal design of off-grid HRES, highlighting the role of hydrogen as a key component for energy storage. They use the Pareto frontier method and the particle swarm optimization (PSO) algorithm to evaluate different combinations of elements such as photovoltaic (PV) panels, wind turbines, batteries, diesel generators and hydrogen storage. They conclude that hydrogen-based storage is essential to improve the penetration of off-grid renewables, allowing them to avoid battery oversizing. An optimal combination is obtained with a LCOE of 0.41 EUR/kWh which is 35% less than a system that relies only on batteries as a storage medium. On the other hand, a reduction of 84 tons of CO_2 per year was achieved.

The authors of (Mokhtara et al., 2021) present an optimization of the off-grid HRES design to electrify residential buildings in rural Algeria. A particle swarm optimization (PSO) algorithm combined with the epsilon constraint (ε-constraint) method is used to minimize the cost of energy (COE) while maximizing the renewable energy fraction (RF) and ensuring system reliability (LPSP). The study analyzes seven selected locations in different climatic zones of the country. The results show that in low energy efficiency buildings, the optimal mix includes solar, wind, diesel and battery storage in areas such as Adrar and Tindouf. A 100% renewable configuration is achieved in Biskra and Tamenrasset in high energy efficiency buildings, with a COE of $0.21/kWh. Building energy performance and climatic conditions significantly influence the optimal HRES size and configuration.

In (Althani & Maheri, 2021) propose an ant colony algorithm (ACO) to optimize the size and configuration of a HRES including solar (PV), wind, batteries, diesel generators, and hydrogen storage. It was applied in three case studies using MOHRES software to find configurations that minimize life cycle cost, carbon emissions, and unused energy while ensuring system reliability. The ACO technique uses Gaussian distribution to generate solutions and the roulette wheel principle to select probabilistic paths. The results show that the PV-battery system is optimal in scenarios with high solar irradiation, while the PV-diesel-battery combination is preferred under limited conditions. Compared with the genetic algorithm (GA), ACO proved equally effective but with fewer manual adjustments.

The authors of (Mahmoud et al., 2022) investigate the optimal configuration of a HRES using solar (PV), wind (WT), batteries, and diesel generators in El-Bahariya Oasis, Egypt. Three optimization algorithms were applied: Salp Swarm Algorithm (SSA), Grey Wolf Optimizer (GWO), and Improved Grey Wolf Optimizer (IGWO). The objective was to minimize the cost of energy (COE) and loss of supply probability (LPSP). The results showed that IGWO was the most efficient algorithm, achieving a COE of $0.21582/kWh and the lowest LPSP, with an optimal configuration of 1100 solar modules, 14 wind turbines, 399.9 battery banks, and 1.89 diesel generators. Furthermore, IGWO demonstrated higher stability than SSA and GWO, with shorter simulation time and higher accuracy across the 30 runs performed.

In (Dufo-López et al., 2016), an optimization of HRES (PV-wind-diesel-battery) for a community in the Sahrawi refugee camps in Tindouf is presented. Using a multi-objective evolutionary algorithm (MOEA) combined with a genetic algorithm (GA), the authors seek to minimize the NPC and maximize the Human Development Index (HDI) and job creation (JC). HDI is considered a new factor since access to electricity improves indicators such as life expectancy and education. In addition,

the JC is calculated according to the technologies employed (PV, wind, diesel). The results show that the PV-wind-diesel-battery configuration optimizes these three objectives, balancing low costs, greater social development, and more jobs. The study concludes that it is possible to design energy systems that improve the economy and the quality of life in remote rural communities.

According to the review, there is a growing trend towards using hybrid algorithms, which could improve the results in the search for the optimal configuration of a hybrid renewable energy system. Most of these systems combine sources such as solar, wind, and batteries, optimizing energy coverage in remote and off-grid areas with a clear focus on reducing the LCOE. The development of new technologies could incorporate fuel cells, capable of generating electricity and heat, expanding the possibilities of HRES. In addition, the growing role of hydrogen storage is highlighted as a promising alternative to avoid battery oversizing and improve the integration of renewable energies.

(b) Iterative methods

These methods, such as linear programming, the DIRECT algorithm, and mixed integer linear programming, among others, allow solutions to be refined through repetitive cycles until the optimal result is reached. Despite being slower than artificial intelligence-based methods, these approaches are still valuable for problems with well-defined constraints and in cases requiring high calculation accuracy.

In (Alberizzi et al., 2020), the authors investigate the optimal design of a hybrid renewable energy system (HRES) to electrify a mountain hut at 2200 meters altitude in South Tyrol, Italy, replacing traditional diesel generators. Using a mixed integer linear programming (MILP) algorithm implemented in MATLAB, the component sizes (solar panels, wind turbines, and batteries) were optimized to minimize total costs, including capital and operating costs. The optimal configuration includes 86 solar panels, a 10-kW wind turbine, and 30-kWh battery storage. The high cost of the system is mainly due to the batteries, which raises the possibility of cost reduction by considering a diesel generator as a backup. The results demonstrate that a 100% renewable system is feasible, albeit with high costs, especially in remote areas.

The authors of (Abdellatif et al., 2023) present the optimization of a hybrid renewable energy system (HRES) using solar, wind, batteries, and diesel generators in an isolated environment. Linear programming (LP), combined with Bender decomposition and lexicographic optimization techniques, was applied to minimize operating costs, CO2 emissions, unmet demand, and excess energy.

The study, performed with a time horizon of a full year, allows a more detailed evaluation compared to other approaches that use only 24 hours. The optimal configuration included solar panels, wind turbines, and batteries, significantly reducing CO_2 emissions and operating costs. Furthermore, using Benders decomposition improved the computational efficiency of the optimization. The study demonstrates the economic and environmental viability of HRES in off-grid systems.

In (Belfkira et al., 2011) an optimization study is presented for sizing a hybrid power generation system combining wind, solar photovoltaic (PV), and diesel power. A deterministic DIRECT (DIviding RECTangles) algorithm was applied to find the optimal number of components (solar panels, wind turbines, batteries, and diesel generators) that minimizes the total system cost while ensuring energy availability. The study used wind speed, solar radiation, and ambient temperature data recorded hourly for six months in Dakar, Senegal. The results show that using batteries significantly reduces the number of operating hours of the diesel generator and the total long-term system cost. In the optimal configuration, the system with batteries had a total cost of €388,540 compared to €2.9775 million for the system without batteries. This study confirms that hybrid systems with batteries are more economical and efficient in remote regions.

Iterative methods are becoming less widely used due to their disadvantages compared to artificial intelligence algorithms. These methods often get stuck in local minimum solutions, are highly sensitive to initial conditions, and are limited in their ability to handle multi-objective functions, making them less effective in complex optimization problems.

(c) Software tools for optimization

Several tools, such as HOMER Pro and iHOGA, are widely used for HRES simulation and optimization. These tools allow designers to model different system configurations and compare scenarios to find the most cost-effective and efficient option regarding cost and energy performance.

The authors in (Nadeem et al., 2024) investigate the design and optimization of a HRES based on solar photovoltaics (PV) and biomass to electrify a rural community in Tharparkar, Pakistan. HOMER Pro was used to optimize the size and configuration of the system components. The main objective was to minimize installation and operation costs while ensuring high system reliability. The results show that the optimal combination of solar and biomass is economically viable, with a lower LCOE compared to diesel-only systems. The optimized solution ensures community energy self-sufficiency, promoting sustainable development.

This approach offers a feasible solution to improve electrification in rural areas of Pakistan.

In (Araoye et al., 2024), a techno-economic modeling and optimization study of a stand-alone hybrid microgrid system for rural electrification in Nigeria is presented. Using HOMER tools, the study seeks to optimally size the components of a system that combines solar photovoltaic (PV), wind, biomass, and batteries. The goal is to ensure energy sustainability at a minimum cost, improving energy accessibility in rural areas. Results show that the optimal combination includes 50 kW of solar panels, 20 kW of wind, 30 kW of biomass, and a battery system with a capacity of 200 kWh. This configuration achieves a LCOE of $0.15/kWh, making it a cost-effective and sustainable solution to improve rural electrification in Nigeria while reducing dependence on diesel generators.

The authors of (Saiprasad et al., 2019) analyze the optimal sizing of a hybrid renewable energy system in Aralvaimozhi community, Tamil Nadu, India, using iHOGA software. The study combines solar photovoltaic (PV), wind (WT), and battery storage to minimize the NPC and maximize social and environmental benefits. Economic, social, and environmental impacts were assessed, showing that the system could provide up to 70% of electricity from renewable sources. The results include a significant reduction in CO2 emissions, job creation for the community, and a cost of energy (LCOE) of 2.8 INR/kWh.

Both HOMER and IHOGA are specialized software for the simulation and optimization of HRES, widely used in research for their ability to combine various energy sources. Although these tools are very powerful, their main disadvantage is the lack of flexibility compared to artificial intelligence algorithms, which allow greater customization and fine-tuning in the optimization processes.

2.1.2 Energy Complementarity

Energy complementarity refers to the level of correlation between two or more energy sources. Regarding resources with temporal variability, such as solar and wind energy, measuring this relationship to estimate their capacity to meet system demand is essential. If the resources are in the same geographic location, we speak of temporal complementarity; if they are distributed in different areas, it is called spatial complementarity.

In (Jurasz et al., 2020b) the authors define complementarity as the degree of correlation existing between different energy sources. **Fig 2-2** defines complementarity as the degree of correlation between different energy sources.

They also describe different ways of measuring complementarity, including metrics such as the Pearson correlation coefficient, Spearman rank coefficient, Kendall coefficient, autocorrelation, and cross-correlation. They mention the wavelet-based complementarity index and the temporal complementarity index.

For their part, the authors of (Pedruzzi et al., 2023), reviewed the methodologies, techniques, and data sets available to assess the complementarity between wind and solar energy. By analyzing the different correlation coefficients and indices, they concluded that no universal methodology or standard exists to measure energy complementarity.

Numerous and varied studies on energy complementarity exist in different countries and regions worldwide. Some relevant current articles are:

In (Vázquez et al., 2024), the authors discuss the importance of combining different renewable energy sources (wind, solar and wave) for hybrid offshore platforms off the coast of Spain. Using ERA5 reanalysis data, the authors assess the potential of these energies in different regions, such as the Atlantic, the Mediterranean and the Canary Islands. The results show that wind energy is the most abundant, but wave energy can help reduce variability in production, especially in areas such as northwestern Spain. Combining these technologies makes it possible to maximize output and achieve a more constant flow of energy, contributing to a more sustainable energy system.

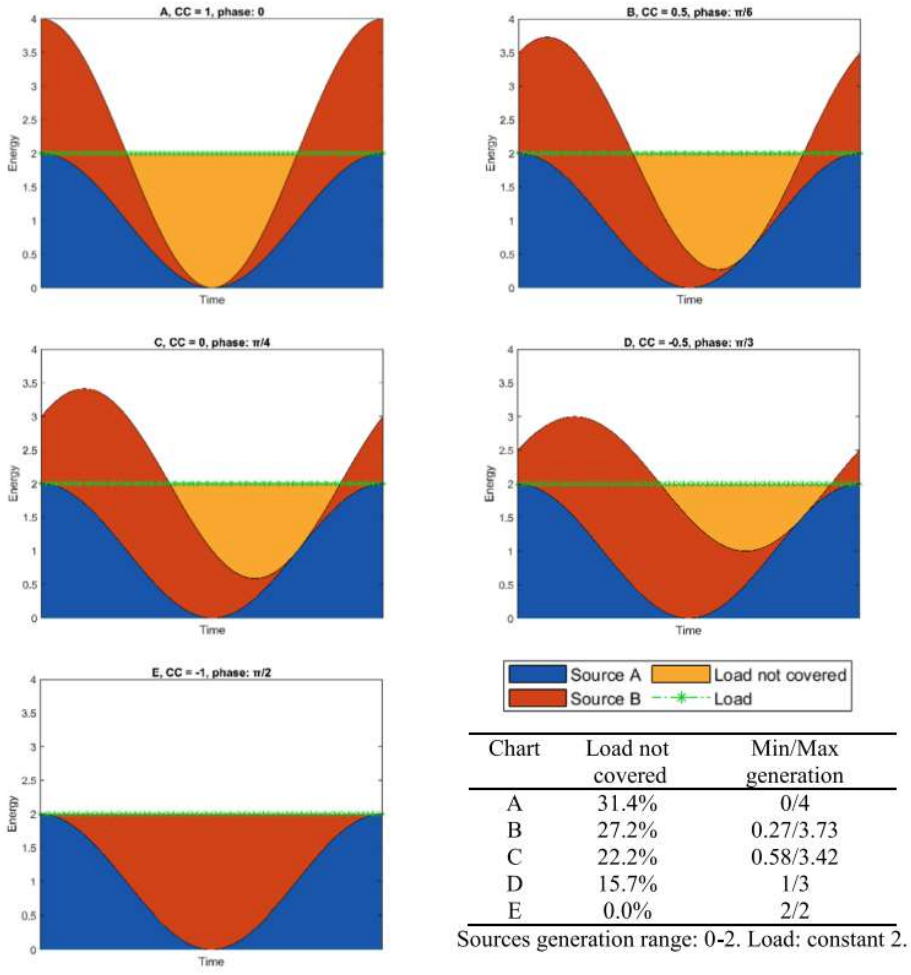

Chart	Load not covered	Min/Max generation
A	31.4%	0/4
B	27.2%	0.27/3.73
C	22.2%	0.58/3.42
D	15.7%	1/3
E	0.0%	2/2

Sources generation range: 0-2. Load: constant 2.

Fig 2-2 The concept of complementarity, explained by a sinusoidal signal. CC – correlation coefficient. Figure original from (Jurasz et al., 2020b).

The authors of (Yang et al., 2024) analyze the spatiotemporal distribution, evolution, and complementarity of wind and wave resources in China's coastal waters. Using ERA5 reanalysis data, the characteristics of wind speed and significant wave height over the past 60 years in different regions are evaluated. The results show decreasing trends in the Bohai Sea and the Yellow Sea, while the East China Sea and the South China Sea show increasing trends. The study introduces the concept of "energy utilization guarantee rate" (EUGR), which measures the synergy between wind and wave resources, showing that these areas are highly complementary for the joint development of green energy. This is particularly important in planning wind and wave energy projects on the southeast coast of China, where the complementarity effects are more significant.

In (López Prol et al., 2024), the authors study the technological, spatial and temporal complementarities between wind and solar energy in Europe, using a portfolio approach. Through the application of Markowitz portfolio theory, it is shown that the optimal combination of installed capacities of these energies in different European countries can increase the efficiency of the electricity system. The analysis shows that, by coordinating the installation of renewable energies between countries with heterogeneous generation patterns, a 22% increase in the capacity factor and a 26% reduction in hourly variability are achieved, which optimizes integration costs and accelerates the transition to clean energies. In addition, the integration of wind farms offers greater benefits due to regional climate diversity, while solar energy, having more homogeneous production profiles across Europe, brings more limited benefits. This approach can guide European energy policymakers towards creating more cost-effective and sustainable electricity systems.

The authors of (Jurasz et al., 2024) analyze the complementarity between solar and wind energy in North Africa. They examine how combining both energy sources can mitigate periods of low energy generation, known as energy droughts. In addition, they analyze how the North Atlantic Oscillation (NAO) influences these energy resources, highlighting that the coastal regions of North Africa show a strong potential for the complementarity of these energies. The study also concludes that the hybridization of solar and wind farms significantly reduces the occurrence of energy droughts and improves supply stability, which is crucial for the energy transition in the region.

In (Gao et al., 2024), the authors analyze the potential of hybrid wind and solar energy in mainland China, highlighting its ability to provide a more stable energy source at various time scales. Using high-resolution data from the ERA-5 reanalysis ensemble, the complementary effects between wind and solar energy are explored, showing that combining the two can increase renewable energy availability by 15% to 25%. The study also notes that adjusting the proportions of these energies can improve the stability of power generation. The results indicate that this combination is especially favorable in regions in northern China, such as Gansu and Inner Mongolia, where the synergy ratio between wind and solar exceeds 50%. This hybrid energy approach is key to overcoming the intermittency of renewable sources and ensuring a continuous energy supply, which is crucial for China’s sustainable energy future.

Finally, in (Muñoz-Pincheira et al., 2024), the authors evaluate the complementarity between solar and wind energy in the Chilean territory. The authors use the Spearman correlation coefficient to analyze hourly solar radiation and wind speed data between 2004 and 2016 at 176 geographic points. The

results show four main zones: the northern coast and valleys (zone A1) with a moderate positive correlation, the north mountain range (zone A2) with a weak negative correlation, the center-south of the country (zone B) with a mild negative correlation, and the extreme south (zone C) with almost zero correlation. This analysis is critical for planning hybrid energy generation facilities in Chile, contributing to the transition towards a 100% renewable matrix by 2030.

According to the literature review, numerous studies have been conducted on the optimal design of HRES that use artificial intelligence techniques, iterative methods, and specialized optimization software. These studies mainly focus on cost minimization, reliability maximization, or evaluating of technological configurations under different operating conditions. However, no study has explicitly quantified the impact of temporal complementarity between solar and wind sources on the optimal design of a stand-alone HRES with storage. Based on this gap, the following research question arises: ¿How does the degree of temporal complementarity between solar and wind resources influence the NPC and the LPSP in the optimal design of such systems?.

2.1.3 Goal and hypothesis

We aim to quantify the influence of temporal complementarity between wind and solar resources on the optimal design of a stand-alone hybrid renewable energy system with storage from micro to medium generation capacity (10MW).

The results provide relevant information for decision-making in territorial energy planning, especially in the transition towards renewable energies. We hypothesized that the evaluation parameters for the optimal design of a stand-alone wind-solar HRES system with storage vary depending on the temporal complementarity between the energy sources.

2.1.4 Limitations and applicability

This study analyzes the influence of temporal complementarity between solar and wind resources on the optimal design of off-grid HRES. In this context, it is crucial to recognize the following limitations of the approach adopted:

- Comparative approach, not global optimization: The implemented genetic algorithm does not guarantee obtaining the global optimum. Its primary function in this work is to compare solutions across different complementarity scenarios

consistently. It keeps the random generator seed constant (equal to the initial solution vector) to avoid bias due to stochastic variability.

- Simplified generation model: The main components of the system, such as photovoltaic panels, wind turbines, and batteries, are modeled, focusing on their generation and storage capacity. However, it does not consider the associated power electronics systems, such as inverters, MPPT controllers, and DC/DC converters. - Optimization of sizing, not operation: The model focuses on finding efficient design configurations for installed capacity (number of panels, turbines, and batteries), but does not consider dynamic optimization of operation or advanced control strategies.

- Off-grid system model: The system is assumed to operate autonomously, without connection to the electrical grid. This implies that the results do not consider possible energy exchanges with the interconnected system or factors such as nodal prices, backup tariffs, or incentive policies.

Despite these simplifications, the developed methodology applies to any geographic region, given that it explicitly incorporates scenarios with different levels of solar-wind complementarity (from $\rho = -0.95$ to $\rho = 0.95$). This allows the analysis to be extrapolated to territories with diverse climatic conditions, provided hourly irradiation and wind speed data are available to characterize local complementarity.

2.2 Methodology

A program is developed in OCTAVE to evaluate the influence of temporal complementarity between wind and solar sources in an HRES with storage. This program employs the metaheuristics of genetic algorithms to optimize the number of wind turbines, photovoltaic panels, and batteries needed to meet a specific energy demand, minimizing the NPC and ensuring compliance with the constraint of a maximum limit for the LPSP.

Different evaluations are designed to determine the impact of temporal complementarity by varying the degree of complementarity between the solar irradiation and wind speed series, keeping the total energy potential of both sources constant to meet a specific energy demand. Two scenarios are evaluated: the first considers a constant load that represents the typical energy consumption of an industry, while the second scenario focuses on a load representative of the consumption of a community of 150 people.

2.2.1 System Description

Fig 2-3 shows the architecture of the stand-alone HRES system, composed of a set of wind turbines (WT), photovoltaic panels (PV), and batteries (BS), each connected to its respective AC/DC or DC/DC converter, as needed. All components are integrated into a direct current bus (DC Bus), which supplies electrical power to meet a specific demand (Load).

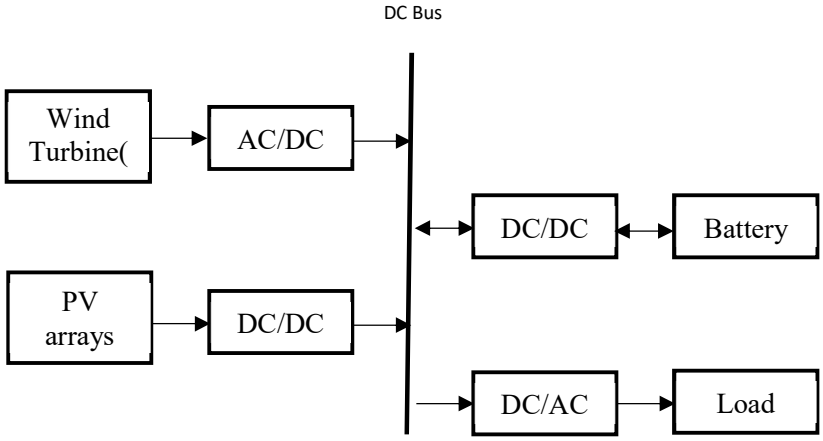

Fig 2-3 Block diagram of a hybrid wind/PV/Battery system.

2.2.2 Modeling of components

2.2.2.1 Wind Turbines

Wind turbines generate electricity from the availability of kinetic energy from the wind. The power generated by a wind turbine is calculated according to (2-1).

$$P_{WT,t}^{single}(v) = \begin{cases} 0, & \text{if } v < v_{\text{cut-in}} \text{ or } v > v_{\text{cut-out}} \\ \kappa_{WT} \cdot \left(\frac{v - v_{\text{cut-in}}}{v_{\text{rated}} - v_{\text{cut-in}}}\right)^3 \cdot \eta_{WT} \cdot \phi_{WT}, & \text{if } v_{\text{cut-in}} \le v < v_{\text{rated}} \\ \kappa_{WT} \cdot \eta_{WT} \cdot \phi_{WT}, & \text{if } v_{\text{rated}} \le v \le v_{\text{cut-out}} \end{cases} \quad (2\text{-}1)$$

Where,

$P_{WT,t}^{single}$: Power generated by one wind turbine.

$v\ \left[\frac{m}{s}\right]$: Hourly wind speed.

$v_{\text{cut-in}}\left[\frac{m}{s}\right]$: Minimum wind speed to start generating energy.

$v_{\text{rated}}\left[\frac{m}{s}\right]$: Nominal wind speed.

$v_{\text{cut-out}}\left[\frac{m}{s}\right]$: Maximum wind speed for safe operation.

$K_{\text{WT}}\ [kw]$: wind turbine nominal capacity.

$\eta_{\text{WT}}\ [\%]$: Wind turbine efficiency.

$\phi_{\text{WT}}\ [\%]$: Wind turbine availability factor.

2.2.2.2 Photovoltaic Panels

The power generated by a photovoltaic panel is calculated according to (2),

$$P_{\text{PV}} = \kappa_{\text{PV}} * \eta_{\text{PV}} * \phi_{PV} \tag{2-2}$$

Where,

$K_{\text{PV}}\ [kW]$: photovoltaic panel nominal capacity.

$\eta_{\text{PV}}\ [\%]$: Photovoltaic panel efficiency.

$\phi_{\text{PV}}\ [\%]$: Photovoltaic panel availability factor.

2.2.3 Mathematical Model

2.2.3.1 Decision variables:

x_1: total capacity of photovoltaic (PV) solar panels in kWp

x_2: total wind turbine (WT) capacity in kW

x_3: total battery storage capacity in kWh

2.2.3.2 Model parameters

C_{PV}: cost per kW of photovoltaic (PV) panels

C_{WT}: cost per kW of wind turbines

C_{BS}: cost per kWh of batteries

OM_{PV}: annual operation and maintenance cost of PV (initial cost fraction)

OM_{WT}: annual operation and maintenance cost of WT (initial cost fraction)

K_{PV}: photovoltaic panel nominal capacity

K_{WT}: wind turbine nominal capacity

K_{BS}: battery nominal capacity per unit

d: discount rate

L: project life (years)

$LPSP_{\max}$: maximum allowed value of LPSP

$FD = \frac{1-(1+d)^{-L}}{d}$: discount factor.

2.2.3.3 Input variables

$C_{\mathrm{load},t}$: energy demand per hour (kWh)

I_t : solar irradiation (kWh/m^2 hour)

v_t : wind speed (m^2/s)

Therefore, the mathematical model is expressed as follows,

$$\min \mathrm{NPC} = x_1 \cdot C_{\mathrm{PV}} + x_2 \cdot C_{\mathrm{WT}} + x_3 \cdot C_{\mathrm{Bat}} + (\mathrm{OM}_{\mathrm{PV}} \cdot x_1 \cdot C_{\mathrm{PV}} + \mathrm{OM}_{\mathrm{Wind}} \cdot x_2 \cdot C_{\mathrm{Wind}}) * FD \quad (2\text{-}3)$$

Subject to:

1. LPSP constraint:

$$\mathrm{LPSP} = \frac{\sum_{t=1}^{24} D_t}{\sum_{t=1}^{24} C_{\mathrm{load},t}} \cdot 100 \leq \mathrm{LPSP}_{max} \quad (2\text{-}4)$$

Where D_t is the energy deficit at hour *t*.

2. Definition of deficit in each hour:

$$D_t = max\left(0, C_{\text{load},t} - \left(E_{\text{PV},t} + E_{\text{WT},t} + E_{\text{Bat},t}\right)\right), \forall t \quad (2\text{-}5)$$

Where $C_{\text{load},t}$ is the hourly energy demand, $E_{\text{PV},t}$ the energy generated by photovoltaic panels on hour t and $E_{WT,t}$ the energy generated by wind turbines on hour t, and $E_{\text{Bat},t}$ the energy provided by the batteries on hour t.

3. Photovoltaic solar generation each hour:

$$E_{\text{PV},t} = x_1 \cdot I_t \cdot \eta_{\text{PV}} \cdot \phi_{\text{PV}}, \forall t \quad (2\text{-}6)$$

$$N_{\text{PV}} = \frac{x_1}{\kappa_{\text{PV}}} \quad (2\text{-}7)$$

Where,

$E_{\text{PV},t}$: total solar energy generated at hour t.

N_{PV}: number of photovoltaic panels

4. Wind power generation: $\mathbf{E_{WT,t}}$

Energy based on wind speed at hour t and total capacity of wind turbines x_2.

$$P_{\text{WT},t}^{single} = \begin{cases} 0 & \text{if } v_t < v_{\text{cut-in}} \text{ or } v_t > v_{\text{cut-out}} \\ \kappa_{\text{WT}} \cdot \left(\frac{v_t - v_{\text{cut-in}}}{v_{\text{rated}} - v_{\text{cut-in}}}\right)^3 \cdot \eta_{\text{WT}} \cdot \phi_{\text{WT}} & \text{if } v_{\text{cut-in}} \le v_t < v_{\text{rated}} \\ \kappa_{\text{WT}} \cdot \eta_{\text{WT}} \cdot \phi_{\text{WT}} & \text{if } v_{\text{rated}} \le v_t \le v_{\text{cut-out}} \end{cases} \quad (2\text{-}8)$$

$$E_{\text{WT},t}^{\text{single}} = P_{\text{WT},t}^{single} * 1h \quad (2\text{-}9)$$

$$E_{\text{WT},t} = N_{\text{WT}} \cdot E_{\text{WT},t}^{\text{single}} \quad (2\text{-}10)$$

$$N_{\text{WT}} = \frac{x_2}{\kappa_{\text{WT}}} \quad (2\text{-}11)$$

Where,

$E_{\text{WT},t}$: total wind energy generated by wind turbines at hour t.

$E_{\text{WT},t}^{\text{single}}$: energy generated by a single wind turbine at hour t.

N_{WT} : number of wind turbines.

5. Energy stored in batteries: $E_{\text{Bat},t}$

The battery bank is modeled using an hourly schedule that considers the charge/discharge efficiency (η_{bat}) and the total storage capacity x_3, defined as a decision variable within the optimization process. The stored energy at the end of each hour t is calculated according to the following expressions:

$$E_{\text{bat},t} = min(max(E_{\text{bat},pre,t}, 0), x_3) \tag{2-12}$$

$$E_{\text{bat},pre,t} = E_{\text{bat},t-1} + \eta_{\text{bat}} \cdot \left(E_{\text{total},t} - C_{load,t}\right) \tag{2-13}$$

$$E_{\text{curt},t} = max(0, E_{\text{bat},pre,t} - x_3) \tag{2-14}$$

$$N_{\text{BT}} = \frac{x_3}{\kappa_{\text{BS}}} \tag{2-15}$$

Where,

$E_{\text{bat},t}$: Energy stored in the batteries at the end of hour t, adjusted for its maximum capacity and previous state of charge.

$E_{\text{bat, pre},t}$: Battery energy before adjustment at time t. Adjusted by adding the excess energy generated in the current hour or subtracting the deficit if demand exceeds generation.

$E_{\text{total},t}$: Energy generated by the system (solar + wind) at hour t.

$C_{load,t}$: Load or demand for energy at hour t.

$E_{\text{curt},t}$: if the battery has more energy than it can store (i.e. $E_{\text{bat, pre},t} > x_3$) the excess energy cannot be stored.

N_{BT}: number of batteries.

Equation (2-12) starts from calculating the preliminary state of the battery $E_{,\text{bat, pre},t}$ which represents the theoretical charge level without capacity restrictions.

The final value $E_{\text{bat},t}$ is obtained by adjusting $E_{\text{bat},pre,t}$ to keep it within the physical limits of the system, i.e., not less than zero and not greater than x_3. When $E_{\text{bat, pre},t} > x_3$, some energy is not produced (curtailment) $E_{\text{curt},t}$, which allows quantifying the fraction of renewable generation not used due to saturation of the storage system.

6. Non-negativity constraints:

$$x_1, x_2, x_3 \geq 0 \tag{2-16}$$

2.2.4 Optimization procedure

We implement a genetic algorithm metaheuristic that is suitable for addressing optimization problems with complex constraints, such as battery storage capacity, solar panel and wind turbine performance, and compliance with a maximum loss of LPSP value. This choice is based on the inherent ability of genetic algorithms to explore non-linear and multidimensional search spaces, where interactions between variables are highly complex and objective functions are not necessarily continuous or differentiable. (Holland, 1992).

In the context of this study, the algorithm must balance several factors, such as minimizing system costs and meeting energy demand, resulting in a highly irregular solution space with multiple local optima. Genetic algorithms are particularly effective in addressing this challenge, as they simultaneously explore different regions of the search space, thus decreasing the probability of converging on suboptimal solutions. The filter-free genetic algorithm proposed by (Mahesh & Sandhu, 2020) is adapted. To ensure reproducible results and allow for consistent comparisons between different levels of complementarity, the algorithm was set to a constant random seed (value 42) throughout the primary analysis. This choice isolates the effect of the complementarity index, preventing stochastic variability in the algorithm from influencing the observed differences between scenarios. **Fig 2-4** shows the flowchart of the implemented optimization algorithm.

2.2.4.1 Genetic algorithm (GA) performance

The performance of the GA was evaluated using three key metrics: convergence speed, stability, and computational requirements. The algorithm showed efficient convergence, reaching stable solutions in less than 20 generations with a population size of 200, indicating adequate exploration and refinement of the solution space. Stability was verified through simulations with different seeds, revealing low NPC variability and confirming the method's robustness. Finally, the model was implemented in GNU Octave and ran on a mid-range computer (Intel Core i7 processor, 16 GB RAM). Each full simulation, including LPSP evaluation, NPC calculation, and graphing, took on average between 1.5 and 3 minutes per scenario. This makes the algorithm suitable for comparative studies with multiple simulations, without requiring advanced computational resources.

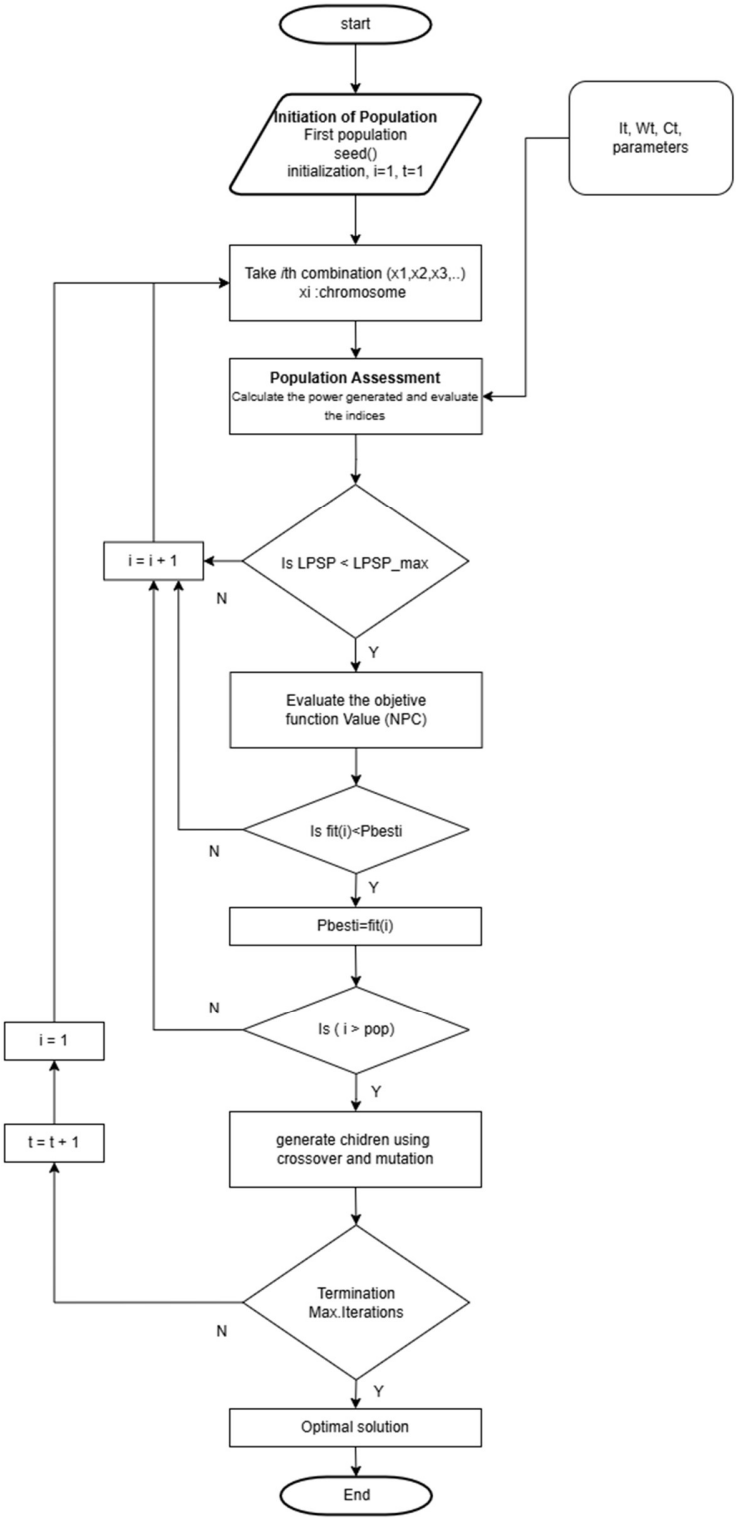

Fig 2-4 Optimization algorithm flowchart.

2.2.5 Wind-Solar Complementarity

To evaluate the influence of the complementarity between wind and solar energy on the optimal design of a stand-alone HRES system, a typical 24-hour solar irradiation curve corresponding to the city of Calama, Chile, was used (Ministerio de Energía, n.d.). From this, various wind speed curves were generated, ensuring that all of them maintained the same wind energy potential but with different levels of complementarity concerning the solar irradiation curve, according to the values presented in ***Table 2-2***. The complementarity was measured using the Spearman correlation index.

Solar irradiation data are approximated using (2-17):

$$I(x) = \begin{cases} 0 & \text{if } 0 \leq x \leq 5, \\ 0.0001466x^4 - 0.007337x^3 + 0.1088x^2 - 0.4178x + 0.244 & \text{if } 5 < x < 21, \\ 0 & \text{if } 21 \leq x \leq 23. \end{cases} \quad \text{(2-17)}$$

Table 2-2 shows the classification of the different complementarity ranges in wind and solar sources.

Table 2-2 *Interpretation of the correlation coefficient. Extracted from (Santabárbara, 2019).*

Correlation	Coefficient' interpretation
-1 a -0.7	Strongly negative
-0.7 a -0.3	Moderately negative
-0.3 a 0	Weakly negative
0	No relationship
0 a 0.3	Weakly positive
0.3 a 0.7	Moderately positive
0.7 a 1	Strongly positive

Note that in each of the following cases, the wind potential of each curve is 1900 kWh using (2-18).

$$\sum_{x=0}^{23} \frac{1}{2} W_i(x)^3 \ = 1900 \quad \text{(2-18)}$$

2.2.5.1 *Strong positive correlation*

A wind speed curve is fitted such that the Spearman correlation index is $\rho = 0.95$.

$$W_1(x) = -0.0454 * (x - 11.5)^2 + 7 \quad \text{(2-19)}$$

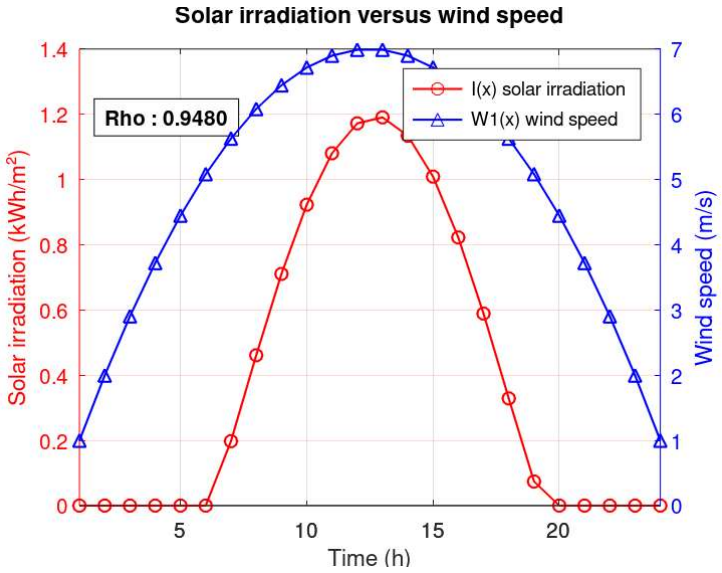

Fig 2-5 Strong positive correlation (ρ=0.95) between wind and solar sources.

2.2.5.2 *Moderate positive correlation*

A new wind speed curve is fitted such that the Spearman correlation index is $\rho = 0.5$.

$$W_2(x) = 0.879 * (-0.005 * (x - 11.5)^2) + 0.212 \cdot \sin(0.3x) + 5.605 \quad \text{(2-20)}$$

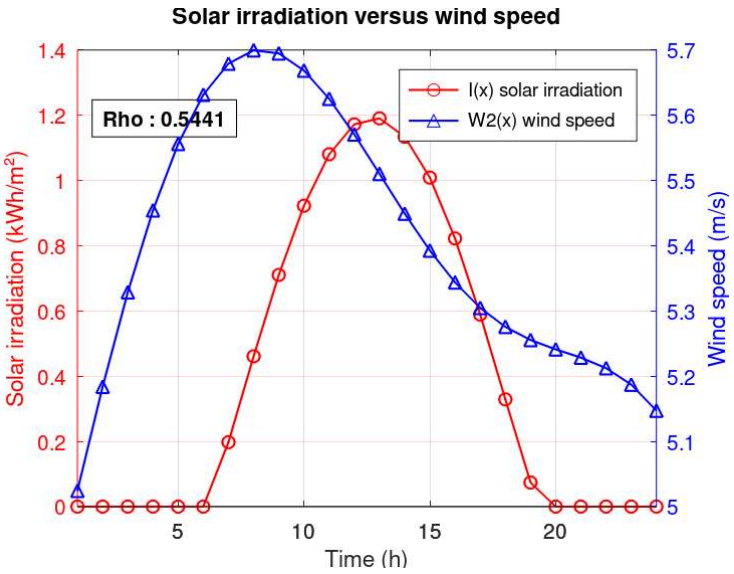

Fig 2-6 Moderate positive correlation (ρ=0.54) between wind and solar sources.

2.2.5.3 Weak negative correlation

A wind speed curve is fitted such that the Spearman correlation index is $\rho = -0.29$.

$$W_3(x) = 0.486 * sin(0.5x) + 0.297 * cos(0.35x) + 5.315 \quad (2\text{-}21)$$

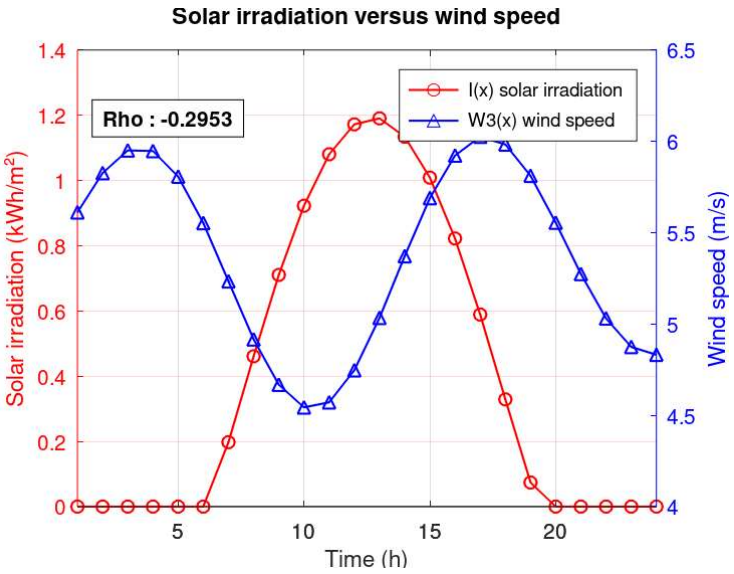

Fig 2-7 Weak negative correlation (ρ=-0.29) between wind and solar sources.

2.2.5.4 *Moderate negative correlation*

A wind speed curve is fitted such that the Spearman correlation index is $\rho = -0.63$.

$$W_4(x) = 0.145 * (5.2 - 0.8 * \sin(0.3x)) + 0.402 * \cos(0.32x) + 4.5 \quad (2\text{-}22)$$

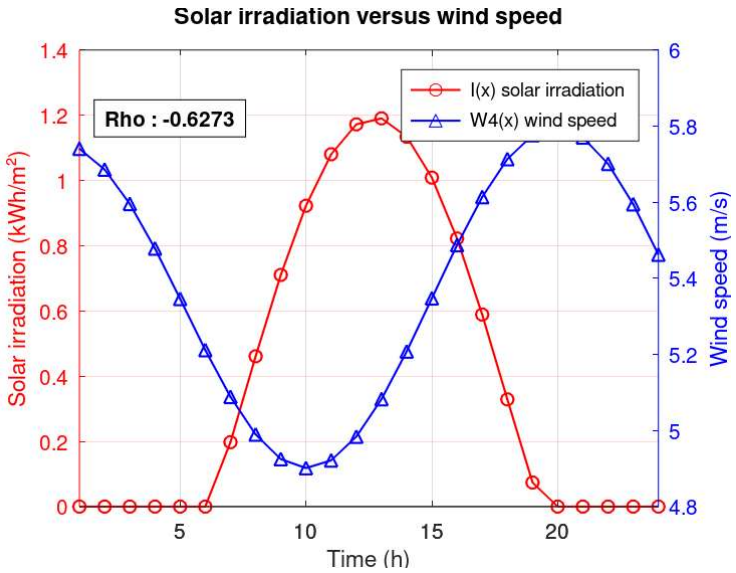

Fig 2-8 Moderate negative correlation (ρ=-0.63) between wind and solar sources.

2.2.5.5 *Strong negative correlation*

A wind speed curve is fitted such that the Spearman correlation index is $\rho = -0.95$.

$$W_5(x) = 0.0379 \cdot (x - 11.5)^2 + 3.077 \quad (2\text{-}23)$$

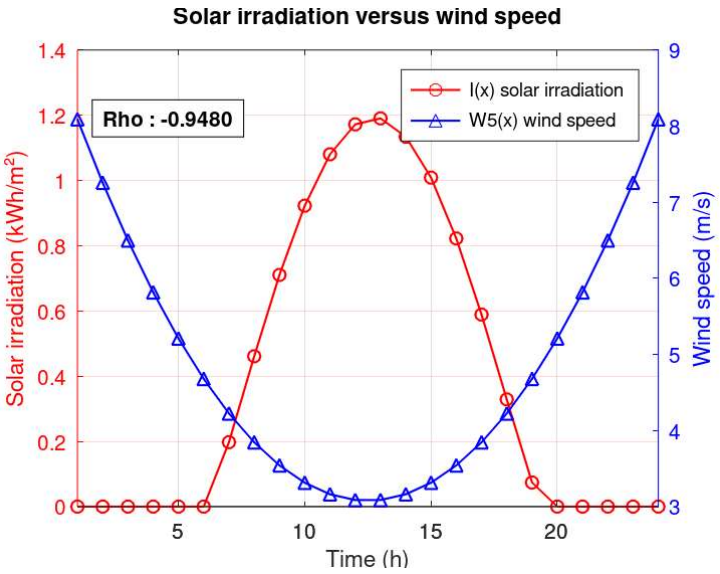

Fig 2-9 Strong negative correlation (ρ=-0.95) between wind and solar sources.

Figures 2-5 to 2-9 show different wind speed curves with the same daily energy potential (1900 kWh). These curves exhibit varying levels of temporal complementarity with the solar irradiation curve, measured using Spearman's coefficient (ρ). Figure 2-5 shows a strongly positive correlation (ρ = 0.95), which implies low complementarity; in contrast, Figure 2-9 displays a strongly negative correlation (ρ = –0.95), indicating maximum temporal complementarity between both sources. The intermediate figures (2-6 to 2-8) represent progressively more negative correlations, with ρ values of 0.54, –0.29, and –0.63, respectively. These curves allow for the analysis of how the degree of solar–wind complementarity impacts the design and performance of stand-alone hybrid renewable energy systems with storage.

2.3 Results

Two tests were proposed to assess whether the complementarity between wind and solar energy impacts the optimal design of a stand-alone HRES system. The first is based on a constant load that simulates the energy consumption of an industry, while the second corresponds to a typical consumption profile of a community of 150 people. For both scenarios, a maximum LPSP < 5% is considered as a constraint. The costs per technology were obtained from the National Energy Commission (Energia, n.d.). The rest of the relevant parameters

used are the following: $C_{\mathrm{PV}} = 871\,\frac{\$}{kwp}$, $C_{WT} = 1255\,\frac{\$}{kw}$, $C_{BS} = 150\,\frac{\$}{kwh}$, $OM_{\mathrm{PV}} = 2\%$ annual, $OM_{\mathrm{WT}} = 3\%$ annual, $\kappa_{\mathrm{PV}} = 0{,}4\ kW$ (400W photovoltaic panels), $\kappa_{\mathrm{WT}} = 100\ kW$ (100 kW wind turbine), $\kappa_{\mathrm{BS}} = 10\ kWh$, $\mathrm{LPSP}_{max} = 5\%$, pop_size (t) = 200 (population size), and max_gen (i) = 20 (maximum generations).

2.3.1 Constant load

A constant load of 61.25 kWh, representative of industrial consumption, is established. The total daily demand is 1470 kWh. The optimal stand-alone HRES configuration is calculated for each wind-solar complementarity combination.

Table 2-3 Results of optimizing an HRES configuration for a constant load considering different degrees of temporal complementarity of the wind-solar sources.

Variable or indicator	Unit	$\boldsymbol{\rho = 0.95}$	$\boldsymbol{\rho = 0.54}$	$\boldsymbol{\rho = -0.29}$	$\boldsymbol{\rho = -0.63}$	$\boldsymbol{\rho = -0.95}$
$\boldsymbol{x_1}$	kWp	4,125	303	1,287	1,088	692
$\boldsymbol{x_2}$	kW	36,371	5,189	3,557	4,517	2,224
$\boldsymbol{x_3}$	kWh	237	7,673	1,566	958.59	1,678
$\boldsymbol{N_{\mathrm{PV}}}$	-	10,314	757	3,219	2,722	1,731
$\boldsymbol{N_{\mathrm{WT}}}$	-	364	52	36	46	23
$\boldsymbol{N_{\mathrm{BS}}}$	-	24	768	157	96	168
NPC	$	$67,234,821	$10,428,003	$7,769,391	$9,116,993	$4,839,986
LCOE	$/kWh	0.8183	1.3543	0.6566	0.782	0.6279
LPSP	%	14.71	4.24	3.3	3.66	2.45
D	kWh	16,790	0	0	205.06	0

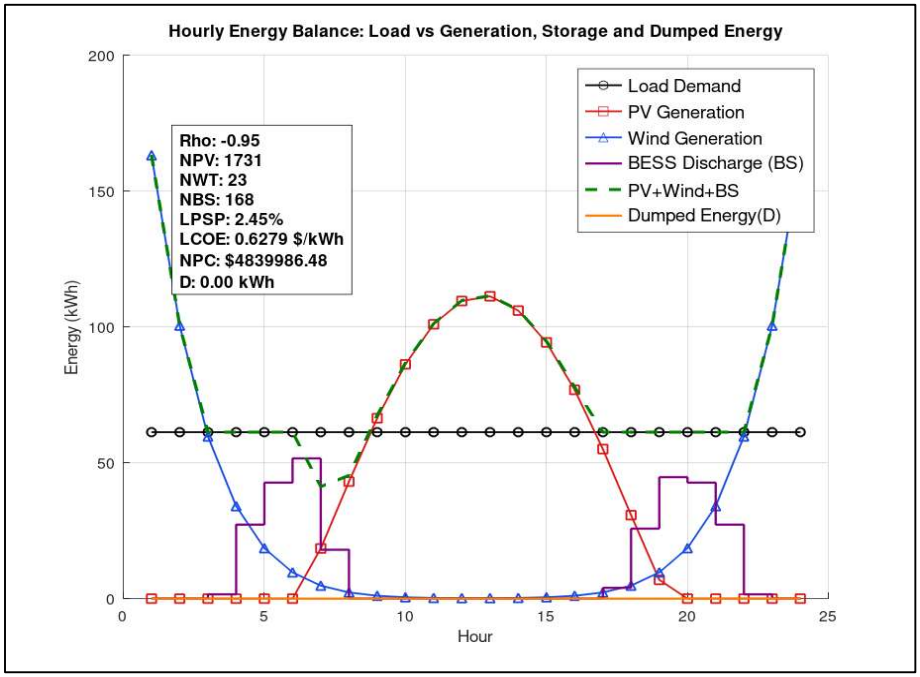

Fig 2-10 Constant load, ρ=-0.95.

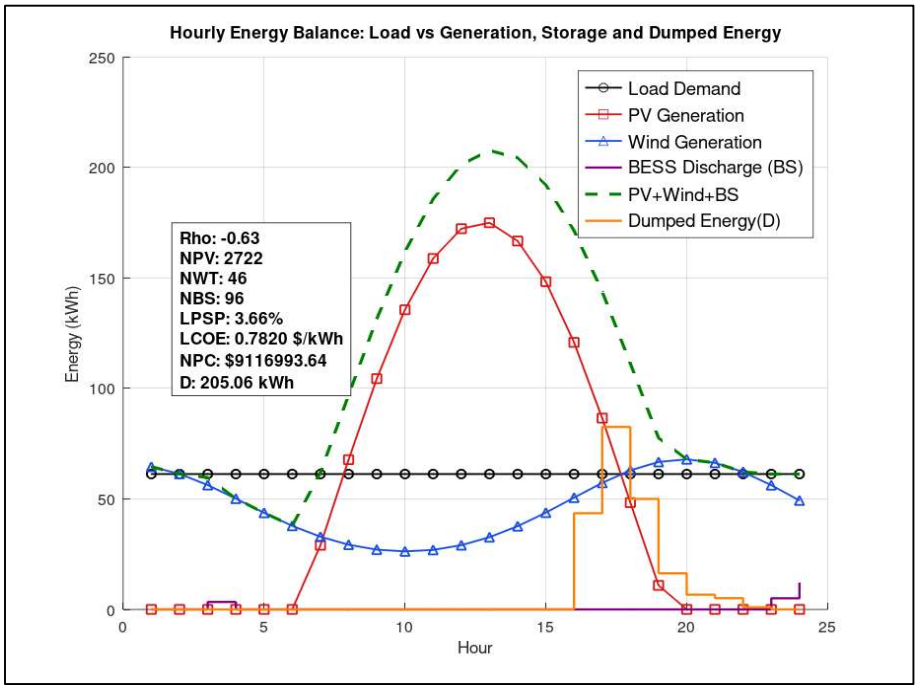

Fig 2-11 Constant load, ρ=-0.63.

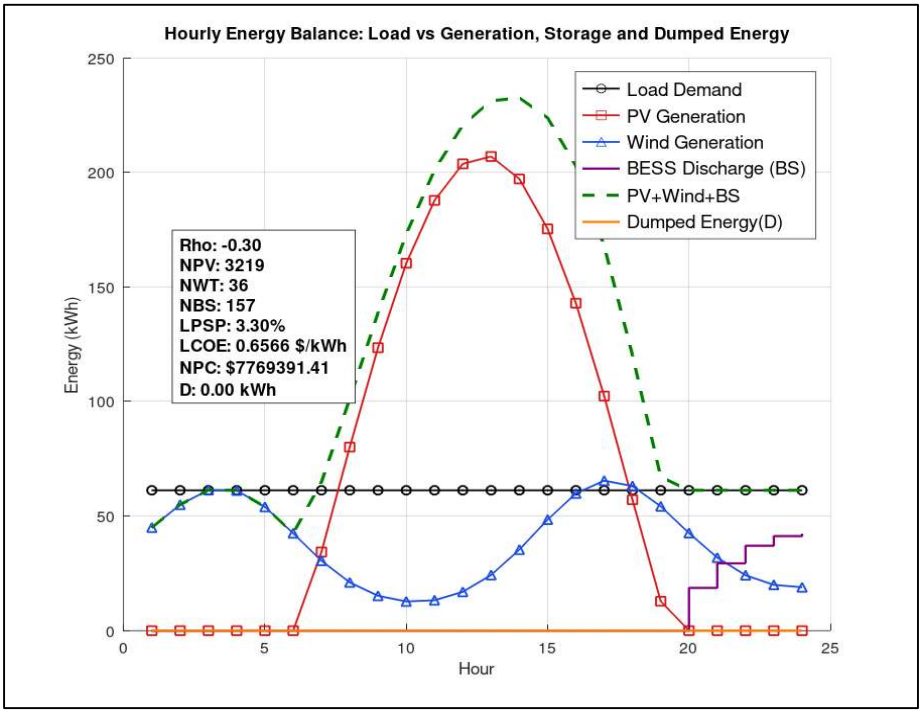

Fig 2-12 Constant load, ρ=-0.29.

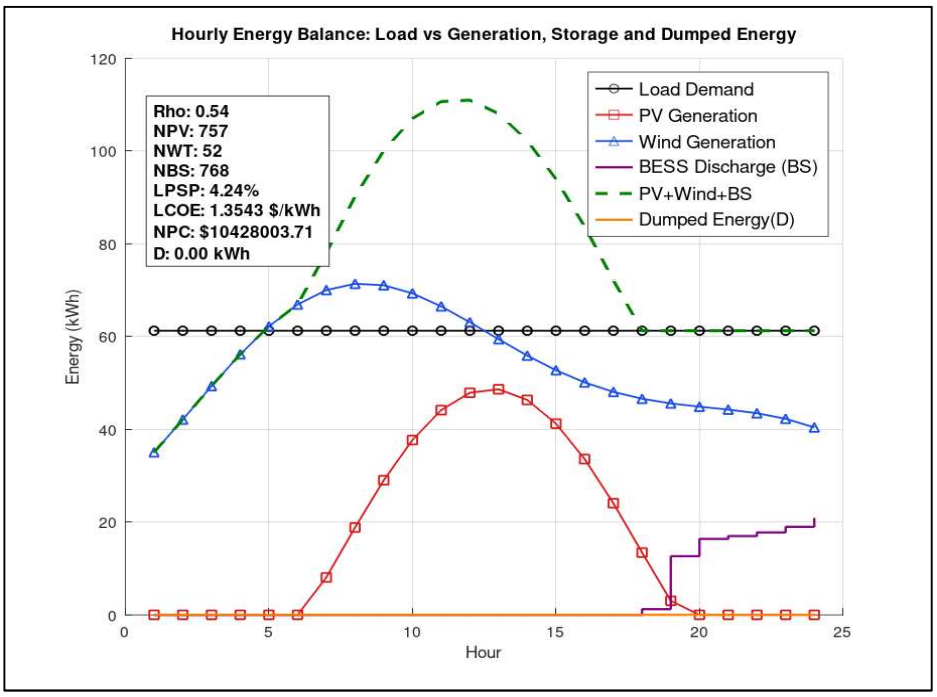

Fig 2-13 Constant load, ρ=0.54.

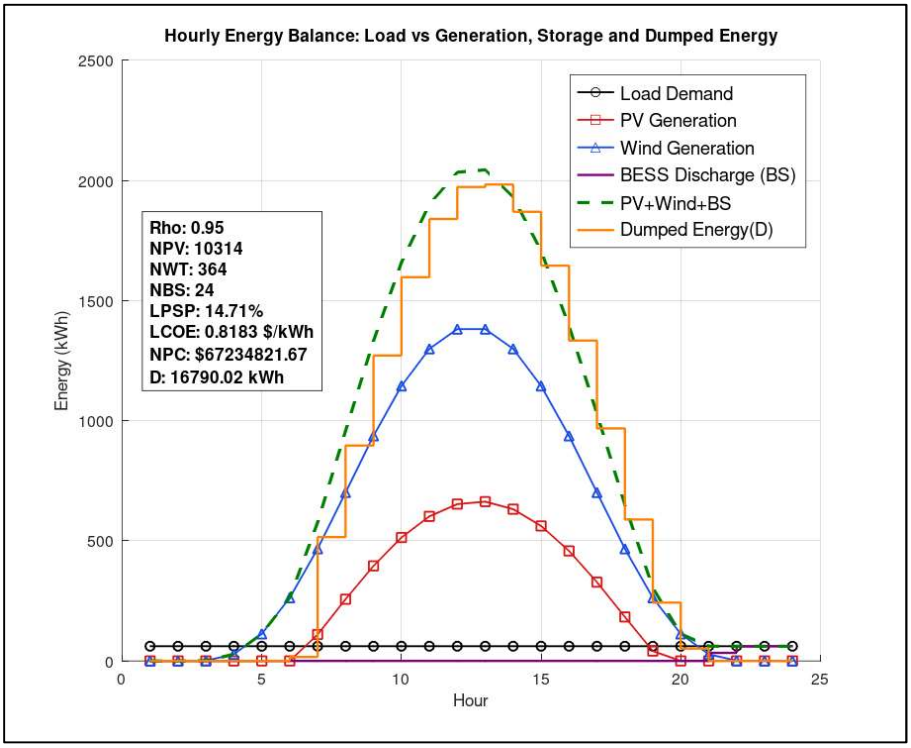

Fig 2-14 Constant load, ρ=0.95.

The results indicate that as the correlation coefficient ρ decreases—that is, as the temporal complementarity between solar and wind resources increases—a significant reduction is observed in both the NPC and the LCOE. This economic improvement is accompanied by improved technical performance, reflected in a LPSP and reduced curtailment.

In particular, the scenario with ρ = –0.95 (see **Fig 2-10**), which represents high negative complementarity, achieves the best overall performance, with an NPC of $4,839,986 and an LCOE of $0.6279/kWh, along with an LPSP of only 2.45% and no energy spillage. In contrast, the case with ρ = 0.95 (see **Fig 2-14**), characterized by low complementarity, requires system oversizing, presents considerable effluent (16,790 kWh), and achieves the worst economic results, with an LCOE of $0.8183/kWh. In this scenario, the LPSP rises to 14.12%, as there is no possible configuration capable of meeting the required threshold of LPSP < 5%.

The decrease in the NPC with increasing complementarity is explained by the reduced need to incorporate wind turbines to cover hours without solar generation. Similarly, the improvement in the LPSP is because wind generation,

complementary to solar, allows not only the load to be covered in real time, but also the batteries to charge to supply periods of deficit, as illustrated in **Fig 2-10.**

2.3.2 Variable Load

A typical consumption variable load is established for a community of 150 people. The total daily demand is 1470 kWh. The optimal stand-alone HRES configuration is calculated for each combination of wind-solar complementarity.

The results obtained for the variable load case under an LPSP threshold < 5% show that the complementarity between renewable resources does not significantly impact the economic or technical indicators of the hybrid system. As shown in Table 4, in all the ρ scenarios analyzed, from low complementarity (ρ = 0.95) to high complementarity (ρ = –0.95), the optimal system configuration remains unchanged, with one wind turbine, 2,742 photovoltaic panels, and 221 batteries, resulting in a NPC of $1,585,025 and a very similar LCOE between cases (varying between $0.2408 and $0.2414/kWh). Furthermore, no energy is dumped, and the LPSP remains around 3.5%.

This stability in the results can be explained by the shape of the variable load curve (see **Fig 2-15**). Since minimum demands are concentrated during nighttime hours (between 00:00 and 06:00), the system can afford a certain degree of supply loss during this period without exceeding the imposed LPSP limit. Consequently, optimization favors solar generation during the day, when demand is highest, and allocates part of this energy to battery charging to cover evening peaks partially. By prioritizing daytime and evening demand fulfillment, the optimal configuration remains independent of the degree of complementarity between solar and wind resources.

Table 2-4 Results of optimizing an HRES configuration for a variable load considering different degrees of temporal complementarity of wind-solar sources.

Variable or indicator	Unit	$\rho = 0.95$	$\rho = 0.54$	$\rho = -0.29$	$\rho = -0.63$	$\rho = -0.95$
x_1	kWp	1097	1097	1097	1097	1097
x_2	kW	36	36	36	36	36
x_3	kWh	2205	2205	2205	2205	2205
N_{PV}	-	2742	2742	2742	2742	2742
N_{WT}	-	1	1	1	1	1
N_{BS}	-	221	221	221	221	221
NPC	$	$1,585,025	$1,585,025	$1,585,025	$1,585,025	$1,585,025
LCOE	$/kWh	0.2408	0.2414	0.2414	0.2414	0.2408
LPSP	%	3.71	3.6	3.53	3.57	3.32
D	kWh	0	0	0	0	0

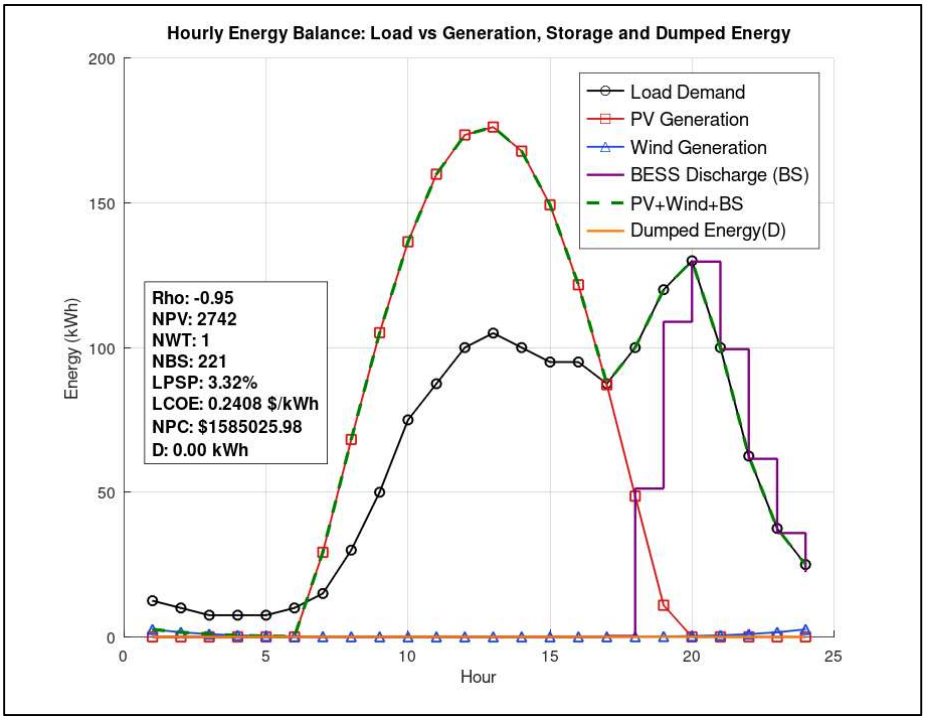

Fig 2-15 Variable load, ρ= {-0.95;-0.65;-0.29;0.50;0.94}.

This demonstrates that, under variable load conditions with moderate reliability constraints (LPSP < 5%), temporal complementarity between renewable sources does not significantly influence the optimal system design, as the model tolerates supply failures during low-demand hours without compromising the objective of minimizing the NPC.

The results for the variable load case change significantly when a higher level of demand fulfillment is required, that is, when a stricter constraint is imposed on the LPSP. As the allowable LPSP value is reduced, sensitivity analysis shows that complementarity between renewable sources becomes more relevant to system performance.

2.3.3 Sensitivity analysis

To evaluate the impact of key parameters on the hybrid system's economic performance, a sensitivity analysis was performed considering three variables: the LPSP (Loss of Power Supply Probability), the battery cost ($/kWh), and the discount rate (%). This analysis was carried out specifically for a variable load curve, representative of a community where demand is low at night and peaks during midday and afternoon. Each variable was modified independently, holding the others constant, to observe their effect on the NPC.

2.3.3.1 Changes on maximum LPSP allowed (%)

A sensitivity analysis was performed on the LPSP parameter, evaluating four levels of system reliability constraints: <5%, <3%, <1%, and 0%. For this analysis, the battery cost (CBS) was constant at $150/kWh, and the discount rate (r) was 5%. Furthermore, the study was conducted under different scenarios of temporal complementarity between solar and wind resources, represented by different values of the coefficient ρ.

The LPSP defines the maximum percentage of demand that the renewable hybrid system cannot meet. Therefore, reducing its allowable value increases the energy coverage requirement, directly impacting the optimal design and system cost. This analysis allows us to observe how complementarity becomes more relevant as stricter reliability constraints are imposed.

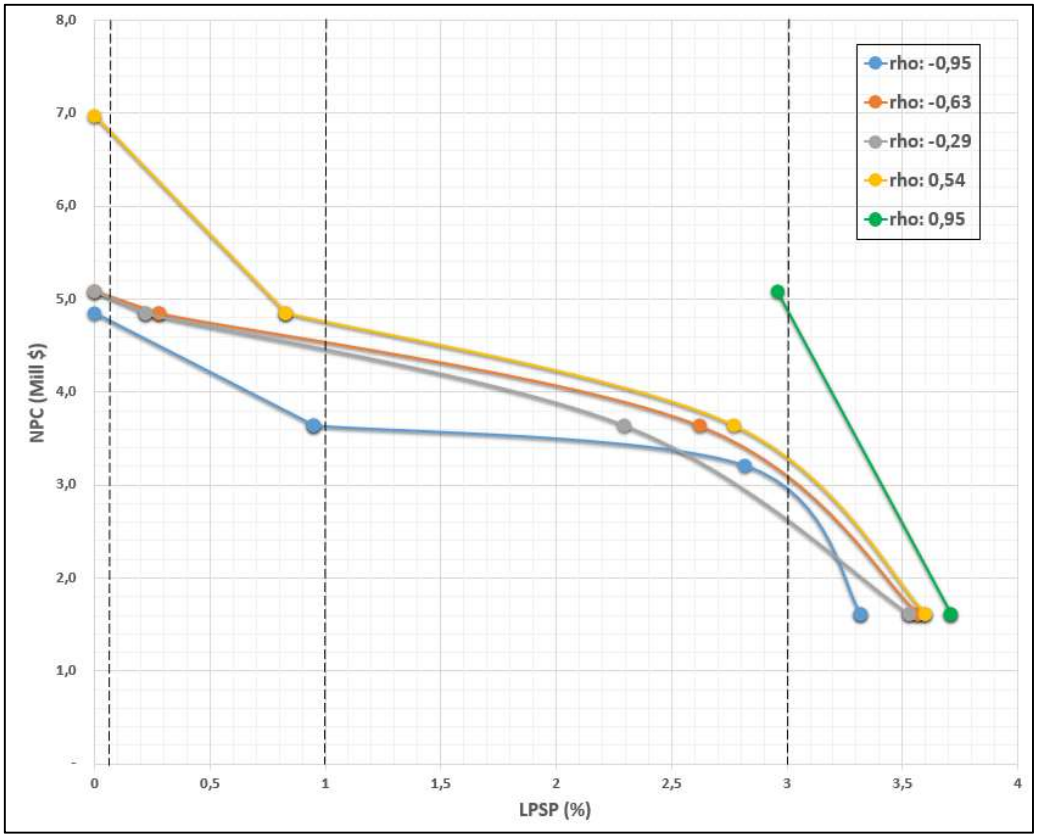

Fig 2-16 NPC (Mill$) versus LPSP variation (%) for different values of ρ (rho).

Fig 2-16 shows the evolution of the NPC as a function of the maximum allowable load shedding level (LPSP) for different levels of complementarity (ρ), holding the battery cost and the discount rate constant. It is observed that, in general, by relaxing the reliability constraint (higher allowed LPSP), the NPC decreases in all scenarios, given that lower installed capacities are required to supply demand. However, as a lower LPSP (higher reliability) is required, the differences between scenarios of different complementarity become more pronounced. In particular, the scenario with ρ = –0.95 (high complementarity) maintains lower NPCs even with stricter constraints. In contrast, the case with ρ = 0.95 (low complementarity) requires greater investment to meet the same levels of reliability. These results confirm that complementarity between renewable sources becomes more critical as greater demands are placed on energy supply reliability.

2.3.3.2 Changes to CBS (cost of batteries).

Sensitivity analysis for battery costs was performed by holding the discount rate constant (5%) and varying the battery cost between $100, $150, and $200/kWh. Different reliability levels represented by the LPSP (less than 5%, 3%, 1%, and 0%) and different levels of temporal complementarity between renewable sources (ρ) were considered.

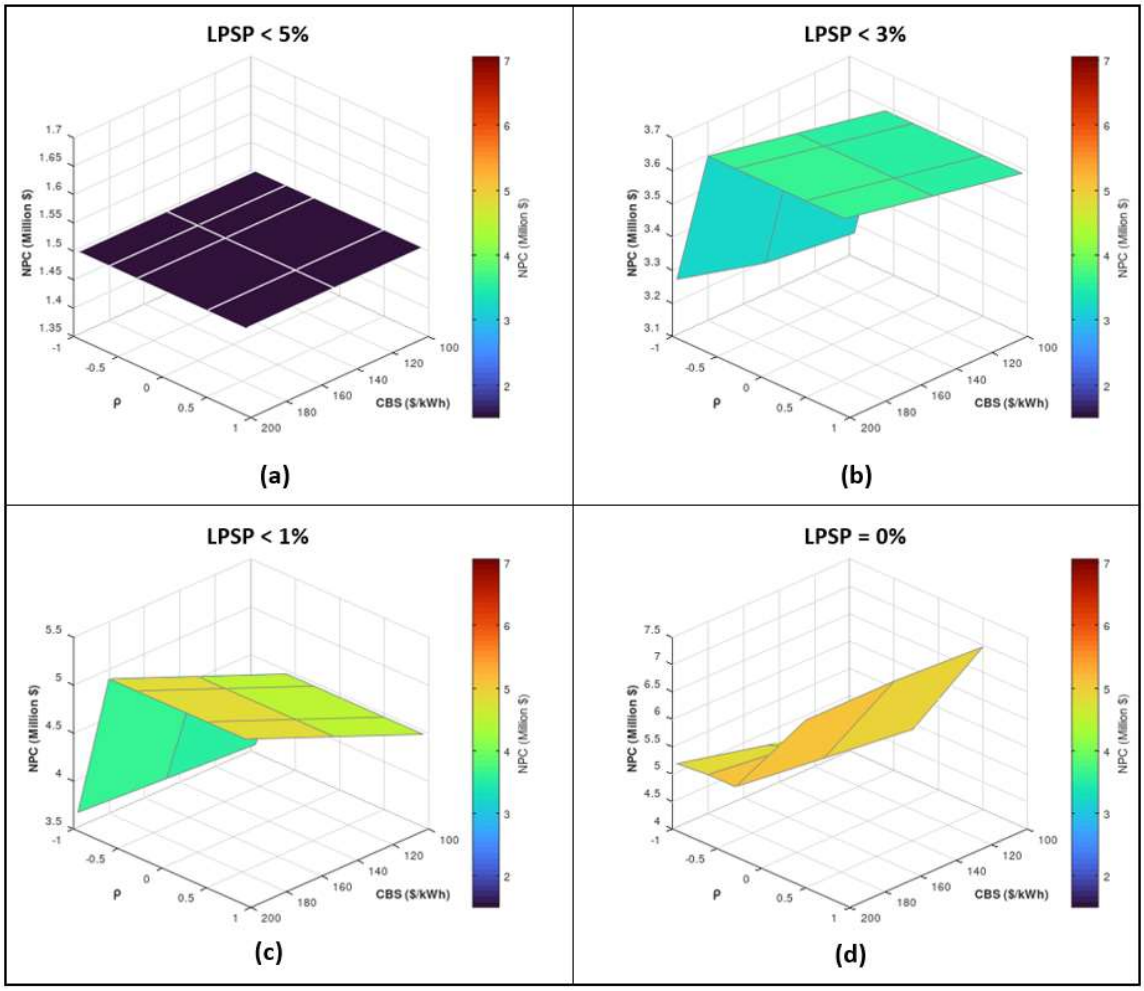

Fig 2-17 Sensitivity analysis of the NPC as a function of the battery cost (CBS) and the complementarity ρ, for different reliability levels defined by the LPSP. (a) LPSP < 5%, (b) LPSP < 3%, (c) LPSP < 1%, (d) LPSP = 0%.

The results, shown in **Fig 2-17**, indicate that as the LPSP becomes more stringent, the impact of battery costs on NPC becomes more pronounced. NPC

values remain constant for LPSP < 5% (**Fig 2-17**a) because the optimal system configuration does not require a large storage capacity. However, in scenarios with higher reliability demands (LPSP < 3%, < 1%, and = 0%), NPC increases significantly with increasing CBS, especially for low complementarity values (positive ρ). Higher reliability requires more energy storage, and its cost directly impacts NPC.

Furthermore, at all LPSP levels, scenarios with high complementarity (negative ρ) have lower NPC than scenarios with lower complementarity, confirming that complementarity between sources allows cost reduction by reducing dependence on storage. Consequently, the analysis highlights the importance of considering storage price and source complementarity when designing hybrid systems with high reliability standards.

2.3.3.3 Changes to discount rate r (%).

A sensitivity analysis of the NPC was performed with variations in the discount rate (r), considering values of 10%, 5%, and 1%, holding the other parameters constant: a battery cost of $150/kWh and a variable load with different reliability levels (LPSP < 5%, 3%, 1%, and 0%). The results are presented in **Fig 2-18**.

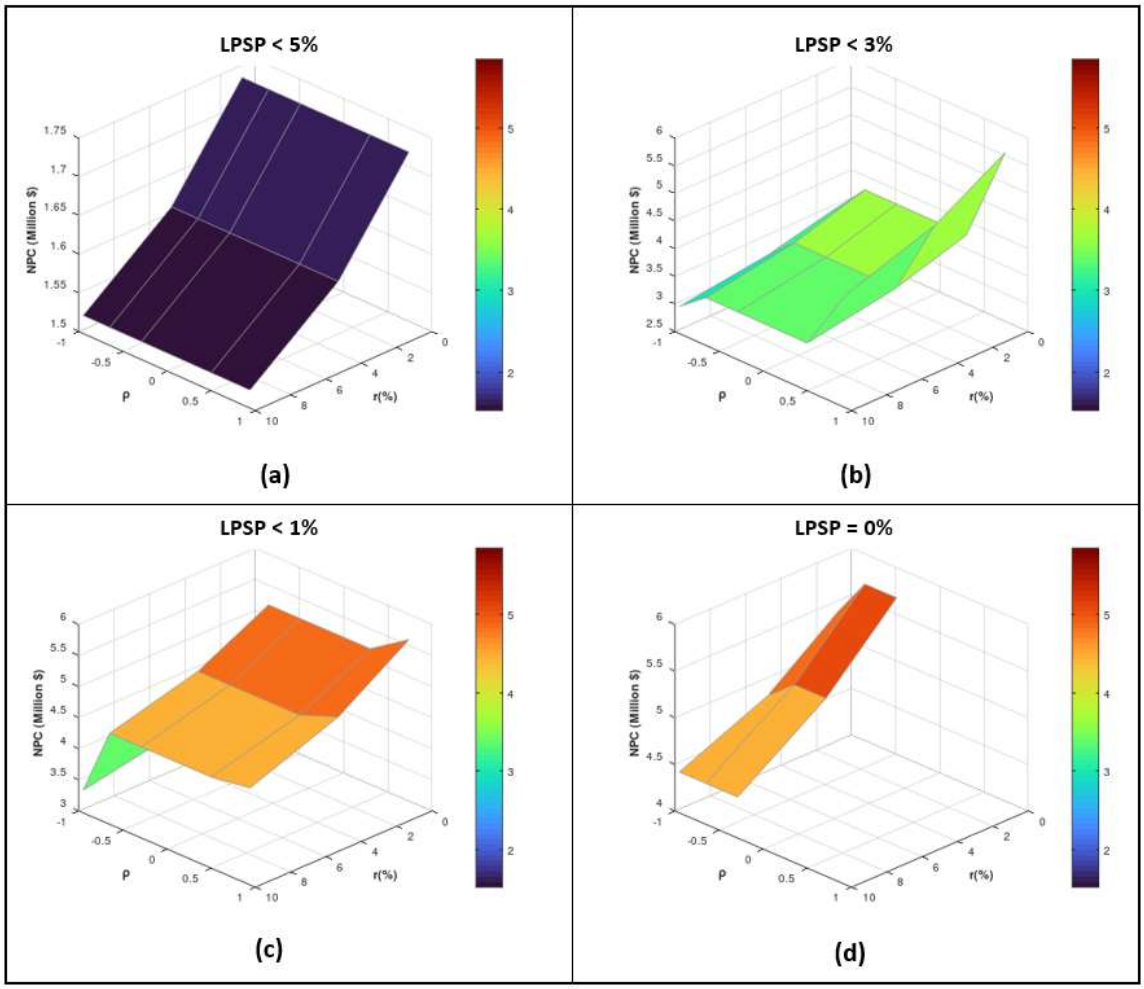

Fig 2-18 NPC sensitivity as a function of the discount rate (r) and complementarity (ρ) for different levels of LPSP: (a) LPSP < 5%, (b) LPSP < 3%, (c) LPSP < 1%, and (d) LPSP = 0%.

The results show that the discount rate increasingly influences the NPC value as reliability conditions become more stringent. At LPSP < 5%, the impact is marginal, while at LPSP = 0%, greater sensitivity is observed: a reduction in the discount rate from 10% to 1% generates a significant increase in the NPC, because future cash flows are not discounted as intensively and, therefore, the present value of future costs is higher. Furthermore, the complementarity between wind and solar sources maintains its positive effect on system performance, especially when a lower LPSP is required. In all discount rate scenarios, a higher degree of complementarity (more negative ρ) allows for lower NPC values, as

generation is distributed more efficiently throughout the day, reducing the need to oversize components.

However, the discount rate's effect is considerably smaller than battery cost. While the discount rate affects the valuation of future cash flows, the storage cost directly impacts the initial investment and system sizing, making it a more decisive factor. Therefore, in the design of off-grid HRES, battery cost represents a much more critical optimization level than the discount rate.

2.3.4 Statistical Analyses

In metaheuristic algorithms, such as the genetic algorithm used in this study, the seed controls the random number generator that defines both the starting point of the search (initial vector) and the stochastic behavior of the evolutionary process. To ensure reproducible results and allow for valid comparisons across different levels of complementarity, a constant seed (seed 42) was used in this work during the primary analysis. This decision guarantees that the differences observed in the results are not due to the randomness inherent in the algorithm, but solely to variations in the complementarity index.

To evaluate the statistical significance of the differences observed in the NPC resulting from the different complementarity conditions, a one-way analysis of variance (ANOVA) was performed. This analysis was based on a series of additional simulations, in which the genetic algorithm seed values varied (10 simulations per scenario) while holding the rest of the design parameters constant. Specifically, three representative levels of temporal complementarity between renewable sources were compared, characterized by correlation coefficients $\rho = -0.95$, $\rho = -0.29$, and $\rho = 0.5$ (see **Table 2-5**).

The analysis considered a variable hourly demand curve representative of a community with a residential profile, and a strict reliability constraint of LPSP = 0% was imposed.

ANOVA indicated statistically significant differences between the groups ($F = 45.81$, $p < 0.001$), which confirms that complementarity has a relevant effect on the NPC value, even considering the variability associated with the solutions delivered by the algorithm. **Fig 2-19** shows the corresponding box plots, where it can be observed that the higher the complementarity (more negative ρ), the NPC values tend to be lower and less dispersed. In contrast, the NPCs are higher for low complementarity ($\rho = 0.5$) and have higher variability.

This result reinforces the conclusion that temporal complementarity between renewable resources improves system performance and contributes to more economically stable and reliable solutions, regardless of the heuristic algorithm's starting point.

Table 2-5 NPC results based on different seeds used in the genetic algorithm for three levels of complementarity (ρ = –0.95, –0.29, and 0.5).

		NPC ($)		
Simulation	**Seed**	**ρ= -0.95**	**ρ= -0.29**	**ρ= 0.5**
1	42	4,846,930	5,088,805	6,967,880
2	1	4,944,320	4,944,319	9,067,321
3	10	3,442,060	5,673,068	8,116,641
4	15	5,304,641	6,615,664	6,615,664
5	20	3,990,440	6,194,326	7,559,987
6	25	3,086,374	3,969,872	8,285,999
7	35	3,876,680	5,811,760	7,340,364
8	40	3,688,535	5,415,291	6,602,672
9	45	3,911,022	4,830,477	8,066,771
10	50	4,673,417	4,673,417	10,048,179

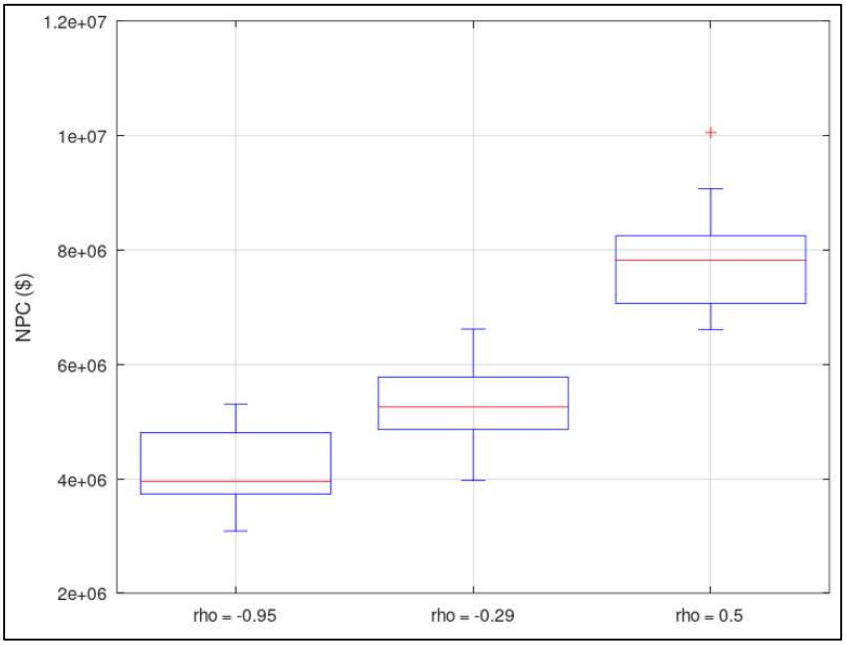

Fig 2-19 Box plot of the NPC for different values of the complementarity index (ρ - rho), considering 10 simulations with different seeds for each scenario.

2.3.5 Environmental benefits: Potential reduction of CO_2 emissions

One of the main indirect benefits of optimal HRES design is the reduction of greenhouse gas emissions, particularly carbon dioxide (CO_2). To estimate this environmental impact, the reduction in carbon dioxide (CO_2) emissions was estimated considering two reference scenarios: diesel generation (off-grid) and supply from the Chilean national electricity grid (on-grid).

(a) Comparison with diesel generation

A typical emission factor of 0.7 kg CO_2/kWh is assumed for diesel generators. Since the dimensioned HRES supplies 1470 kWh/day, the estimated daily reduction is:

$$Daily\ reduction = 1{,}470\ kWh * 0.7\ \frac{kg\ CO_2}{kWh} = 1{,}029\ \frac{kg\ CO_2}{day} \quad (2\text{-}24)$$

$$Annual\ reduction = 1{,}029\ \frac{kg\ CO_2}{day} * 365\ days = 375{,}585\ \frac{kg\ CO_2}{year} \quad (2\text{-}25)$$

(b) Comparison with the national electricity matrix

According to the Chilean National Electric System (SEN), the average emission factor has progressively decreased thanks to the incorporation of renewable energy, reaching approximately 0.2021 kg CO_2/kWh in recent years (*Factores de Emisión – Energía Abierta | Comisión Nacional de Energía,* 2024). Under this scenario, the environmental benefit of the HRES is maintained, although to a lesser extent.

$$Daily\ reduction = 1{,}470\ kWh * 0.2021\ \frac{kg\ CO_2}{kWh} = 297\ \frac{kg\ CO_2}{day} \quad (2\text{-}26)$$

$$Annual\ reduction = 297\ \frac{kg\ CO_2}{day} * 365\ days = 108{,}405\ \frac{kg\ CO_2}{year} \quad (2\text{-}27)$$

These results show that HRES is not only technically and economically competitive in a high-complementarity scenario but can also avoid between 108 and 375 tons of CO_2 annually, depending on the reference source. This impact is especially relevant for isolated communities or industrial applications with grid access restrictions, contributing to decarbonization and energy sustainability goals.

2.3.6 Example of applicability

The Chilean government has decisively promoted the green hydrogen market's development as a strategic decarbonization pillar, encouraging large-scale renewable generation projects. In this context, incorporating the criterion of temporal energy complementarity between solar and wind resources could significantly improve location selection processes by favoring more stable and continuous renewable energy generation. This is especially relevant in applications that require a constant electricity supply, such as electrolysis. For example, a plant that produces 200 kg of green hydrogen daily requires approximately 10,400 kWh daily. (Muñoz-Pincheira et al., 2024) created a temporal complementarity map for Chile. If a location for the electrolysis plant with high solar-wind complementarity (Spearman coefficient ρ = -0.95) is compared with another with equal energy potential but low complementarity (ρ = 0.5), the former could reduce the NPC by around 60% and the LCOE by 50%, thanks to a better utilization of the electrolyzer and a lower need for storage.

2.4 Conclusions

This study has demonstrated that temporal complementarity between solar and wind sources is a key factor in the optimal design of off-grid HRES. Explicitly incorporating this parameter into the optimization process significantly reduces the NPC and the LCOE, while also improving system reliability as measured by the LPSP. This evidence reinforces the need to consider complementarity metrics as a fundamental technical criterion in the planning and sizing of hybrid systems.

From a critical perspective, the results show that the effect of complementarity is not uniform: under constant demand and strict reliability requirements (LPSP < 1%), higher negative complementarity ($\rho \approx -0.95$) enables up to a 60% reduction in NPC compared to low-complementarity scenarios ($\rho \approx 0.95$), avoiding system oversizing—especially in storage. Moreover, it is observed that as the reliability requirement increases (i.e., lower LPSP values), temporal complementarity becomes more relevant, as it allows for a more balanced distribution of generation throughout the day and reduces the need for costly backup or storage systems. In contrast, for variable demand profiles with moderate reliability thresholds, the impact of complementarity is attenuated, since the flexibility of the load profile allows demand to be met without depending on a favorable correlation between sources.

The validity of the results is supported by sensitivity analyses of key technical and economic parameters (LPSP, battery cost, discount rate), as well as by multiple simulations using different random seeds in the genetic algorithm. An ANOVA test confirmed that the differences observed in NPC across complementarity scenarios are statistically significant ($p < 0.001$), which supports the robustness of the model and its applicability to real-world conditions.

This study presents an original and significant contribution compared to the existing literature. While many studies have explored HRES design using artificial intelligence techniques, iterative methods, or specialized software, none have explicitly quantified the effect of temporal complementarity on design indicators. This study is the first to incorporate such a metric into an optimization model using hourly data and constant energy potential, allowing the real impact of complementarity to be isolated and measured.

Accordingly, the results directly answer the research question: the degree of temporal complementarity between solar and wind resources significantly influences the NPC and LPSP's optimal design of stand-alone hybrid renewable energy systems with storage. This influence is more pronounced in high-reliability

scenarios or under constant demand conditions, and less relevant in contexts with flexible load profiles.

From a practical standpoint, the findings provide clear recommendations: identifying areas with high solar-wind complementarity and adjusting HRES design accordingly leads to more efficient, reliable, and cost-effective configurations. This is especially relevant for applications requiring a continuous power supply, such as green hydrogen production. Furthermore, from a public policy perspective, promoting distributed generation in areas with high complementarity can help reduce curtailment, ease transmission congestion, and improve the resilience of national power systems.

In summary, this study provides quantitative, validated, and comparative evidence that temporal solar-wind complementarity should be considered a fundamental technical parameter in designing and planning renewable hybrid systems with storage.

3 GENERAL DISCUSSION AND CONCLUSIONS

The increasing penetration of variable renewable energy sources in power systems poses significant challenges for their efficient and reliable integration. The variability, intermittency, and high geographic concentration of resources such as solar and wind energy create difficulties in centralized power systems, namely transmission congestion, energy curtailment, and the need for fossil backup. In this context, a technical alternative worth considering is the implementation of off-grid HRES, aimed at decentralizing electricity generation and enhancing local energy autonomy.

This thesis tackled how the temporal complementarity between solar and wind generation can influence the optimal techno-economic configuration of an HRES with storage. To this end, two main objectives were defined: (1) to characterize solar-wind complementarity across Chilean territory, and (2) to quantitatively assess temporal complementarity in designing stand-alone hybrid systems under various load profiles and reliability levels.

The results demonstrate that solar-wind temporal complementarity significant affects on system costs, reliability, and sizing, but its impact depends strongly on the load profile and required reliability (LPSP). In particular, for a daily demand of 1,470 kWh:

For systems with constant loads and LPSP ≤ 5%, high complementarity ($\rho \approx -0.95$) enabled:

- Up to a 17-fold reduction in NPC,
- A 12.7 % decrease in LPSP,
- A drop in LCOE from 0.81 to 0.63 USD/kWh,
- Complete elimination of energy curtailment.

By contrast, complementarity had only a marginal effect on the evaluated indicators for residential type variable loads, highlighting that its relevance hinges on system reliability and load profile. Moreover, complementarity becomes a decisive factor as the continuity requirement grows (i.e., lower LPSP).

Furthermore, technology cost has a more significant impact on NPC than financing cost. This suggests that, for example, a reduction in storage system prices could substantially improve HRES project profitability, making them more attractive to potential investors.

In comparison to grid-connected projects, an HRES with an LCOE of 0.38 USD/kWh (obtained with ρ = –0.95 complementarity and genetic-algorithm seed = 1) is not economically competitive, since generator revenues on the market typically range from 0.03 to 0.06 USD/kWh, and end-user energy prices are around 0.15 USD/kWh (CNE, 2025). However, in isolated areas where diesel generation costs lie between 0.80 and 1.20 USD/kWh, HRES becomes a viable technical and economic alternative. Its competitiveness could improve with higher curtailment rates, lower technology costs, and policies promoting distributed generation.

This thesis contributes to scientific knowledge in three dimensions:

- Theoretical: It quantitatively demonstrates that temporal complementarity is not secondary but a critical variable in the optimal design of hybrid systems, especially under high-reliability requirements.
- Methodological: It develops an optimization model in GNU Octave based on genetic algorithms, enabling evaluation of different HRES configurations across varying levels of temporal complementarity. The model compares scenarios using financial, operational, and technical metrics, facilitating comprehensive system performance analysis.
- Applied: It produces the first national map of solar-wind temporal complementarity in Chile and shows how incorporating this metric into design reduces costs, improves reliability, and lowers storage needs.

Key limitations of this work include:

- Metaheuristic approach constraints: Genetic algorithms do not guarantee global optima due to their heuristic nature. Nevertheless, the model was configured to ensure comparability of feasible solutions under controlled initial conditions, enabling consistent scenario analyses.
- Simplified generation modeling: Although the system represents PV panels, wind turbines, and batteries, it omits power-electronics components (inverters, MPPT controllers, DC/DC converters), which could increase total system cost.
- Design-only optimization: The model focuses on sizing optimization, i.e., determining the most efficient installed capacities of panels, turbines, and batteries, without optimizing dynamic operation or advanced control strategies, which are vital for system operation.
-

Future research directions proposed are:

- Explore and compare other optimization techniques (e.g., Particle Swarm Optimization, Tabu Search, Simulated Annealing, and machine learning-based algorithms), assessing their efficacy, convergence, and robustness against the genetic algorithm used.
- Develop integrated design-operation models that include dynamic behavior and explicit representation of power-electronics components (inverters, DC/DC converters, MPPT controllers) for a more realistic system assessment.
- Extend complementarity analysis to other renewable sources (wave, tidal, geothermal, biomass) and examine their integration in complex hybrid systems with high energy diversification.

Finally, it is vital to highlight the implications for decentralized energy planning: incorporating temporal complementarity as a design criterion not only enhances HRES technical and economic performance but also reduces CO_2 emissions, promotes generation decentralization, strengthens energy resilience in isolated communities, and advances more sustainable energy solutions. Accordingly, this thesis proposes adopting temporal complementarity as a key metric in public policy development, investment instruments, and incentives designed to foster distributed generation in regions with high solar-wind complementarity.

3. DISCUSIÓN GENERAL Y CONCLUSIONES

El aumento en la penetración de fuentes de energía renovable variable en los sistemas eléctricos plantea desafíos significativos para su integración eficiente y confiable. La variabilidad, intermitencia y alta concentración geográfica de recursos como la energía solar y eólica generan dificultades en los sistemas centralizados, tales como congestión en la transmisión, vertimiento de energía y la necesidad de respaldo fósil. En este contexto, una alternativa técnica que merece consideración es la implementación de Sistemas Híbridos de Energía Renovable autónomos (HRES), orientados a descentralizar la generación eléctrica y fortalecer la autonomía energética local.

Esta tesis abordó cómo la complementariedad temporal entre la generación solar y eólica puede influir en la configuración tecnoeconómica óptima de un HRES con almacenamiento. Para ello, se definieron dos objetivos principales: (1) caracterizar la complementariedad solar-eólica en el territorio chileno, y (2) evaluar cuantitativamente el impacto de dicha complementariedad en el diseño de sistemas híbridos autónomos bajo distintos perfiles de carga y niveles de confiabilidad.

Los resultados demuestran que la complementariedad temporal solar-eólica tiene efectos significativos sobre los costos del sistema, su confiabilidad y dimensionamiento, aunque su impacto depende fuertemente del perfil de carga y del nivel de confiabilidad requerido (LPSP). En particular, para una demanda diaria de 1.470 kWh:

Para sistemas con carga constante y un LPSP ≤ 5%, una alta complementariedad ($\rho \approx -0{,}95$) permitió:

- Una reducción del NPC de hasta 17 veces,
- Una disminución del LPSP del 12,7 %,
- Una caída del LCOE de 0,81 a 0,63 USD/kWh,
- La eliminación total del vertimiento de energía.

En contraste, la complementariedad tuvo solo un efecto marginal sobre los indicadores evaluados en cargas variables tipo residencial, lo que destaca que su relevancia depende del perfil de carga y del requerimiento de continuidad del sistema. Además, la complementariedad se vuelve un factor decisivo a medida que aumentan las exigencias de continuidad (es decir, menor LPSP).

Por otro lado, se observó que el costo tecnológico tiene un mayor impacto sobre el NPC que el costo del financiamiento. Esto sugiere que, por ejemplo, una disminución en los precios de los sistemas de almacenamiento podría mejorar sustancialmente la rentabilidad de los proyectos HRES, haciéndolos más atractivos para potenciales inversionistas.

En comparación con proyectos conectados a la red, un HRES con un LCOE de 0,38 USD/kWh (obtenido con una complementariedad ρ = –0,95 y semilla del algoritmo genético = 1) no resulta competitivo económicamente, dado que los ingresos de los generadores en el mercado suelen oscilar entre 0,03 y 0,06 USD/kWh, y los precios de la energía para el usuario final se sitúan en torno a los 0,15 USD/kWh (CNE, 2025). Sin embargo, en zonas aisladas donde los costos de generación diésel se encuentran entre 0,80 y 1,20 USD/kWh, los HRES se convierten en una alternativa técnica y económicamente viable. Su competitividad podría mejorar con mayores tasas de vertimiento, menores costos tecnológicos y políticas que fomenten la generación distribuida.

Esta tesis contribuye al conocimiento científico en tres dimensiones:

Teórica: Demuestra cuantitativamente que la complementariedad temporal no es una variable secundaria, sino un factor crítico en el diseño óptimo de sistemas híbridos, especialmente bajo exigencias altas de confiabilidad.

Metodológica: Desarrolla un modelo de optimización en GNU Octave basado en algoritmos genéticos, que permite evaluar distintas configuraciones de HRES bajo diferentes niveles de complementariedad temporal. El modelo compara escenarios utilizando métricas financieras, operativas y técnicas, facilitando un análisis integral del desempeño del sistema.

Aplicada: Genera el primer mapa nacional de complementariedad temporal solar-eólica en Chile y demuestra cómo la incorporación de esta métrica en el diseño reduce costos, mejora la confiabilidad y disminuye los requerimientos de almacenamiento.

Las principales limitaciones de este trabajo incluyen:

Restricciones del enfoque metaheurístico: Los algoritmos genéticos no garantizan óptimos globales debido a su naturaleza heurística. No obstante, el modelo fue configurado para asegurar la comparabilidad de soluciones factibles bajo condiciones iniciales controladas, permitiendo un análisis consistente entre escenarios.

Modelación simplificada de la generación: Aunque el sistema representa paneles fotovoltaicos, aerogeneradores y baterías, omite componentes

electrónicos de potencia (inversores, controladores MPPT, convertidores DC/DC), los cuales podrían incrementar el costo total del sistema.

Optimización solo del diseño: El modelo se centra en la optimización del dimensionamiento, es decir, en determinar las capacidades instaladas más eficientes de paneles, turbinas y baterías, sin considerar la optimización de la operación dinámica ni estrategias avanzadas de control, aspectos clave para el funcionamiento real del sistema.

Las futuras líneas de investigación propuestas son:

- Explorar y comparar otras técnicas de optimización (por ejemplo, Optimización por Enjambre de Partículas, Búsqueda Tabú, Recocido Simulado y algoritmos basados en aprendizaje automático), evaluando su eficacia, convergencia y robustez frente al algoritmo genético utilizado.
- Desarrollar modelos integrados de diseño y operación que incluyan el comportamiento dinámico y la representación explícita de componentes de electrónica de potencia (inversores, convertidores DC/DC, controladores MPPT), para una evaluación más realista del sistema.
- Ampliar el análisis de complementariedad a otras fuentes renovables (oleaje, mareas, geotermia, biomasa) y examinar su integración en sistemas híbridos complejos con alta diversificación energética.

Finalmente, es fundamental destacar las implicancias para la planificación energética descentralizada: incorporar la complementariedad temporal como criterio de diseño no solo mejora el desempeño técnico y económico de los HRES, sino que también reduce las emisiones de CO_2, fomenta la descentralización de la generación, fortalece la resiliencia energética en comunidades aisladas y promueve soluciones energéticas más sostenibles. En consecuencia, esta tesis propone adoptar la complementariedad temporal como una métrica clave en el desarrollo de políticas públicas, instrumentos de inversión e incentivos destinados a promover la generación distribuida en regiones con alta complementariedad solar-eólica.

REFERENCES

Abdellatif, H., Syed, M. N., Hossain, M. I., & Abido, M. A. (2023). Standalone Hybrid Renewable Energy System Optimization Using Linear Programming. *Arabian Journal for Science and Engineering*, *48*(5), 6361–6376. https://doi.org/10.1007/s13369-022-07363-7

Agajie, T. F., Ali, A., Fopah-Lele, A., Amoussou, I., Khan, B., Velasco, C. L. R., & Tanyi, E. (2023). A Comprehensive Review on Techno-Economic Analysis and Optimal Sizing of Hybrid Renewable Energy Sources with Energy Storage Systems. *Energies*, *16*(2), Article 2. https://doi.org/10.3390/en16020642

Akrouch, M. A., Chahine, K., Faraj, J., Hachem, F., Castelain, C., & Khaled, M. (2023). Advancements in cooling techniques for enhanced efficiency of solar photovoltaic panels: A detailed comprehensive review and innovative classification. *Energy and Built Environment*. https://doi.org/10.1016/j.enbenv.2023.11.002

Al Sumarmad, K. A., Sulaiman, N., Wahab, N. I. A., & Hizam, H. (2022). Energy Management and Voltage Control in Microgrids Using Artificial Neural Networks, PID, and Fuzzy Logic Controllers. *Energies*, *15*(1), Article 1. https://doi.org/10.3390/en15010303

Alberizzi, J. C., Rossi, M., & Renzi, M. (2020). A MILP algorithm for the optimal sizing of an off-grid hybrid renewable energy system in South Tyrol. *Energy Reports*, *6*, 21–26. https://doi.org/10.1016/j.egyr.2019.08.012

Al-falahi, M. D. A., Jayasinghe, S. D. G., & Enshaei, H. (2017). A review on recent size optimization methodologies for standalone solar and wind hybrid renewable energy system. *Energy Conversion and Management*, *143*, 252–274. https://doi.org/10.1016/j.enconman.2017.04.019

Althani, M., & Maheri, A. (2021). An Ant Colony Algorithm for HRES Size and Configuration Optimisation. *2021 6th International Symposium on Environment-Friendly Energies and Applications (EFEA)*, 1–6. https://doi.org/10.1109/EFEA49713.2021.9406256

Araoye, T. O., Ashigwuike, E. C., Mbunwe, M. J., Bakinson, O. I., & Ozue, T. I. (2024). Techno-economic modeling and optimal sizing of autonomous hybrid microgrid renewable energy system for rural electrification sustainability using HOMER and grasshopper optimization algorithm. *Renewable Energy*, *229*, 120712. https://doi.org/10.1016/j.renene.2024.120712

Auguadra, M., Ribó-Pérez, D., & Gómez-Navarro, T. (2023). Planning the deployment of energy storage systems to integrate high shares of renewables: The Spain case study. *Energy*, *264*, 126275. https://doi.org/10.1016/j.energy.2022.126275

Belfkira, R., Zhang, L., & Barakat, G. (2011). Optimal sizing study of hybrid wind/PV/diesel power generation unit. *Solar Energy*, *85*(1), 100–110. https://doi.org/10.1016/j.solener.2010.10.018

Beluco, A., de Souza, P. K., & Krenzinger, A. (2008). A dimensionless index evaluating the time complementarity between solar and hydraulic energies. *Renewable Energy*, *33*(10), 2157–2165. https://doi.org/10.1016/j.renene.2008.01.019

Camargo, L. R., Valdes, J., Macia, Y. M., & Dorner, W. (2019). Assessment of on-site steady electricity generation from renewable energy sources in Chile. *Energy Procedia*, *158*, 1099–1104. https://doi.org/10.1016/j.egypro.2019.01.266

Canales, F. A., & Acuña, G. J. (2022). Chapter 2—Metrics and indices used for the evaluation of energetic complementarity—A review. In J. Jurasz & A. Beluco (Eds.), *Complementarity of Variable Renewable Energy Sources* (pp. 35–55). Academic Press. https://doi.org/10.1016/B978-0-323-85527-3.00020-0

Cantão, M. P., Bessa, M. R., Bettega, R., Detzel, D. H. M., & Lima, J. M. (2017). Evaluation of hydro-wind complementarity in the Brazilian territory by means of correlation maps. *Renewable Energy*, *101*, 1215–1225. https://doi.org/10.1016/j.renene.2016.10.012

Cantor, D., Ochoa, A., & Mesa, O. (2022). Total Variation-Based Metrics for Assessing Complementarity in Energy Resources Time Series. *Sustainability*, *14*(14), Article 14. https://doi.org/10.3390/su14148514

Coordinador eléctrico nacional. (2022). *Hoja de ruta para una transición energética acelerada, visión del coordinador eléctrico nacional*. https://www.coordinador.cl/wp-content/uploads/2022/06/8_digital_Informe_Coordinador_2.5.pdf

Costoya, X., deCastro, M., Carvalho, D., & Gómez-Gesteira, M. (2023). Assessing the complementarity of future hybrid wind and solar photovoltaic energy resources for North America. *Renewable and Sustainable Energy Reviews*, *173*, 113101. https://doi.org/10.1016/j.rser.2022.113101

Couto, A., & Estanqueiro, A. (2021). Assessment of wind and solar PV local complementarity for the hybridization of the wind power plants installed in Portugal. *Journal of Cleaner Production*, *319*, 128728. https://doi.org/10.1016/j.jclepro.2021.128728

Cuesta, M. A., Castillo-Calzadilla, T., & Borges, C. E. (2020). A critical analysis on hybrid renewable energy modeling tools: An emerging opportunity to include social indicators to optimise systems in small communities. *Renewable and Sustainable Energy Reviews*, *122*, 109691. https://doi.org/10.1016/j.rser.2019.109691

Daszkiewicz, K. (2020). Policy and Regulation of Energy Transition. In M. Hafner & S. Tagliapietra (Eds.), *The Geopolitics of the Global Energy Transition* (pp. 203–226). Springer International Publishing. https://doi.org/10.1007/978-3-030-39066-2_9

Delgado, R. (2007). *Probabilidad y Estadística para Ciencias e Ingenierias.* Delta. https://books.google.cl/books?id=xbiCKj0vV6kC

Dufo-López, R., Cristóbal-Monreal, I. R., & Yusta, J. M. (2016). Optimisation of PV-wind-diesel-battery stand-alone systems to minimise cost and maximise human development index and job creation. *Renewable Energy*, *94*, 280–293. https://doi.org/10.1016/j.renene.2016.03.065

Energia, S. I.-C. N. (n.d.). *Costos de Tecnologías de Generación—Comisión Nacional de Energía*. Retrieved September 25, 2024, from https://www.cne.cl/tarificacion/electrica/costos-de-inversion/

ESRI Chile. (2024, January 1). *ArcGIS Pro | Software de representación cartográfica SIG 2D, 3D y 4D*. https://www.esri.cl/es-cl/productos/arcgis-pro/overview

Factores de Emisión – Energía Abierta | Comisión Nacional de Energía. (2024). http://energiaabierta.cl/visualizaciones/factor-de-emision-sic-sing/

Fernandes, P. C. B., Risso, A., & Beluco, A. (2022). Chapter 5—A survey on temporal and spatial complementarity between wind and solar resources along the coast of northeastern Brazil. In J. Jurasz & A. Beluco (Eds.), *Complementarity of Variable Renewable Energy Sources* (pp. 99–120). Academic Press. https://doi.org/10.1016/B978-0-323-85527-3.00011-X

Gallardo, R. P., Ríos, A. M., & Ramírez, J. S. (2020). Analysis of the solar and wind energetic complementarity in Mexico. *Journal of Cleaner Production*, *268*, 122323. https://doi.org/10.1016/j.jclepro.2020.122323

Gao, Y., Meng, Y., Dong, G., Ma, S., Miao, C., Xiao, J., Mao, S., & Shao, L. (2024). The wind-solar hybrid energy could serve as a stable power source at multiple time scale in China mainland. *Energy*, *305*, 132294. https://doi.org/10.1016/j.energy.2024.132294

Garcia G., M., & Oliva H., S. (2023). Technical, economic, and CO2 emissions assessment of green hydrogen production from solar/wind energy: The case of Chile. *Energy*, *278*, 127981. https://doi.org/10.1016/j.energy.2023.127981

Gelaro, R., McCarty, W., Suárez, M. J., Todling, R., Molod, A., Takacs, L., Randles, C. A., Darmenov, A., Bosilovich, M. G., Reichle, R., Wargan, K., Coy, L., Cullather, R., Draper, C., Akella, S., Buchard, V., Conaty, A., Silva, A. M. da, Gu, W., … Zhao, B. (2017). The Modern-Era Retrospective Analysis for Research and Applications, Version 2 (MERRA-2). *Journal of Climate*, *30*(14), 5419–5454. https://doi.org/10.1175/JCLI-D-16-0758.1

Generadoras de Chile. (2023). *Boletin generadoras de Chile-septiembre 2023*. https://generadoras.cl/documentos/boletines/boletin-generadoras-de-chile-septiembre-2023

Gonzalez-Salazar, M., & Poganietz, W. R. (2021). Evaluating the complementarity of solar, wind and hydropower to mitigate the impact of El Niño Southern Oscillation in Latin America. *Renewable Energy*, *174*, 453–467. https://doi.org/10.1016/j.renene.2021.04.048

Guo, Y., Ming, B., Huang, Q., Yang, Z., Kong, Y., & Wang, X. (2023). Variation-based complementarity assessment between wind and solar resources in China. *Energy Conversion and Management*, *278*, 116726. https://doi.org/10.1016/j.enconman.2023.116726

Henao, F., Viteri, J. P., Rodríguez, Y., Gómez, J., & Dyner, I. (2020). Annual and interannual complementarities of renewable energy sources in Colombia. *Renewable and Sustainable Energy Reviews*, *134*, 110318. https://doi.org/10.1016/j.rser.2020.110318

Holland, J. H. (1992). *Adaptation in natural and artificial systems: An introductory analysis with applications to biology, control, and artificial intelligence*.

IEA. (2023). *Net Zero Roadmap: A Global Path to Keep the 1.5°C Target Within Reach, IEA, Paris*. https://www.iea.org/reports/net-zero-roadmap-a-global-pathway-to -mantener-el-objetivo-15-0c-al-alcance

IGM. (n.d.). *Instituto Geográfico Militar de Chile*. Grilla IGM Escala 1:25000 KMZ. Retrieved January 15, 2024, from https://www.igm.cl/?page=descargas-gratuitas-igm&menu=1

International Energy Agency. (2020). World Energy Outlook 2020. *IEA Publications*.

International Energy Agency. (2023). *The Evolution of Energy Efficiency Policy to Support Clean Energy Transitions*. OECD. https://doi.org/10.1787/18f6db00-en

International Energy Agency. (2024). Electricity Information database. *Electricity Information*. http://wds.iea.org/wds/pdf/ele_documentation.pdf.

IPCC. (2023). *Climate Change 2023: Synthesis Report. Contribution of Working Groups I, II and III to the Sixth Assessment Report of the Intergovernmental Panel on Climate Change*.

Jurasz, J., Canales, F. A., Kies, A., Guezgouz, M., & Beluco, A. (2020a). A review on the complementarity of renewable energy sources: Concept, metrics, application and future research directions. *Solar Energy*, *195*, 703–724. https://doi.org/10.1016/j.solener.2019.11.087

Jurasz, J., Canales, F. A., Kies, A., Guezgouz, M., & Beluco, A. (2020b). A review on the complementarity of renewable energy sources: Concept,metrics, application and future research directions. *Solar Energy*, *195*, 703–704. https://doi.org/10.1016/j.solener.2019.11.087

Jurasz, J., Guezgouz, M., Campana, P. E., Kaźmierczak, B., Kuriqi, A., Bloomfield, H., Hingray, B., Canales, F. A., Hunt, J. D., Sterl, S., & Elkadeem, M. R. (2024). Complementarity of wind and solar power in North Africa: Potential for alleviating energy droughts and impacts of the North Atlantic Oscillation. *Renewable and Sustainable Energy Reviews*, *191*, 114181. https://doi.org/10.1016/j.rser.2023.114181

Kavadias, K. A., & Triantafyllou, P. (2021). Hybrid Renewable Energy Systems' Optimisation. A Review and Extended Comparison of the Most-Used Software Tools. *Energies*, *14*(24), Article 24. https://doi.org/10.3390/en14248268

Khan, K. A., Quamar, M. M., Al-Qahtani, F. H., Asif, M., Alqahtani, M., & Khalid, M. (2023). Smart grid infrastructure and renewable energy deployment: A conceptual review of Saudi Arabia. *Energy Strategy Reviews*, *50*. https://doi.org/10.1016/j.esr.2023.101247.

Kharrich, M., Selim, A., Kamel, S., & Kim, J. (2023). An effective design of hybrid renewable energy system using an improved Archimedes Optimization Algorithm: Acase study of Farafra,Egypt. *Energy Conversion and Management*, *283*, 116907. https://doi.org/10.1016/j.enconman.2023.116907

López Prol, J., de Llano Paz, F., Calvo-Silvosa, A., Pfenninger, S., & Staffell, I. (2024). Wind-solar technological, spatial and temporal complementarities in Europe: A portfolio approach. *Energy*, *292*, 130348. https://doi.org/10.1016/j.energy.2024.130348

Magaña-González, R. C., Rodríguez-Hernández, O., & Canul-Reyes, D. A. (2023). Analysis of seasonal variability and complementarity of wind and solar resources in Mexico. *Sustainable Energy Technologies and Assessments*, *60*, 103456. https://doi.org/10.1016/j.seta.2023.103456

Mahesh, A., & Sandhu, K. S. (2020). A genetic algorithm based improved optimal sizing strategy for solar-wind-battery hybrid system using energy filter algorithm. *Frontiers in Energy*, *14*(1), 139–151. https://doi.org/10.1007/s11708-017-0484-4

Mahmoud, F., Diab, A., Ali, Z., Ahmed, A.-H., Alquthami, T., Ahmed, M., & Ramadan, H. (2022). Optimal sizing of smart hybrid renewable energy system using different optimization algorithms. *Energy Reports*, *8*, 4935–4956. https://doi.org/10.1016/j.egyr.2022.03.197

Marocco, P., Ferrero, D., Lanzini, A., & Santarelli, M. (2022). The role of hydrogen in the optimal design of off-grid hybrid renewable energy systems. *Journal of Energy Storage*, *46*, 103893. https://doi.org/10.1016/j.est.2021.103893

Merei, G., Berger, C., & Sauer, D. U. (2013). Optimization of an off-grid hybrid PV–Wind–Diesel system with different battery technologies using genetic algorithm. *Solar Energy*, *97*, 460–473. https://doi.org/10.1016/j.solener.2013.08.016

Ministerio de Energía. (n.d.). *Explorador Solar*. Retrieved September 24, 2024, from https://solar.minenergia.cl/exploracion

Ministerio de energía, Gobierno de Chile. (2022). *Plan nacional de eficiencia energética 2022-2026*. https://energia.gob.cl/sites/default/files/documentos/plan_nacional_de_eficiencia_energetica_2022-2026.pdf

Mishra, S., Panigrahi, C. K., & Kothari, D. P. (2016). Design and simulation of a solar–wind–biogas hybrid system architecture using HOMER in India. *International Journal of Ambient Energy*, *37*(2), 184–191. https://doi.org/10.1080/01430750.2014.915886

Mokhtara, C., Negrou, B., Settou, N., Settou, B., & Samy, M. M. (2021). Design optimization of off-grid Hybrid Renewable Energy Systems considering the effects of building energy performance and climate change: Case study of Algeria. *Energy*, *219*, 119605. https://doi.org/10.1016/j.energy.2020.119605

Molina, A., Falvey, M., & Rondanelli, R. (2017). A solar radiation database for Chile. *Scientific Reports*, *7*(1), Article 1. https://doi.org/10.1038/s41598-017-13761-x

Muñoz-Pincheira, J. L., Salazar, L., Sanhueza, F., & Lüer-Villagra, A. (2024). Temporal Complementarity Analysis of Wind and Solar Power Potential for Distributed Hybrid Electric Generation in Chile. *Energies*, *17*(8), Article 8. https://doi.org/10.3390/en17081890

Nadeem, T. B., Ahmed, A., Saad, M., & Naqvi, A. A. (2024). Design and optimization of off-grid solar PV and biomass-based hybrid renewable energy system (HRES) for electrification of a rural community in Tharparkar, Pakistan. *Environment, Development and Sustainability*. https://doi.org/10.1007/s10668-024-05146-8

Naderipour, A., Kamyab, H., Klemeš, J. J., Ebrahimi, R., Chelliapan, S., Nowdeh, S. A., Abdullah, A., & Hedayati Marzbali, M. (2022). Optimal design of hybrid grid-connected photovoltaic/wind/battery sustainable energy system improving reliability, cost and emission. *Energy*, *257*, 124679. https://doi.org/10.1016/j.energy.2022.124679

Nogueira, E. C., Morais, R. C., & Pereira, A. O. (2023). Offshore Wind Power Potential in Brazil: Complementarity and Synergies. *Energies*, *16*(16), Article 16. https://doi.org/10.3390/en16165912

Ogunjuyigbe, A. S. O., Ayodele, T. R., & Akinola, O. A. (2016). Optimal allocation and sizing of PV/Wind/Split-diesel/Battery hybrid energy system for minimizing life cycle cost, carbon emission and dump energy of remote residential building. *Applied Energy*, *171*, 153–171. https://doi.org/10.1016/j.apenergy.2016.03.051

ONU. (2015). *Acuerdo de París de la Convención Marco de las Naciones Unidas sobre el Cambio Climático (UNFCCC)*. https://www.refworld.org.es/docid/602021b64.html

Pedruzzi, R., Silva, A. R., Soares dos Santos, T., Araujo, A. C., Cotta Weyll, A. L., Lago Kitagawa, Y. K., Nunes da Silva Ramos, D., Milani de Souza, F., Almeida Narciso, M. V., Saraiva Araujo, M. L., Medrado, R. C., Camilo Júnior, W. O., Neto, A. T., de Carvalho, M., Pires Bezerra, W. R., Costa, T. T., Bione de Melo Filho, J., Bandeira Santos, A. Á., & Moreira, D. M. (2023). Review of mapping analysis and complementarity between solar and wind energy sources. *Energy*, *283*, 129045. https://doi.org/10.1016/j.energy.2023.129045

Pérez Odeh, R., & Watts, D. (2019). Impacts of wind and solar spatial diversification on its market value: A case study of the Chilean electricity market. *Renewable and Sustainable Energy Reviews*, *111*, 442–461. https://doi.org/10.1016/j.rser.2019.01.015

Pérez Uc, D. A., de León Aldaco, S. E., & Aguayo Alquicira, J. (2024). Trends in Hybrid Renewable Energy System (HRES) Applications: A Review. *Energies*, *17*(11), Article 11. https://doi.org/10.3390/en17112578

Ren, G., Wan, J., Liu, J., & Yu, D. (2019). Spatial and temporal assessments of complementarity for renewable energy resources in China. *Energy*, *177*, 262–275. https://doi.org/10.1016/j.energy.2019.04.023

REN21. (2023). *Renewables 2023 Global Status Report Collection*. https://www.ren21.net/gsr-2023/

Rey-Costa, E., Elliston, B., Green, D., & Abramowitz, G. (2023). Firming 100% renewable power: Costs and opportunities in Australia's National Electricity Market. *Renewable Energy*, *219*, 119416. https://doi.org/10.1016/j.renene.2023.119416

Ross, C. (2023, September 15). *We've Got a Transmission Traffic Jam: Why this problem is costing consumers billions*. Default. https://www.ecmag.com/magazine/articles/article-detail/we-ve-got-a-transmission-traffic-jam-why-this-problem-is-costing-consumers-billions

Rueger, J., Smith Morton, L., & McLean, M. (2023, November 10). *DOE Study Finds US Must Double Regional Transmission Capacity To Meet 2035 Clean Energy Goal | Perkins Coie*. https://perkinscoie.com/insights/update/doe-study-finds-us-must-double-regional-transmission-capacity-meet-2035-clean

Saiprasad, N., Kalam, A., & Zayegh, A. (2019). Triple Bottom Line Analysis and Optimum Sizing of Renewable Energy Using Improved Hybrid Optimization Employing the Genetic Algorithm: A Case Study from India. *Energies*, *12*(3), Article 3. https://doi.org/10.3390/en12030349

Santabárbara, J. (2019). Cálculo del intervalo de confianza para los coeficientes de correlación mediante sintaxis en SPSS. *Revista d'Innovació i Recerca En Educació*, *12*, 1–14. https://doi.org/10.1344/reire2019.12.228245.

Singh, R., & Bansal, R. C. (2018). Review of HRESs based on storage options, system architecture and optimisation criteria and methodologies. *IET Renewable Power Generation*, *12*(7), 747–760. https://doi.org/10.1049/iet-rpg.2017.0603

Sinha, A., Venkatesh, A., Jordan, K., Wade, C., Eshraghi, H., de Queiroz, A. R., Jaramillo, P., & Johnson, J. X. (2024). Diverse decarbonization pathways under near cost-optimal futures. *Nature Communications*, *15*(1), 8165. https://doi.org/10.1038/s41467-024-52433-z

Sistema Nacional de Areas Protegidas, Pub. L. No. Ley 21600. https://bcn.cl/3evks

Sleeper, A. (2011). *Minitab Demystified*. Mcgraw-hill. https://books.google.cl/books?id=cy6E5R2Zv3kC

Song, X., Zhang, H., Fan, L., Zhang, Z., & Peña-Mora, F. (2023). Planning shared energy storage systems for the spatio-temporal coordination of multi-site renewable energy sources on the power generation side. *Energy*, *282*, 128976. https://doi.org/10.1016/j.energy.2023.128976

Torres-Madroñero, J. L., Nieto-Londoño, C., & Sierra-Pérez, J. (2020). Hybrid Energy Systems Sizing for the Colombian Context: A Genetic Algorithm and Particle Swarm Optimization Approach. *Energies*, *13*(21), Article 21. https://doi.org/10.3390/en13215648

US EPA, O. (2015, August 4). *Centralized Generation of Electricity and its Impacts on the Environment* [Overviews and Factsheets]. https://www.epa.gov/energy/centralized-generation-electricity-and-its-impacts-environment

Vargas-Ferrer, P., Álvarez-Miranda, E., Tenreiro, C., & Jalil-Vega, F. (2022). Assessing flexibility for integrating renewable energies into carbon neutral multi-regional systems: The case of the Chilean power system. *Energy for Sustainable Development*, *70*, 442–455. https://doi.org/10.1016/j.esd.2022.08.010

Vázquez, R., Cabos, W., Nieto-Borge, J. C., & Gutiérrez, C. (2024). Complementarity of offshore energy resources on the Spanish coasts: Wind, wave, and photovoltaic energy. *Renewable Energy*, *224*, 120213. https://doi.org/10.1016/j.renene.2024.120213

Vendoti, S., Muralidhar, M., & Kiranmayi, R. (2019). GA Based Optimization of an Stand-alone Hybrid Renewable Energy System for Electrification in a Cluster of Villages in India. *2019 Fifth International Conference on Science Technology Engineering and Mathematics (ICONSTEM)*, 319–324. https://doi.org/10.1109/ICONSTEM.2019.8918728

Viviescas, C., Lima, L., Diuana, F. A., Vasquez, E., Ludovique, C., Silva, G. N., Huback, V., Magalar, L., Szklo, A., Lucena, A. F. P., Schaeffer, R., & Paredes, J. R. (2019). Contribution of Variable Renewable Energy to increase energy security in Latin America: Complementarity and climate change impacts on wind and solar resources. *Renewable and Sustainable Energy Reviews*, *113*, 109232. https://doi.org/10.1016/j.rser.2019.06.039

von Papp, J., Moraga, F., & Henríquez, A. (2022). Vertimiento de energía de centrales eólicas y solares fotovoltaicas del Sistema Eléctrico Nacional (SEN) en Chile durante 2022. *Fraunhofer Chile Research*. Available from: mailto:julius.vonpapp@fraunhofer.cl

Wiernga, J. (1993). Representative roughness parameters for homogeneous terrain. *Boundary-Layer Meteorol*, *63*, 323–363. https://doi.org/10.1007/BF00705357

Yang, M., Shao, H., Zhao, X., Cheng, G., Dai, S., Wang, L., & Mao, X. (2024). Spatiotemporal distribution, evolution, and complementarity of wind and waves in China's offshore waters and its implications for the development of green energy. *Energy Conversion and Management*, *312*, 118567. https://doi.org/10.1016/j.enconman.2024.118567

Zhang, N., Lu, X., McElroy, M. B., Nielsen, C. P., Chen, X., Deng, Y., & Kang, C. (2016). Reducing curtailment of wind electricity in China by employing electric boilers for heat and pumped hydro for energy storage. *Applied Energy*, *184*, 987–994. https://doi.org/10.1016/j.apenergy.2015.10.147

APPENDICES

1. Pseudocode for HRES Optimization Algorithm:

```
BEGIN
    Set random seed for reproducibility (rng(42))

    Read hourly input data:
        - Load demand (C_load_hourly)
        - Solar irradiation (Irradiacion_solar_hourly)
        - Wind speed (Viento_hourly)

    Define technical and economic parameters:
        - Efficiencies (PV, Wind, Battery)
        - Availability factors
        - Costs (investment, O&M)
        - Constraint: LPSP_max

    Compute Spearman correlation between solar irradiation and wind speed

    Initialize population (pop_size) randomly within bounds [lb, ub]

    FOR each generation g in [1, max_gen] DO
        FOR each individual i in population DO
            Evaluate individual:
                - Compute PV and wind energy generation for each hour
                - Simulate battery use, dumped energy, and power deficit
                - Calculate LPSP

            IF LPSP > LPSP_max THEN
                Repair solution: proportionally increase PV, wind, and battery capacities
                Re-evaluate constraints

            Compute total cost and levelized cost of energy (LCOE)

            IF solution is valid AND better than best_cost THEN
                Update best_solution, best_cost, best_LPSP, best_results, best_COE
        END FOR

        Select best individuals using tournament selection
        Replace population with new solutions (mutation/crossover optional)
    END FOR

    IF no valid solution found THEN
        Notify: No optimal solution met the constraints

    ELSE
        Compute number of PV panels, wind turbines, and batteries
        Export results to text file
        Generate plots:
            - Hourly energy balance: load, PV, wind, battery, dumped
            - Solar-wind correlation plot

END
```